INFORMATION TO USERS

NUMERICAL AND EXPERIMENTAL ANALYSIS OF BENDING AND VIBRATION OF STIFFENED LAMINATED COMPOSITE PANELS

A Dissertation

Submitted to the Graduate Faculty of the
Louisiana State University and
Agricultural and Mechanical College
in partial fulfillment of the
requirements for the degree of
Doctor of Philosophy

in

The Department of Mechanical Engineering

by

Aruna Kumar Tripathy
B.Sc, Berhampur University, Berhampur, India, 1982
A.M.I.E., Institution of Engineers, Calcutta, India, 1986
M.E., Anna University, Madras, India, 1989
December, 1995

UMI Number: 9618329

UMI

ACKNOWLEDGEMENTS

TABLE OF CONTENTS

LIST OF TABLES

LIST OF FIGURES

vii

ABSTRACT

The objective of this study is to develop a method of analysis for fiber glass composite skew plates subjected to static and dynamic loading. An investigation has been carried out on the stress and deflection characteristics of stiffened parallelogramic plates with different skew angles. The numerical solution with assumed displacement function was developed using finite element analysis. Experiments using aluminum and Scotchply composite laminated plates were conducted to verify the results. Cantilever and simply supported boundary conditions were included in the analysis and an optimized angular stiffener for a particular swept back panel was achieved.

A finite element model for these types of composite stiffened plates has been formulated by combining the nine-node plate element with the three noded beam element. The effect of the stiffener orientation and eccentricity has been taken into account by proper transformation matrix. The analysis has been carried out using this finite element model for plates of rectangular and skew plan form. Three different boundary conditions have been considered in the analysis: only one side clamped, two opposite edges clamped, and all sides free. Fundamental frequencies and the mode shapes for these plates with no stiffener, single stiffener and two stiffeners parallel to one boundary have been obtained. For validation of these results, experiments were conducted on Scotchply glass-fiber composite plates with all the above mentioned boundary conditions. The modal analysis software STAR has been

used to analyze the experimental data and to prepare the mode shapes. The results are found to be in good agreement with the finite element results. A finite element analysis for a three dimensional composite aircraft wing consisting of skin, stiffener and ribs was carried out and the mode shapes were obtained.

CHAPTER 1. INTRODUCTION

In recent years, it has been assumed that composite materials and structures provide enhanced static and vibrational properties. These materials have found their applications in various fields such as aerospace, automotive, marine, electronics, and housing industries for their noted properties of high strength-to-weight and stiffness-to-weight ratios. Their advantage over conventional materials is due to their low structure weight, high stiffness, high static and dynamic strength. The anisotropic nature of the composites in their mechanical and thermal characteristics which occurs due to the different properties of fiber and matrix makes them of greater importance in various fields. The desired orientation and stacking sequence of fiber layers also adds to their advantage over conventional metals.

Plates with angle of sweep in plan form in any structure calls for the attention of design engineers irrespective of the structures where it is applied. The stress singularity at the root triangle of a swept cantilever plate is an important problem in many practical applications. However, the analysis of such plates presents greater difficulties than that of rectangular plates due to the variation of stresses at the fixed end. It has been known that as the angle of sweep increases, a concentration of stress occurs at the trailing edge and the numerical accuracy decreases. Despite the complexity of stress analysis of such plates, thin skew plates of various aspect ratios are in extensive use in

aeroplane and missile canard, wing, stabilizer and fin structures. The present trend of replacing isotropic materials by glass fiber composites makes the analysis of skew plates more complicated as the material non-linearity is added with stress singularity in such structures.

Skew panels with integrally attached stiffeners is a problem of growing importance especially in the area of aeronautical engineering. The design of stiffened skew plate structures under static and dynamic loading is of considerable interest in many engineering practices. Such structures are incorporated in modern high speed aircraft such as aircraft wings, fuselage and floor panels, guided missiles, ship bottom structures, etc. The skin-stringer connections of the airplane body can be considered as a specific problem. The deflection and stress analysis of these structures is the first step towards a final design. The stress singularities at the fixed corners of a skew plate is a major determinant of stress variation. Hence the study of the stiffened skew panels under static transverse loading is of primary importance. Schematic diagrams of a few commonly used stiffened plates are shown in Fig. 1.

The wide use of stiffened structural elements in engineering began in the nineteenth century, mainly with the application of steel plates for hulls of ships and with the development of steel bridges and aircraft. The most important engineering problems associated with the stiffened plates may be divided into the three main groups:
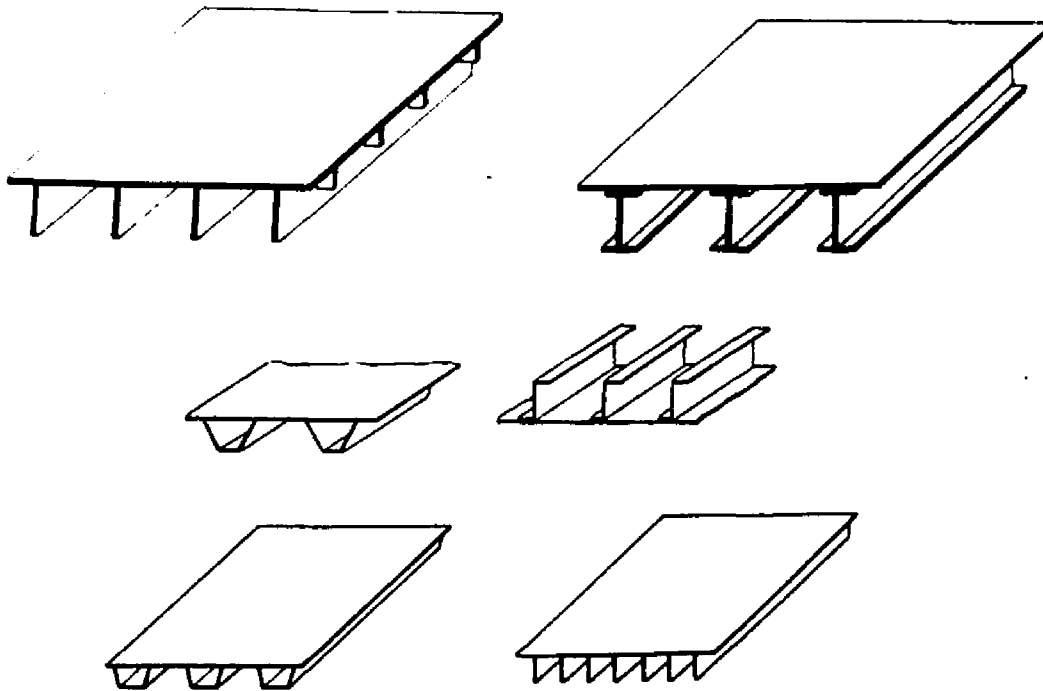
Fig. 1 Typical Stiffened Plates

a) Bending

b) Stability and

c) Vibration

The fundamentals of the method of analysis based on the analogy between a ribbed plate and an orthotropic plate, however, was established long ago by M.T. Huber in 1904. There are various methods known to date for the analysis of stresses, based on Huber's theory. Of all the proposed methods, however, the most practical one is that the stiffened plate be assumed as a continuous orthotropic plate. Based primarily on this approach, the American Institute of Steel Construction published the Design Manual in 1963 for the design of orthotropic steel plate deck bridges. Modern aircraft structures are

built primarily from sheet metal. These elements are very efficient in resisting shear or tension loads in the planes of the webs, but must usually be stiffened by members more capable of resisting compression loads and loads normal to the web. In such members stiffeners resist compression forces in the plane of the web, or small distributed loads normal to the plane of the web. Replacement of orthogonally stiffened plates by an equivalent orthotropic plate of constant thickness is appropriate, when the ribs are disposed symmetrically with respect to the middle plane of the plate. However, for stiffened plates having ribs only on one side of the plate which are asymmetric with respect to the mid-plane of the plate, the unknown location of the neutral surface increases the complexity of determining the orthotropic rigidity factors.

For such cases, the analysis of the problem should be extended to include the effect of the strain in the middle plane of the plate, which produces additional shear stress disregarded in Huber's method. Therefore, the Huber's theory of equivalent orthotropic plate presents only an approximate solution to the stiffened plate problem.

The presence of intermediate stiffeners makes the structure inhomogeneous for the estimation of overall bending deflection, stresses as well as natural frequencies and mode shapes. The analysis of skew cantilever plates, however, presents greater difficulty than that of rectangular ones due to the variation of stresses at the fixed end. As the skew angle increases, a concentration of stress occurs at the trailing edge, and numerical accuracy

diminishes. Hence for bending deflection and stress estimation in such inhomogeneous structures, the plate may be conceptually replaced by an equivalent homogeneous plate of constant thickness with equal stiffness characteristics. This is done by comparing the properties of the basic plate and the stiffener over a repeating interval of the tee cross-section. This concept is applicable provided the ratio of stiffener spacing, s, to plate boundary dimensions, a, is small enough (i.e., $s/a \ll 1$) to ensure approximate homogeneity of stiffness.

CHAPTER 2. LITERATURE REVIEW

2.1 Unstiffened Plates

Several methods of analyzing the stress variation along the root of the skew cantilever plate have been carried out by many investigators. The practical importance of the methods for the analysis of such structures is indicated by the large number of papers devoted to this subject. Although much of work has been done on dynamic analysis and for isotropic plates, only few papers are available on static analysis of composite plates as described in the following.

Employing the principle of least work, a study for the calculation of direct stress of swept cantilever plates of low aspect ratio is carried out by Coull [1]. He has assumed that the load and stress components may be represented with sufficient accuracy by a power series. It was noticed that the agreement between the theoretical and experimental results became poorer as the angle of sweep was increased, since the simple assumed stress polynomials become increasingly less able to deal adequately with the large edge values and the consequent high boundary layer stress gradients which are prescribed at the trailing edge. A Galerkin approach for such clamped swept-back plates in bending has been studied by Mukhopadhyay [2]. The stress singularity in swept cantilever isotropic plates has been studied by Somashekar and Prathap [3]. Torres et al. [4] developed a C^1 finite element family for Kirchhoff plate

bending problems. Dawe [5] conducted a finite element analysis of parallelogramic elements considering rhombic cantilever plate problems by use of consistent load method. A single Fourier series formulation was used by Kan and Ito [6] to obtain an analytical solution of unsymmetrical cross-ply rectangular plates with simply supported boundary conditions. The effect of shear deformations on the bending of rectangular plates with simply supported boundary conditions was studied by Salerno and Goldberg [7]. Rajaiah [8] has studied a direct method of solution for elastically restrained rhombic plates under uniform pressure and central concentrated loads employing simple collocation method for approximate satisfaction of boundary conditions.

2.2 Bending Analysis of Stiffened Plates

The earliest treatment of stiffened panels as orthotropic plates have been provided by Huber [9] and Pfluger [10]. Several technical papers have considered this concept by taking the equivalence of strain energies of the actual and its equivalent orthotropic plate. Hoppmann [11] and Hoppmann, et al. [12] have taken the rectangular and circular plates grooved on one and both sides as the ones shown in Fig. 2, and experimentally obtained the bending stiffness of the stiffened plate.

Huffington and Blackberg [13] gave the theoretical verification of the rigidity properties by the strain energy equivalence method. Huffington also conducted experiments to verify his theoretical results by taking stiffened

plates grooved on one side and on both sides as shown in the Fig. 3. Schade [14] has presented a bending theory for the stiffened ship bottom structures utilizing the orthotropic equivalent thickness plate principle as defined by Huber.
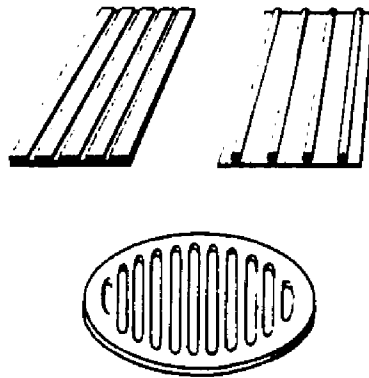
Fig. 2 Stiffened Experimental Plates

Cross Section of Plate
Grooved On One Side Only

Cross Section of Plate
Grooved On Both Sides
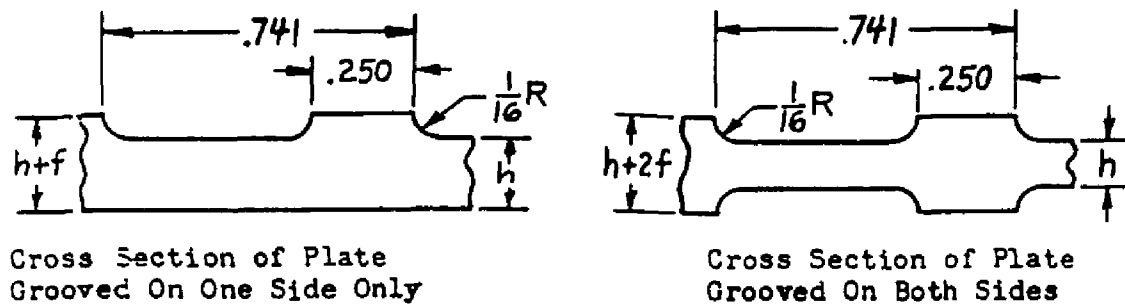
Fig. 3 Plates Grooved on One and Both Sides

A report by Smith, et al. [15] presented the theoretical estimation of the shift of the neutral axis and the effective stiffness added to the plate by a stiffener. The analysis of the shear-flexible orthotropic panels was carried out

by Karamanlidis and Agrawal [16]. Davis [17] and many other NASA projects have dealt with experimental and numerical analysis of graphite-epoxy stiffened panels using STAGS and other computer codes. The J-type composite Stiffeners used by them are shown in Fig. 4.

A numerical solution is presented by Wegmuller [18] based on the layered system of beam and plate elements to analyze the eccentrically stiffened plate as shown in Fig. 5. The layered plate model is attached to the layered beam model in order to describe the actual beam-plate model for isotropic elastic materials. A finite element analysis capable of determining the elastic-plastic response of complex shaped and loaded eccentrically stiffened plate structures is presented. There is an extensive literature of the buckling and post buckling behavior of stiffened plates and shells.
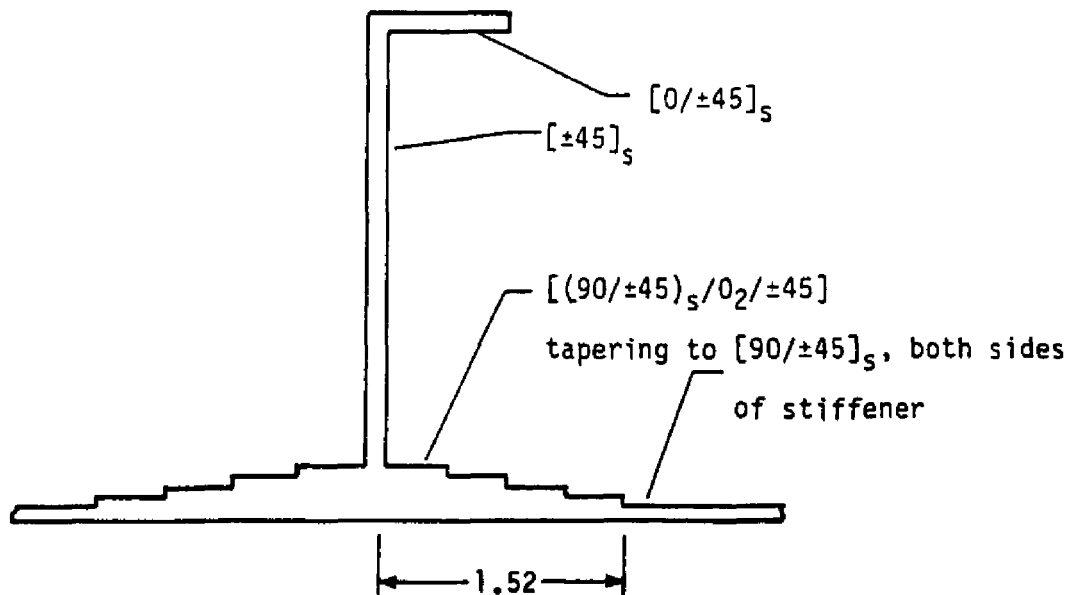
Fig. 4 The J-type Stiffener
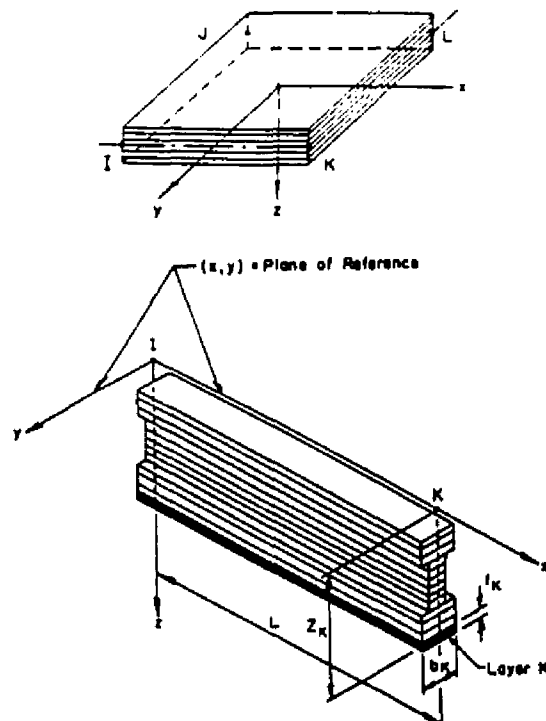
Fig. 5 Layered Beam and Plate Model

In recent years, numerous work has also been done at Lockheed Missiles and Space Research Center, Palo Alto. PANDA, a computer code has been developed at this Lockheed Research Laboratory by Bushnell [19, 20, 21] to create an interactive computer program for engineers which derives minimum weight design of stiffened panels under combined in plane loads N_x, N_y and N_{xy}. A minimum weight design of Tee-stiffened panels is also carried out by Bushnell and Bushnell [22] using the code PANDA2, which served as input to STAGS, a general purpose non-linear finite element code. STAGS is then used to evaluate the optimum design for buckling and post buckling of panels under in plane loads.

The non-linear equations for stiffened laminated panels modeled by plate and elements are derived by Sheinman [23] by applying the variational principle on the potential energy. These non-linear equations characterize the post buckling behavior of stiffened panels. Another numerical technique for large deflection elasto-plastic analysis of stiffened plates is presented by Koko and Olson [24] using super finite elements. New plate and beam finite elements are developed for the non-linear analysis of stiffened plate structures subjected to lateral pressure. Only one plate element per bay and one stiffener per span are considered and the results are compared with those of ADINA. Though their results seem reasonable, they are not close to ADINA stress distributions along a line perpendicular to the stiffener.

2.3 Vibration Analysis of Stiffened Plates

The vibrational analysis of laminated plates also have expanded position in the literature. A method of computing the natural frequencies of vibration of flat plates of arbitrary shape using the minimum energy principle is presented by Dawe [25]. He also has extended this method to include isotropic rectangular plates of variable thickness [26]. An analytical type solution based on the superposition method is developed by Gorman and Singal [27] for the free vibration frequencies and mode shapes of rectangular plates resting on arbitrarily located rigid point supports. Singh et al. [28] have studied the presence of bending extension coupling in antisymmetric cross-ply plates

subjected to large amplitude free vibration. It was also shown that the extensively used perturbation method fails depending on the severity of the bending extension coupling term. The effect of fiber orientation and boundary conditions on the vibration behavior of orthotropic rhombic plates was studied by Malhotra et al. [29] using parallelogramic finite elements and different skew angles. Their results indicate that for a given skew angle and boundary conditions, the fiber orientation of such plates can be chosen to achieve the desired natural frequency.

Krishnan and Deshpande [30, 31] have studied the lowest natural frequency of free vibration of trapezoidal isotropic plates and plates made up of composite materials by using the well known D.K.T. plate bending element. Their study reveals that it is possible to nullify the twisting inherent in the plate due to the asymmetry in the plan form by choosing specific fiber orientation depending on the skew angle. They have also observed that the decrease in the fundamental frequency due to the shear deformation is a function of skew angle too. A linear analysis was presented by Bert and Mayberry [32] for determining the natural frequencies of vibration of laminated anisotropic rectangular plates by use of Rayleigh-Ritz energy method . Dawe and Roufaeil [33] have also used the Rayleigh-Ritz method to predict the natural frequencies of flexural vibration of square plates based on Mindlin plate theory. An isoparametric quadrilateral plate bending element was introduced and its use for the free vibration analysis of both thick and

thin plates of orthotropic material was examined by Rock and Hinton [34]. The governing equations of motion for a laminated plate consisting of an arbitrary number of fiber reinforced composite material layers was derived by Alam and Asnani [35] using the variational principle. Srinivas and Rao [36] presented a unified exact analysis for the static and dynamics of simply supported thick orthotropic rectangular plates and laminates. For free vibration of plates, their analysis yields a triply infinite spectrum of frequencies instead of only one doubly infinite spectrum by thin plate theory.

In recent years Chen and Liu [37] have applied the Mindlin plate theory to study the static deflections and natural frequencies of isotropic, orthotropic/laminated composite plates using a Levy type solution. The influence of aspect ratio, thickness/length ratio, fiber orientation angle, laminate-layer arrangement and ratio of the elastic moduli were also investigated.

There are a few methods available in the literature regarding the natural frequency analysis of stiffened plates. Kirk [38] has studied the natural frequencies of the first symmetric and first antisymmetric modes of a simply-supported rectangular plate reinforced by a single integral stiffener placed along one of its center lines. Their results show a maximum increase in frequency for the symmetric mode of about three times, whereas the frequency of the antisymmetric mode is generally lower than that of the unstiffened plate. An increase in the symmetric mode frequency and a

decrease in the antisymmetric mode frequency makes it possible for both modes to possess equal frequencies for a particular (a/b) ratio and certain size of stiffener. Stiffened plates have also found their application in the field of acoustics. Fahy and Wee [39] have carried out some experiments on stiffened mild steel plates under acoustic excitation. Here, the stiffeners are added to the plate either for reasons of static stability or to reduce the vibration. They have found that the point attachments such as rivets can be preferable to line attachments such as welds.

Free vibration characteristics of rectangular stiffened plates having a single stiffener have been studied by Aksu and Ali [40] using finite difference method along with a variational technique to minimize the total energy of the stiffened plate. A stiffness-type analysis of the vibration of rectangular stiffened plates having stiffeners in one direction was studied by Long [41]. Bhandari et al. [42] presented an approximate analysis using Lagrange's equation to obtain the natural frequencies and mode shapes of integrally stiffened skew plates. The vibration properties of composite materials and structures was studied by Lu et al. [43] and they defined a criterion for performance comparison between composite materials and conventional materials. A super finite element was presented by Koko [44] for non-linear static and dynamic analysis of stiffened plate structures. A study of the effect of stiffness discontinuities and structural parameters on the response of continuous filament grid stiffened flat panels was recently presented in 1993

by Ambur and Rehfield [45]. Non-solid stiffener cross-section such as a foam-filled blade or hat with a 0-deg dominant cap as shown in the following Fig. 6, are found structurally very efficient for wing and fuselage applications.
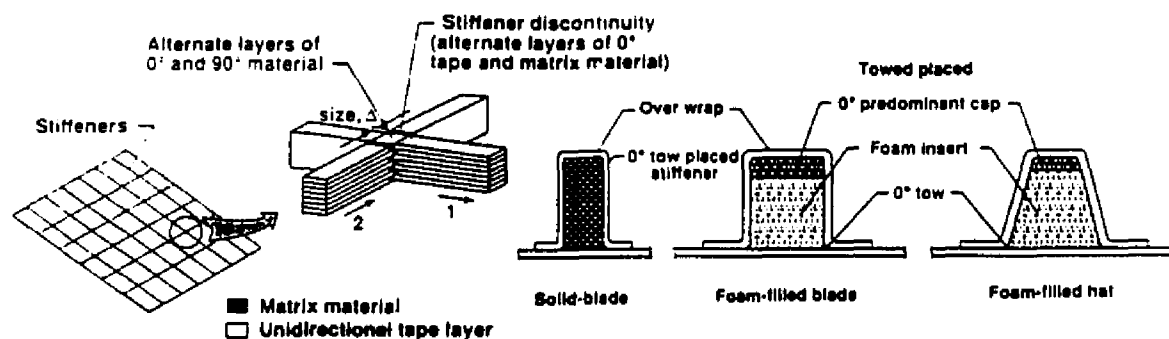
Fig. 6 Foam Type Stiffener Cross-Sections

Liao and Sun [46] have investigated the flutter instability of stiffened and non-stiffened laminated composite plates and shells subjected to aerodynamic forces in the supersonic flow. The natural frequency, critical dynamic pressure and corresponding flutter mode shapes are obtained by them. An experimental and analytical study of the postbuckling behavior of stiffened graphite-epoxy panels, loaded in pure shear are presented by Hachenberg and Kossira [47]. Kassapoglou and DiNicola in 1992 [48] have developed solutions for the stresses at the skin stiffener interface of composite stiffened panels, These solutions can be used to screen design candidates and to obtain an accurate idea of the stress field near dropped plies without resorting to time-consuming finite element or other solutions. The typical assembly of their skin stiffener interface is shown in Fig. 7.
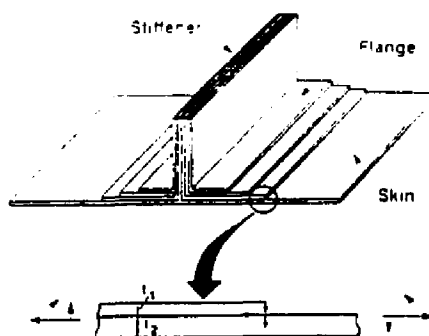
Fig. 7 Skin Stiffener Geometry

Free vibration characteristics of stiffened plates possessing symmetrical

stiffeners have been investigated by Mukherjee and Mukhopadhyay [49] using

a finite element method. Their formulation was based on Mindlin's hypothesis.

The analysis for the free vibration of a stiffened shallow shell numerically by

the collocation method within the frame of the theory of classical thin

orthotropic shallow shells has been carried out by Mecitoglu and Dokmeci [50].

The vibration characteristics of unidirectionally and orthogonally stiffened

shallow shells have also been studied by them for various geometrical and

material parameters. Mequita and Kamat [51] have studied the simultaneous

design and control of stiffened laminated composite structures by the

minimization of an appropriate performance index. A continuum-based

laminated stiffened shell element is used by Liao and Reddy [52] to investigate

the static, geometrically non-linear response of composite shells. The element

is developed from a three-dimensional continuum element based on the incremental total Lagrangian formulation.

2.4 Motivation for the Present Work

The literature review reveals that, in most of the cited references, the analysis has been done only for rectangular cases where stiffeners are parallel to the boundaries of the plate. Also their material selections are limited to the use of isotropic materials only. Though there are a few published works on stiffened plates made of composite materials, they are again for only rectangular plates. But as mentioned earlier, there are wide uses of skew plates where the stiffeners are not parallel to the boundaries of the plate.

Composite materials have found wide applications in various fields in the present scientific world. Since the skew composite plates have high strength/weight ratio, high stiffness and high static and dynamic strength, the development of a method for their bending and vibrational analysis may add further impetus towards the advancement of this technology. The number of researchers working presently on this topic indicates its importance in the field. Hence, in the present work, the motivation is to develop a method of analysis for the static and dynamic analysis of the fiber reinforced composite stiffened skew plates. An attempt has been made to analyze such plates with various angles of sweep and their stiffeners making different angles with the plate boundaries.

CHAPTER 3. CURRENT RESEARCH WORK

3.1 Objective of the Present Work

The objective of this study is to develop a method of analysis for the stiffened composite plates, validate the method by experiment, and to apply this to bending and vibration of fiber reinforced composite skew plates. Analytical solutions of stiffened plates with geometric and material non-linearity subjected to any type of loading is very difficult, though not impossible. Recently, the finite element method is the most commonly used numerical technique to analyze such structures.

As a first step to the current research, a finite element investigation based on the principle of minimum strain energy was carried out to study the stress variation around the root triangle. Parallelogramic plate bending elements are considered with twelve degrees of freedom per element. The stiffness matrices for the isotropic as well as fiber reinforced composite plate elements are developed based on the assumed displacement function. The computer code was written for deflection analysis for isotropic as well as laminated composite swept back plates. Experiments were conducted by taking specific angles of sweep and the results were compared with other existing results. The effect of fiber orientation on the stress singularity has also been studied for a specific swept cantilever composite plate. It has been thought that the excess deflection at the rear tip of a cantilever plate can be

18

reduced by applying stiffeners along the length of the plate. These stiffeners can also reduce the stresses at the root drastically. Here the motivation was to develop a method of analyzing the stiffened plate not only to reduce the deflections, but also to control the natural frequencies of such structures.

Having studied the bending analysis of unstiffened plates, the finite element approach is extended to include Huber's theory of equivalent orthotropic plate for the calculation of the deflections and stresses of stiffened composite plates. A short description of the Huber's theory for stiffened plates is given in the next page. The results of this approach are first confirmed by comparing with the available results for rectangular plates. Experiments using aluminum (6061 T6) and Scotchply composites with cross-ply and angle-ply laminates are also conducted to verify the analytical results. The results of the bending experiment are found to be in good agreement with the present analytical results. Cantilever and simply supported type boundary conditions were included in the analysis and an optimized angular stiffener for a particular swept back panel is achieved.

The above method is only suitable for the plates with many stiffeners having a very close stiffener spacing. So another finite element formulation was carried out by combining a nine node plate element with a three noded beam element. This element can be used even for single stiffened plate with any orientation of the stiffener. This method was used to find the natural frequencies and mode shapes calculation of stiffened laminated plates. Results

of rectangular and skew stiffened plates are computed and compared with those available in literature. Fundamental frequencies for Scotchply composite laminates are evaluated experimentally and are compared with the present analytical results and NASTRAN results. The dynamic user interface STAR software was used to obtain the first few natural frequencies experimentally. A finite element analysis for a three dimensional composite wing with ribs and stiffeners was also carried out for its natural frequencies.

A brief review of the Huber's theory will be necessary here. The differential equation of equilibrium for isotropic plate bending problem is given as:

$$\frac{\partial^4 w}{\partial x^4} + 2\frac{\partial^4 w}{\partial x^2 \partial y^2} + \frac{\partial^4 w}{\partial y^4} = \frac{q}{D} \tag{1}$$

where w is the deflection of plate, q is the uniform pressure applied on the plate, and D is the flexural rigidity. But for an anisotropic plate, this reduces to

$$D_x\frac{\partial^4 w}{\partial x^4} + 2H\frac{\partial^4 w}{\partial x^2 \partial y^2} + D_y\frac{\partial^4 w}{\partial y^4} = q \tag{2}$$

This is the general differential equation of the plate, deduced by Huber and known in the technical literature as "Huber's Equation". The value $2H$ is called "the effective torsional rigidity". The basic assumption proposed by Huber for estimating overall bending deflections and bending stresses in a stiffened plate, was to replace such a plate by an equivalent orthotropic plate

of constant thickness having the same stiffness characteristics. The previous theoretical and experimental investigations indicate that this theory is applicable under the following provisions:

a)   The ratios of stiffener spacing to plate boundary dimensions are small enough to insure approximate homogeneity of stiffness.

b)   It is assumed that the rigidities are uniformly distributed in both directions of the plate.

c)   Flexural and twisting rigidities do not depend on the boundary conditions of the plate or on the distribution of the vertical load.

d)   A perfect bond exists between plate and stiffener.

This concept of elastic equivalence for structural orthotropy is explained diagrammatically in Fig. 8. The flexural and twisting constants D_x, D_y and H are conceived as applying to a homogeneous orthotropic plate of constant thickness which is equivalent to the actual plate-stiffener combination. The precise meaning of the term "equivalent" requires careful definition, since the orthotropic plate can not be equivalent to the stiffened plate in every respect. However, on the basis of the experimental tests and analytical studies, Huffington and Blackberg [13], based on their theoretical and experimental investigation, state that the orthotropic plate theory is applicable to stiffened plates, provided that the ratios of stiffener spacing to the plate boundary

dimensions are small enough , or $(s/a < 1)$. In admitting the applicability of the orthotropic plate theory to the problem of stiffened plates, the next thing s to consider the flexural rigidities.
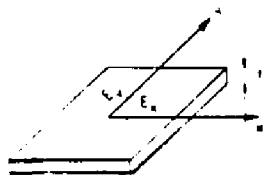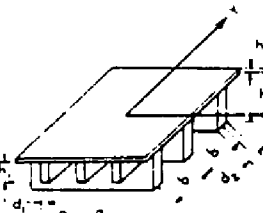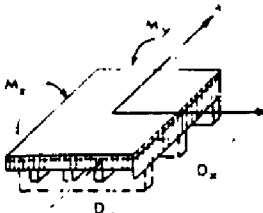
NATURALLY ORTHOTROPIC PLATE	TECHNICALLY ORTHOTROPIC PLATE	EQUIVALENT ORTHOTROPIC PLATE

Fig. 8 Principle of Elastic Equivalence [13]

For a plate reinforced symmetrically with respect to its middle plane, as shown in Fig. 9, the flexural rigidities are

$$D_x = H = \frac{Eh^3}{12(1-v^2)}$$

$$D_y = \frac{Eh^3}{12(1-v^2)} + \frac{EI}{a_1}$$

(3)

and for the plate with stiffeners only on one side of the plate and in one direction (Fig. 9), the rigidities are
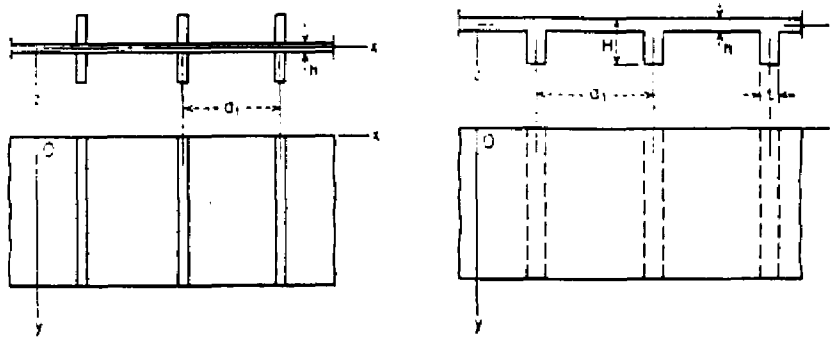
Fig. 9 Symmetrically and Asymmetrically Stiffened Plates

$$D_x = \frac{Ea_1 h^3}{12(a_1 - t + a^3 t)}$$

$$D_y = \frac{EI}{a_1} \tag{4}$$

$$D_{xy} = D'_{xy} + \frac{C}{2a}$$

where I is the moment of inertia about the middle of plate, D_{xy} and D'_{xy} are the torsional rigidities of the slab with and without the ribs respectively, and C the torsional rigidity of one rib.

3.2 Scope of the Proposed Research

The goal of this study can be summarized as follows:

1)   To study the stress distribution along the root of a skew cantilever unstiffened composite plate under bending load.

2)   Extend the finite element method developed for the previous study to

analyze stiffened skew plates under bending load by application of the Huber's theory of equivalent orthotropic plate.

3) Conduct experiments on isotropic as well as fiber reinforced composite plates under transverse loading for both cases of unstiffened and stiffened plates to validate the analytical approach.

4) Develop a finite element to analyze stiffened plates with low aspect to stiffener spacing ratio and study the natural frequencies and mode shapes of stiffened composite skew plates.

5) Apply the second finite element model to rectangular stiffened plates and compare the natural frequencies with those from literature results.

6) Carry out experimental investigation for studying natural frequencies and mode shapes of stiffened laminated composite skew panels using STAR pre and post processor.

7) Obtain the natural frequencies and mode shapes of the composite plates by use of finite element software package MSC/NASTRAN.

8) Model in finite element a three dimensional aircraft wing consisting of skin, ribs and stiffeners and analyze for the natural frequencies.

CHAPTER 4. BENDING ANALYSIS OF STIFFENED PLATE

4.1 Plate Bending Finite Element Formulation

- The plate bending problem is currently analyzed using an assumed displacement function as an incomplete third order polynomial with the stiffness matrix as a function of flexural stiffness. A parallelogramic plate bending element with three degrees of freedom at each node is considered. The plate element with dimensions $a \times b$, the stiffener angle θ and the plate skew angle γ are shown in Fig. 10. The node and element numberings are shown in Fig. 11.

The three degrees of freedom are

$$
\begin{aligned}
w \quad &- \quad \textit{The displacement along the vertical } z\textit{-direction} \\
\frac{\partial w}{\partial \xi} \quad &- \quad \textit{The rotational deformation about } \eta \textit{ axis} \\
\frac{\partial w}{\partial \eta} \quad &- \quad \textit{The rotational deformation about } \xi \textit{ axis}
\end{aligned}
\tag{5}
$$

A fourth-order polynomial with twelve unknown constants, A_i (i = 1,12), has been chosen to fit the displacement function for the element as

$$
\begin{aligned}
w = A_1 + A_2\frac{\xi}{a} + A_3\frac{\eta}{b} + A_4\frac{\xi^2}{a^2} + A_5\frac{\xi\eta}{ab} + A_6\frac{\eta^2}{b^2} + A_7\frac{\xi^3}{a^3} \\
+ A_8\frac{\xi^2\eta}{a^2b} + A_9\frac{\xi\eta^2}{ab^2} + A_{10}\frac{\eta^3}{b^3} + A_{11}\frac{\xi^3\eta}{a^3b} + A_{12}\frac{\xi\eta^3}{ab^3}
\end{aligned}
\tag{6}
$$

or in a short form

$$
w = \{m\}^T\{A\}
\tag{7}
$$

θ = Stiffener Angle
γ = Plate Skew Angle
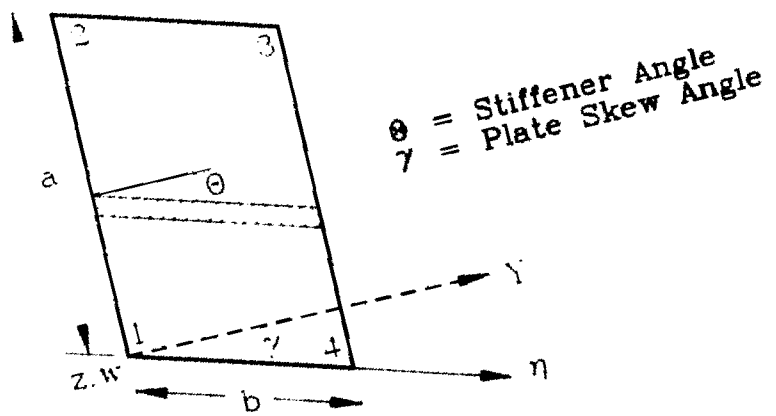
Fig. 10 The Plate Element
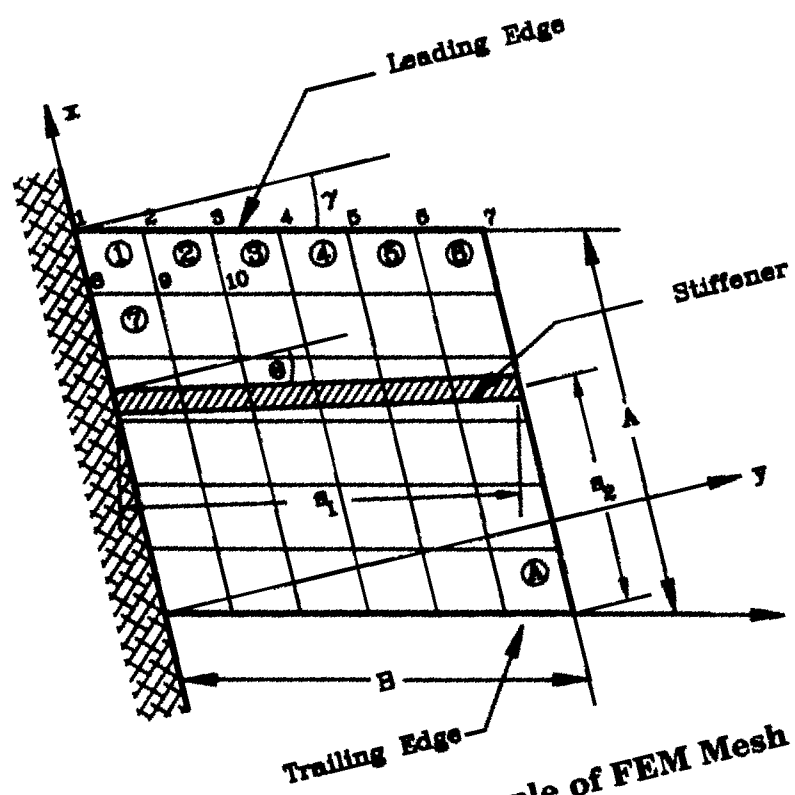
Fig. 11 Example of FEM Mesh

where

$$\{m\}^T = \{1, \frac{\xi}{a}, \frac{\eta}{b}, \frac{\xi^2}{a^2}, \frac{\xi\eta}{ab}, \frac{\eta^2}{b^2}, \frac{\xi^3}{a^3}, \frac{\xi^2\eta}{a^2b}, \frac{\xi\eta^2}{ab^2}, \frac{\eta^3}{b^3}, \frac{\xi^3\eta}{a^3b}, \frac{\xi\eta^3}{ab^3}\} \tag{8}$$

and

$$A = \{A_1, A_2, A_3, A_4, A_5, A_6, A_7, A_8, A_9, A_{10}, A_{11}, A_{12}\}^T. \tag{9}$$

The coordinate transformation is done by

$$\begin{aligned} \xi &= x + y\tan\gamma \\ \eta &= y\sec\gamma \end{aligned} \tag{10}$$

Differentiating Eq. 6, the twelve degrees of freedom of an element can be written as

$$\{V\} = [B]\{A\} \tag{11}$$

where $\{V\}$ is the twelve elemental displacements given by

$$\begin{aligned} \{V\} &= \{w_1, b\psi_1, a\chi_1, w_2, b\psi_2, a\chi_2, w_3, b\psi_3, a\chi_3, w_4, b\psi_4, a\chi_4\}^T \\ \textit{with} \qquad \psi &= \frac{\partial w}{\partial \eta}, \quad \chi = \frac{\partial w}{\partial \xi} \end{aligned} \tag{12}$$

and $[B]$ is a constant matrix of size (12 x 12). This matrix is obtained by taking the first and second derivatives of the displacement function w as given in the equation 6 and then divided by the plate element edges a and b and expressed as

$$[B] = \begin{vmatrix} 1 & 0 & 0 & 0 & 0 & 0 & 0 & 0 & 0 & 0 & 0 & 0 \\ 0 & 0 & 1 & 0 & 0 & 0 & 0 & 0 & 0 & 0 & 0 & 0 \\ 0 & 1 & 0 & 0 & 0 & 0 & 0 & 0 & 0 & 0 & 0 & 0 \\ 1 & 1 & 0 & 1 & 0 & 0 & 1 & 0 & 0 & 0 & 0 & 0 \\ 0 & 0 & 1 & 0 & 1 & 0 & 0 & 1 & 0 & 0 & 1 & 0 \\ 0 & 1 & 0 & 2 & 0 & 0 & 3 & 0 & 0 & 0 & 0 & 0 \\ 1 & 1 & 1 & 1 & 1 & 1 & 1 & 1 & 1 & 1 & 1 & 1 \\ 0 & 0 & 1 & 0 & 1 & 2 & 0 & 1 & 2 & 3 & 1 & 3 \\ 0 & 1 & 0 & 2 & 1 & 0 & 3 & 2 & 1 & 0 & 3 & 1 \\ 1 & 0 & 1 & 0 & 0 & 1 & 0 & 0 & 0 & 1 & 0 & 0 \\ 0 & 0 & 1 & 0 & 0 & 2 & 0 & 0 & 0 & 3 & 0 & 0 \\ 0 & 1 & 0 & 0 & 1 & 0 & 0 & 0 & 1 & 0 & 0 & 1 \end{vmatrix} \qquad (13)$$

Now the bending strain energy is given by

$$U = \frac{1}{2}\int\int_A \{C\}^T[D]\{C\} \, dx \, dy \qquad (14)$$

where

$$\{C\} = \{\frac{\partial^2 w}{\partial x^2} \quad \frac{\partial^2 w}{\partial y^2} \quad \frac{\partial^2 w}{\partial x \partial y}\}^T \qquad (15)$$

and $[D]$ is the bending stiffness matrix of the equivalent orthotropic plate.

The curvature vector $\{C\}$ can now be written as

$$\{C\} = [G]\{C_{ob}\} = [G][E]\{A\} \qquad (16)$$

where $\{C_{ob}\}$ is the oblique curvature, $[G]$ is related to the skew angle γ, and $[E]$ is related to the transformed coordinates as follows:

$$\{C_{ob}\} = \{\frac{\partial^2 w}{\partial \xi^2} \quad \frac{\partial^2 w}{\partial \eta^2} \quad \frac{\partial^2 w}{\partial \xi \partial \eta}\}^T \qquad (17)$$

$$[G] = \begin{bmatrix} 1 & 0 & 0 \\ \dfrac{\sin^2\gamma}{\cos^2\gamma} & \dfrac{1}{\cos^2\gamma} & \dfrac{2\sin\gamma}{\cos^2\gamma} \\ \dfrac{\sin\gamma}{\cos\gamma} & 0 & \dfrac{1}{\cos\gamma} \end{bmatrix} \tag{18}$$

and

$$[E] = \begin{bmatrix} 0 & 0 & 0 & \dfrac{2}{a^2} & 0 & 0 & \dfrac{6\xi}{a^3} & \dfrac{2\eta}{a^2 b} & 0 & 0 & \dfrac{6\xi\eta}{a^3 b} & 0 \\ 0 & 0 & 0 & 0 & 0 & \dfrac{2}{b^2} & 0 & 0 & \dfrac{2\xi}{ab^2} & \dfrac{6\eta}{b^3} & 0 & \dfrac{6\xi\eta}{ab^3} \\ 0 & 0 & 0 & 0 & \dfrac{1}{ab} & 0 & 0 & \dfrac{2\xi}{a^2 b} & \dfrac{2\eta}{ab^2} & 0 & \dfrac{3\xi^2}{a^3 b} & \dfrac{3\eta^2}{ab^3} \end{bmatrix} \tag{19}$$

Hence the strain energy of Eq. 14 can be written as

$$U = \frac{1}{2}\iint_A \{A\}^T [E]^T [G]^T [D][G][E]\{A\}\ dxdy \tag{20}$$

Using Eq. 11 as

$$\{A\} = [B]^{-1}\{V\} \tag{21}$$

the strain energy reduces to

$$U = \frac{1}{2}\{V\}^T (\cos\gamma [B^{-1}]^T \int_0^b \int_0^a [E]^T [G]^T [D][G][E]\ d\xi d\eta [B^{-1}])\{V\} \tag{22}$$

or

$$U = \frac{1}{2}\{V\}^T [K]\{V\} \tag{23}$$

where

$$[K] = \cos\gamma [B^{-1}]^T \int_0^b \int_0^a [E]^T [G]^T [D][G][E] \, d\xi d\eta \, [B^{-1}] \qquad (24)$$

is the stiffness matrix having the only unknown bending stiffness $[D]$.

This $[D]$ matrix for a uniform thick isotropic plate is

$$[D] = \frac{Eh^3}{12(1-v^2)} \begin{bmatrix} 1 & v & 0 \\ v & 1 & 0 \\ 0 & 0 & 2(1-v) \end{bmatrix} \qquad (25)$$

and for a uniform thick laminated composite plate is (Vinson and Sierakowski [53])

$$[D] = \begin{bmatrix} D_{11} & D_{12} & D_{16} \\ D_{12} & D_{22} & D_{26} \\ D_{16} & D_{26} & D_{66} \end{bmatrix} \qquad (26)$$

where

$$D_{ij} = \frac{1}{3} \sum_{k=1}^N (\overline{Q_{ij}})_k (z_k^3 - z_{k-1}^3) \qquad (27)$$

($i = 1, 2, 6; j = 1, 2, 6;$ N = number of layers)

The stiffnesses $\overline{Q}_{ij}$ are given as

$$\overline{Q_{11}} = Q_{11}\cos^4\theta + 2(Q_{12} + 2Q_{66})\sin^2\theta\cos^2\theta + Q_{22}\sin^4\theta$$
$$\overline{Q_{12}} = (Q_{11} + Q_{22} - 4Q_{66})\sin^2\theta\cos^2\theta + Q_{12}(\sin^4\theta + \cos^4\theta)$$
$$\overline{Q_{22}} = Q_{11}\sin^4\theta + 2(Q_{12} + 2Q_{66})\sin^2\theta\cos^2\theta + Q_{22}\cos^4\theta$$
$$\overline{Q_{16}} = (Q_{11} - Q_{12} - 2Q_{66})\sin\theta\cos^3\theta + (Q_{12} - Q_{22} + 2Q_{66})\sin^3\theta\cos\theta \qquad (28)$$
$$\overline{Q_{26}} = (Q_{11} - Q_{12} - 2Q_{66})\sin^3\theta\cos\theta + (Q_{12} - Q_{22} + 2Q_{66})\sin\theta\cos^3\theta$$
$$\overline{Q_{66}} = (Q_{11} + Q_{22} - 2Q_{12} - 2Q_{66})\sin^2\theta\cos^2\theta + Q_{66}(\sin^4\theta + \cos^4\theta)$$

where

$$Q_{11} = \frac{E_1}{(1-v_{12}v_{21})}$$

$$Q_{12} = \frac{v_{12}E_2}{(1-v_{12}v_{21})}$$

$$Q_{22} = \frac{E_2}{(1-v_{12}v_{21})}$$ (29)

$$Q_{66} = G_{12}$$

and

$$v_{21}E_1 = v_{12}E_2$$ (30)

Now, the $[D]$ matrix for a stiffened plate can be taken from Timoshenko and

Woinowsky-Krieger [55] for a plate with stiffeners only in one direction and only on

one side of the plate as

$$D_{11} = D_x = \frac{E_x I}{s}$$

$$D_{22} = D_y = \frac{E_y h^3}{12(s-t+\alpha^3 t)}$$ (31)

$$D_{66} = D_{xy} = D'_{xy} + \frac{C}{2s}$$

$$D_{12} = D_{16} = D_{26} = 0$$

where E_x and E_y = Young's Modulus in the x and y directions,

I = moment of inertia of the repeating tee cross-section,

s = stiffener spacing,

h = plate thickness at each groove,

t = width of the stiffener,

C = torsional rigidity of the stiffener,

D'_{xy} = twisting rigidity of the plate without stiffeners, and

α is the ratio of plate thickness at a groove to total thickness.

The stiffness matrix has been derived from Eq. 24, and as per Castigliano's theorem

$$\frac{\partial U}{\partial V_i} = F_i \tag{32}$$

the stiffness matrix reduces to

$$\{F\} = [K]\{V\} \tag{33}$$

where $\{F\}$ is the set of nodal forces given by:

$$\{F\} = \{w_1, \frac{M_{\psi 1}}{b}, \frac{M_{\chi 1}}{a}, \dots \dots \frac{M_{\chi 4}}{a}\}^T \tag{34}$$

The uniformly distributed load, q, is considered as a set of consistent nodal

loads

$$N = q \cos\gamma [B^{-1}]^T \int_0^b \int_0^a \{m\}\, d\xi d\eta \tag{35}$$

giving

$$N = \frac{q\ ab\ \cos\gamma}{24} \{6,1,1,6,1,-1,6,-1,-1,6,-1,1\}^T \tag{36}$$

Equation (33) has been solved after assembling the stiffness and load matrices of all the elements and applying appropriate boundary conditions. Having obtained the deflections and rotations at the nodal points, one can

obtain the strains $\{\epsilon\}_e$ and stresses $\{\sigma\}_e$ at any point using classical theory from the following relationship:

$$\{\epsilon\}_e = -\{C\} = -[G][E][B^{-1}]\{V\}_e \qquad (37)$$

$$\{\sigma\}_e = z[D]\{\epsilon_e\} \qquad (38)$$

where z is the distance of the stress point from the neutral plane.

The following steps summarize the solution procedure for the skew plate analysis using the above theory. The elemental stiffness matrix is first obtained from Eq. (24), and the skewness of the plate γ is provided by the axis transformation from x, y to ξ, η as per Eq. 10. The bending stiffness $[D]$ for the equivalent orthotropic plate is then calculated per Eq. 30. The $[D]$ matrix for orthotropic cross-ply and angle-ply composites is obtained from Lekhnitskii [54]. For stiffeners making an angle θ with the boundary, the bending stiffness $[D]$ of Eq. 30 is calculated by a coordinate transformation and then substituted in the previously obtained elemental stiffness matrix. The uniformly distributed transverse load, q, is considered as consistent nodal loads and the elemental loads are calculated as per Equation (35). Having obtained the load and stiffness matrices, a finite element program is developed to solve the unknown displacements of Eq. (33), and to obtain the related strains and stresses. A typical example of the nodes and elements of the finite element mesh is shown in Fig. 11.

4.2 Experimental Approach

4.2.1 Static Analysis of Unstiffened Skew Plate

To compare and validate the analytical results, experiments are conducted on both isotropic (Aluminum 6061 T6) and Scotchply fiber glass composite plates. As a preliminary test towards the proposed research, experiment was conducted for rhombic isotropic plate of angle of sweep 30". The finite element results are compared with the experimental ones. The dimensions with material properties of the isotropic and composite plates under consideration are listed in Table 1. One edge of the test plate was clamped firmly to a support bar as shown in the Fig. 12. Rectangular rosettes of strain gauges are used for measuring the strains at the root of the skew cantilever plate. These rosettes of strain gauges were connected to a 10 channeled strain indicator. Load is applied on the plate in steps and the strains were measured each time. Three dial gauges were also used at the free end of the cantilever plate to measure the deflections.

4.2.2 Static Analysis of Stiffened Plate

Having validated the results of the unstiffened plate, the next step is to look forward for experiments of stiffened plates. Three types of tests were conducted with arbitrarily chosen stiffened plates for the comparison of theoretical and experimental results. One of these plates was isotropic (aluminum 6061 T6), and the remaining two were Scotchply glass-epoxy

orthotropic composite plates consisting of thirteen alternating plies with fibers [0°/90°] and [±45°]. The properties for each plate are listed in Table 1. Square plates with simply supported boundary conditions were chosen for simplicity of the experiment. Grooves were machined on one side of these plates to produce the necessary stiffening configuration. Dial gauges were utilized to measure the deflections at three different locations, including the maximum deflection point located at the plate centerline. Eight strain gauges, six on top and two on the bottom of the plate, were attached to measure the strains in two principal directions. Details of specific stiffening geometries, including dial gauge and strain gauge locations for these plates may be found in Table 1 and Fig. 13.

The comparison of strain along the root of the plate for experiment and finite element results are plotted in Fig. 14. The linear strains ε_x and ε_y are obtained directly from the experiment whereas the shear strain v_{xy} were not measured from the experiment. The values of shear strains plotted in Fig. 14 are the ones calculated from the experimental linear strains. The stiffener angle and the plate skew angle (not necessarily same) are varied for different plates and the results are compared. The dial gage deflections for different loading cases are measured and are tabulated later in the results and discussion section.

Table 1. Material Properties and Plate Dimensions

Serial No.	Properties	Symbol Used	Aluminum	Composite
1	Young's Modulus	E	$0.7 \times 10^6 kg/cm^2$	-
2	Poisson's Ratio	v	0.3	-
3	Length of plate	a	30.0 cm	30.0 cm
4	Breadth of plate	b	30.0 cm	30.0 cm
5	Plate Thickness	H	0.32 cm	0.325 cm
6	Thickness at groove	h	0.19 cm	0.200 cm
7	Groove Depth	d	0.13 cm	0.125 cm
8	Width of Stiffener	t	2.5 cm	2.5 cm
9	Stiffener Spacing	s	5.0 cm	5.0 cm

For Scotchply Composite

$$E_{11} = 39.3 \ GPa$$

$$E_{22} = 8.30 \ GPa$$

$$v_{12} = 0.26$$

$$G_{12} = 4.14 \ GPa$$

Specific Gravity = 1.85

Resin Content = 38 % (by weight)
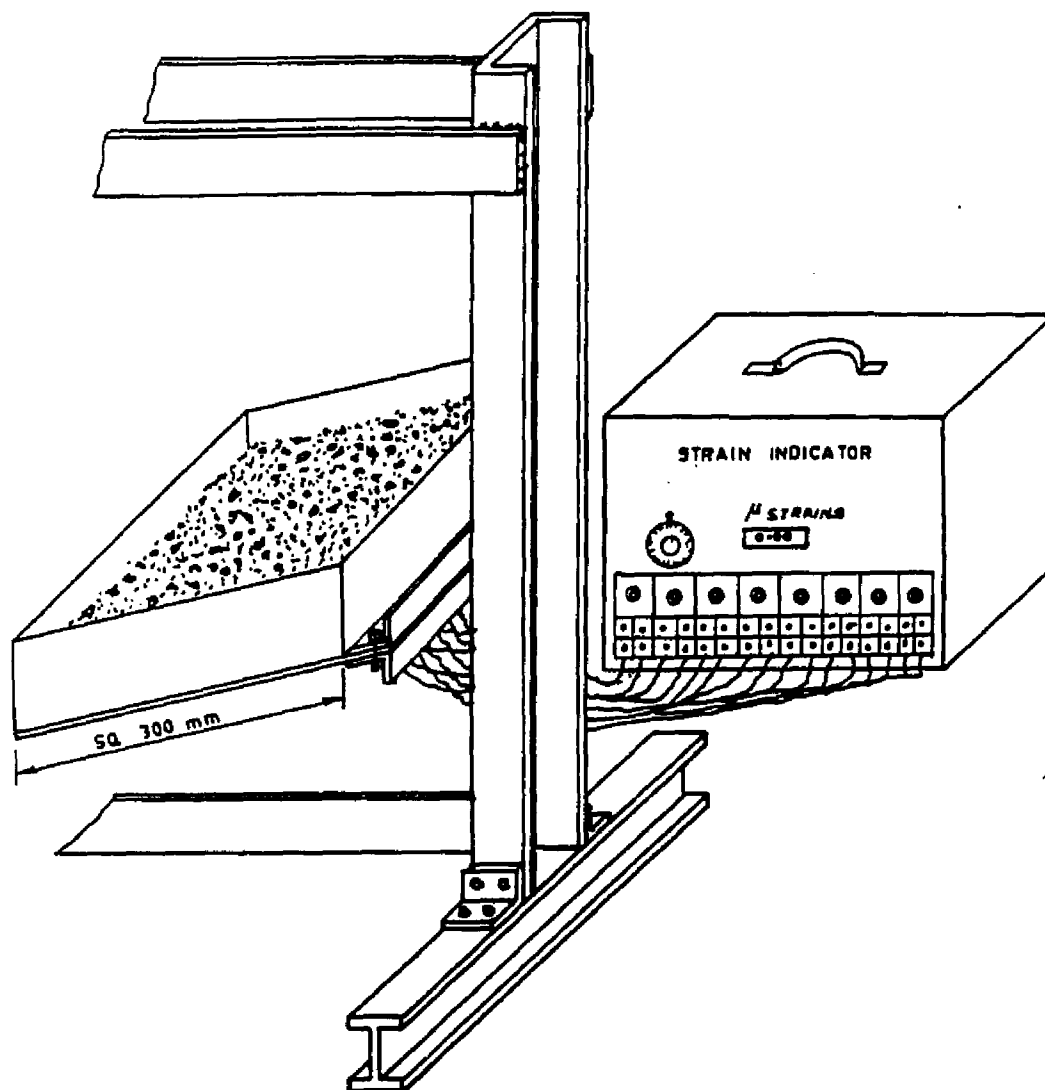
Fig. 12 Experimental Setup for Unstiffened Skew Plate
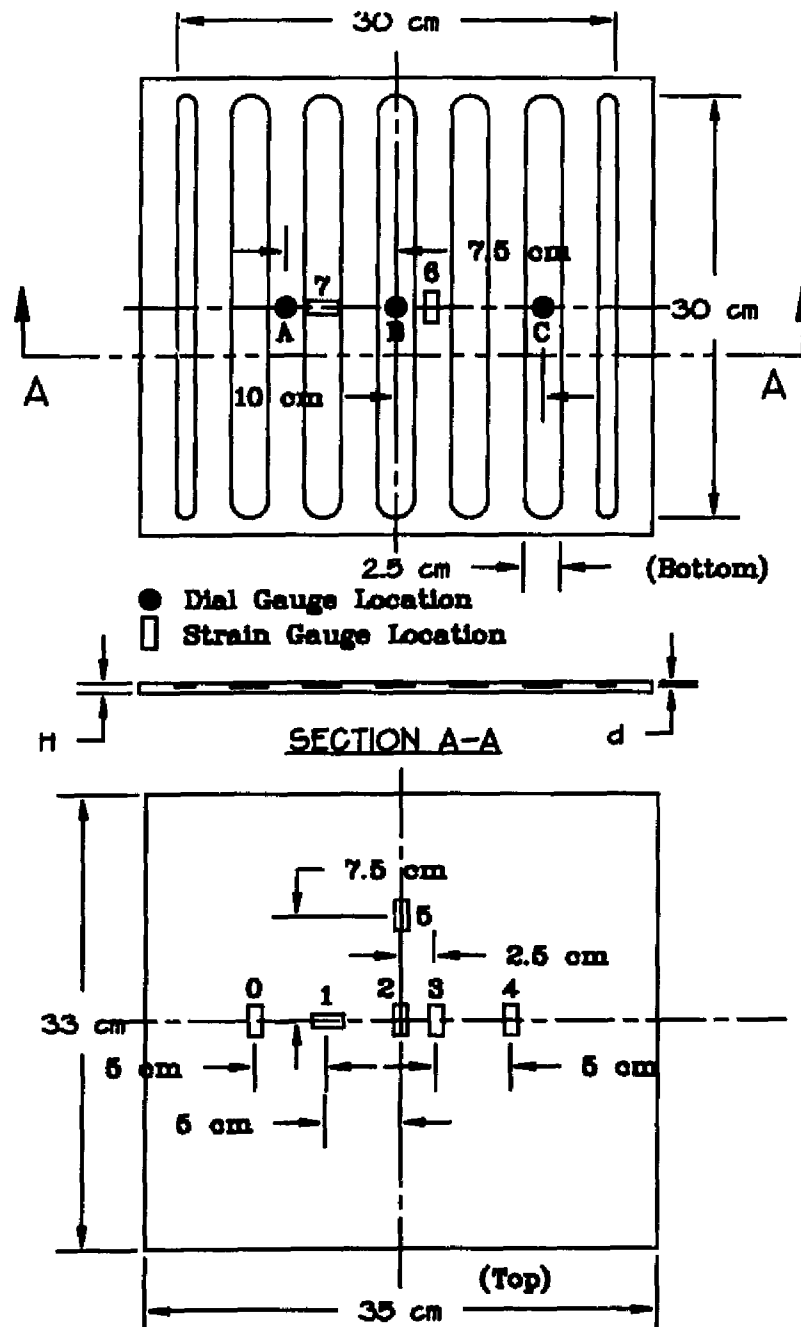
Fig. 13 Test Specimen of Stiffened Plate

4.3 Results and Discussion for Bending Analysis

A quarter plate with 81 elements has been considered for bi-symmetric plates, and a full plate with 78 elements has been taken for unsymmetric inclined plates. A finite element program has been developed to assemble the elemental stiffness and load matrices calculated above for all elements resulting in a set of simultaneous equations given by Eq. 33. Two types of boundary conditions, cantilever and simply supported, have been applied to the above set of simultaneous equations for the boundary nodes. These equations are solved by using Gaussian elimination, resulting in the nodal displacements. Having obtained the deflections, w, at the nodes, the strains and stresses at different locations of the plate are then calculated. The deflection and stress values are computed for different stiffener angles, θ, and the optimized angle for minimum values has been obtained.

The accuracy of the present finite element solution is first confirmed by comparing its results with those available in the literature, for both unstiffened and stiffened plates, as listed in Table 2. The non-dimensional deflections are compared with those obtained by Naiver's analytical method by assuming the deflection as a double Fourier sine series and the load as a single Fourier sine series. As indicated by Timoshenko and Woinowsky-Krieger [55], the Naiver's solution errors are 2.5 percent greater than those of the finite element results. The present solutions are also in agreement with those of others cited in [55]. The primary bending stiffnesses are also verified with the

existing results. The stiffness added to a plate due to an attached stiffener as

per Smith, et al. [15] has been computed, compared and found to be within an

error limit of 2.5 percent and is shown in Table 2.

Table 2. Analytical Comparison of Simply Supported Plate

Properties for Comparison	Present Solution	Naiver's Solution	Other's Solution
$(wD/qa^4)x10^2$ Uniform Thick	0.405	0.416	0.406
Stiffened Plate $(w/a)x10^2$	0.1836	0.1889	-
Bending Rigidity $D/(Eh_3)$	0.1584	0.1619 Huber (1914)	0.1606 Smith (1946)

4.3.1 Bending Analysis of Unstiffened Plate

The finite element strains and the experimental strains for unstiffened

plates were compared and found to be in good agreement. The experimental

results were 3 to 5% greater than those of finite element results. This

discrepancy may be attributed to the uneven load distribution on the plate

after it started bending. The specific values for the strains ε_x, ε_y and γ_{xy} are

plotted in Fig. 14.

The leading and trailing edge deflections at free corners for angles of

sweep ranging from 0° to 60° are computed and are plotted in Fig. 15 as non-

dimensional parameters (wD/qA^4) where w is the deflection, D is the bending
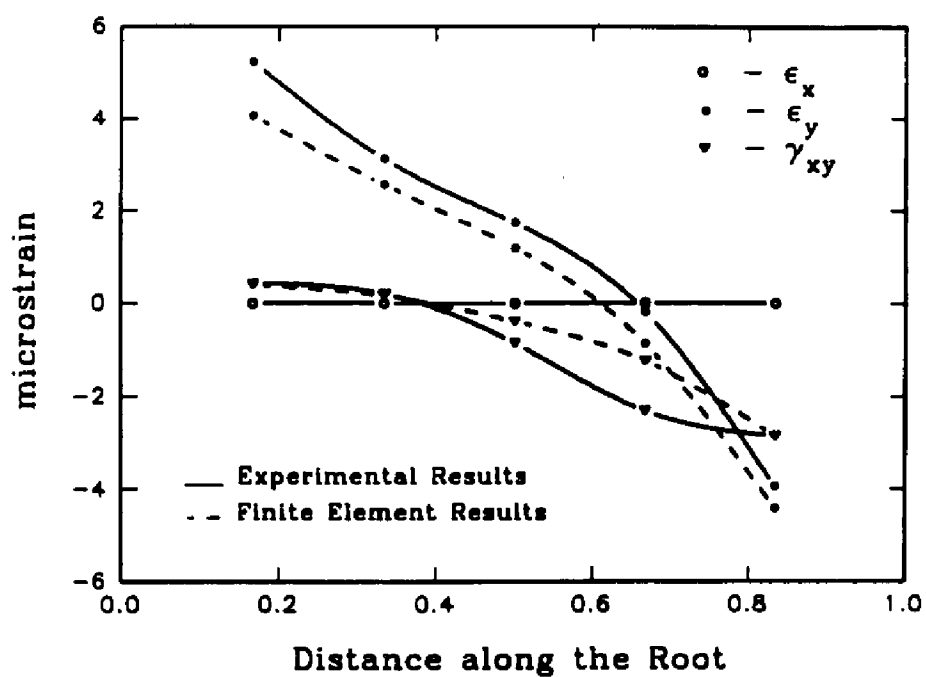
Fig. 14 Comparison of Strains Along the Root
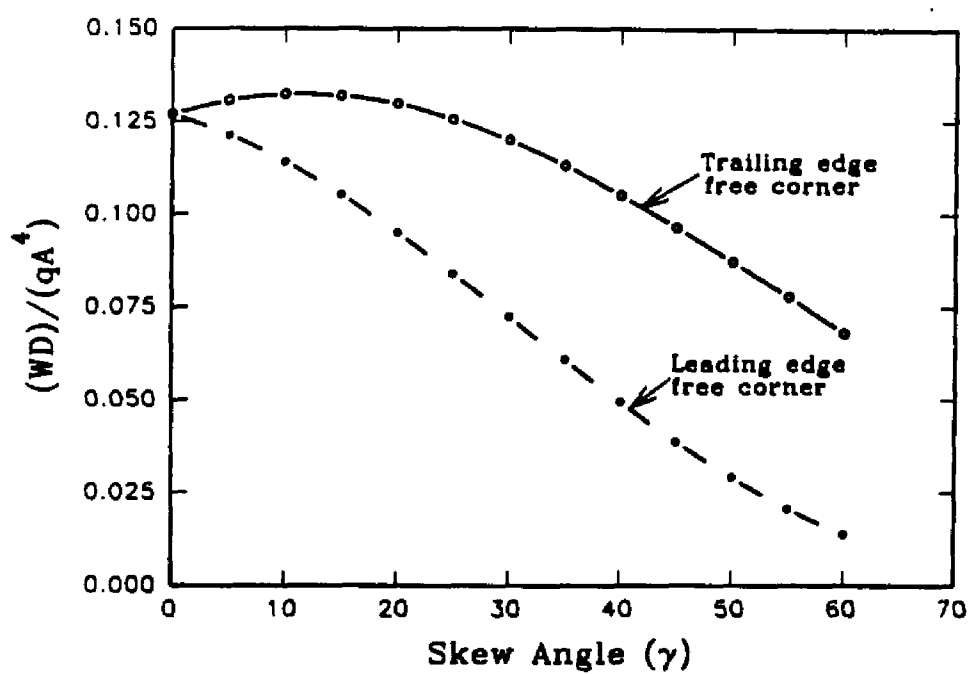
Fig. 15   Non-dimensional Deflections For Isotropic Plate (Finite
           Element Results)

stiffness, q is the uniform transverse load, A is the side of the rhombic plate. The deflections are also computed for a thirteen layer cross-ply fiber glass composite plate for different angles of sweep and are plotted in Fig. 16. The deflections in both isotropic and composite case follow the same pattern. The dependence of deflection on the fiber angle for a plate of specific angle of sweep also has been studied. For any angle of sweep a fiber angle of $90°$ gave the least deflection.

The non-dimensional stress variations along the root of the cantilever plate for different angles of sweep are obtained and plotted in Fig. 17. The stress singularity at the trailing end of the root increases rapidly and becomes undefined as the angle of sweep increases. But, at a point about $0.15A$ from the trailing end of the root, the stress remains nearly the same for all angles of sweep. This point of constant stress gradually moves towards the trailing edge as one moves away from the root, forming a triangle of undefined stress called the root triangle.

4.3.2 Bending Analysis of Stiffened Plate

The results obtained from the experiment for bending of a stiffened plate are listed in Tables 3 and 4 while the maximum deflections and strains, compared with theoretical ones are shown in Figs. 18 and 19, respectively. The deflections are also compared with the analytical results by Naiver's solutions in Table 3. It was found that the experimental results are five
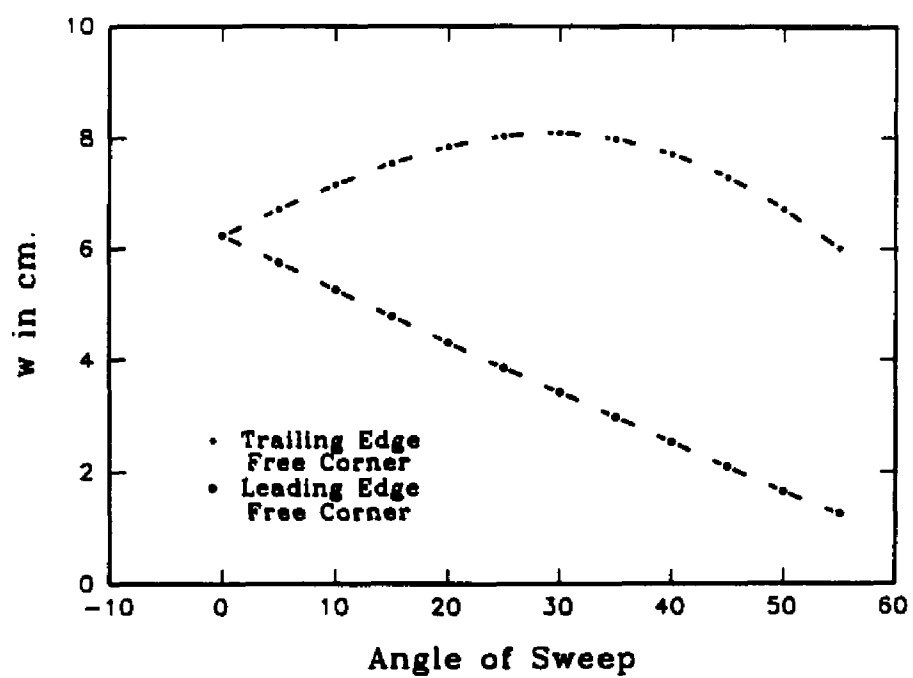
Fig. 16   **Non-dimensional deflections for composite plate. (Finite Element Results)**
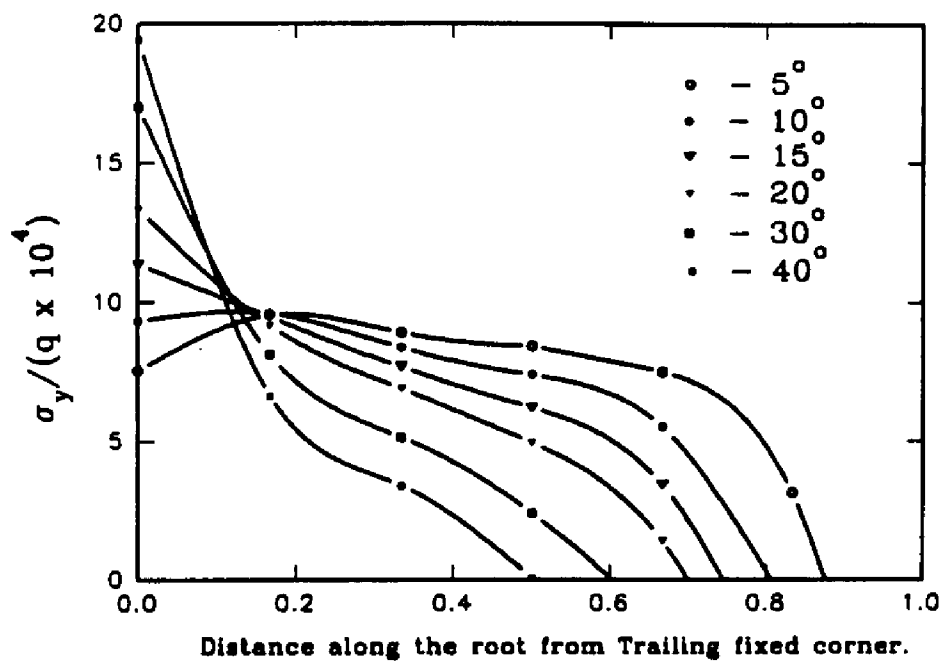
Fig. 17   **Non-Dimensional Stress Along the Root For Different Angles of Sweep**
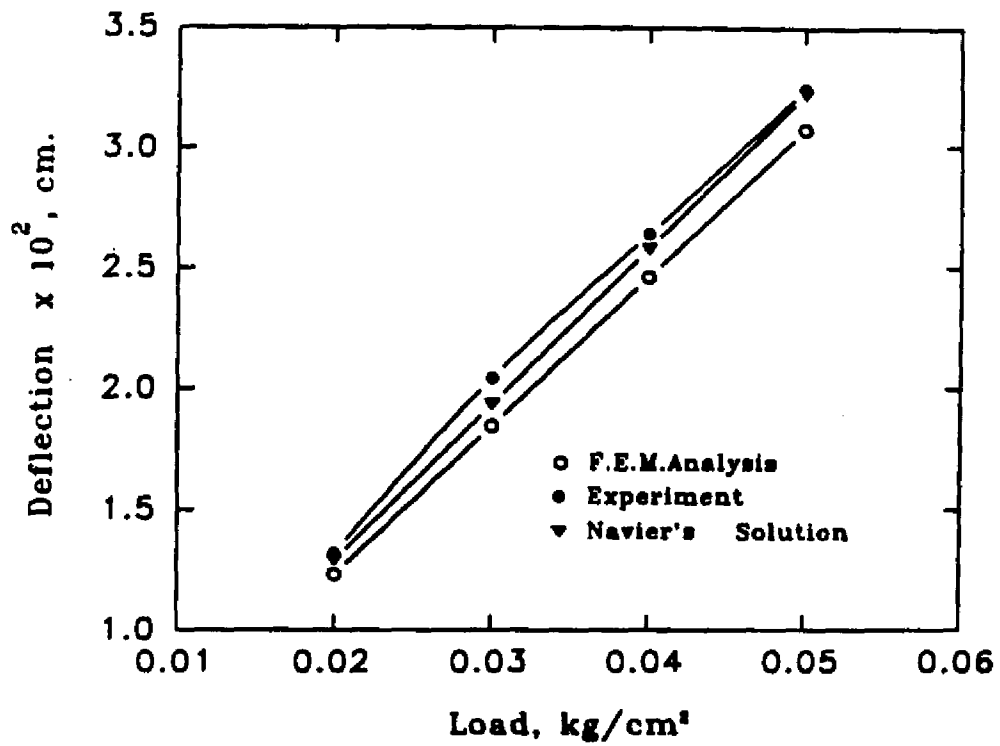
Fig. 18   Maximum Central Deflections of Simply Supported Aluminum Plate
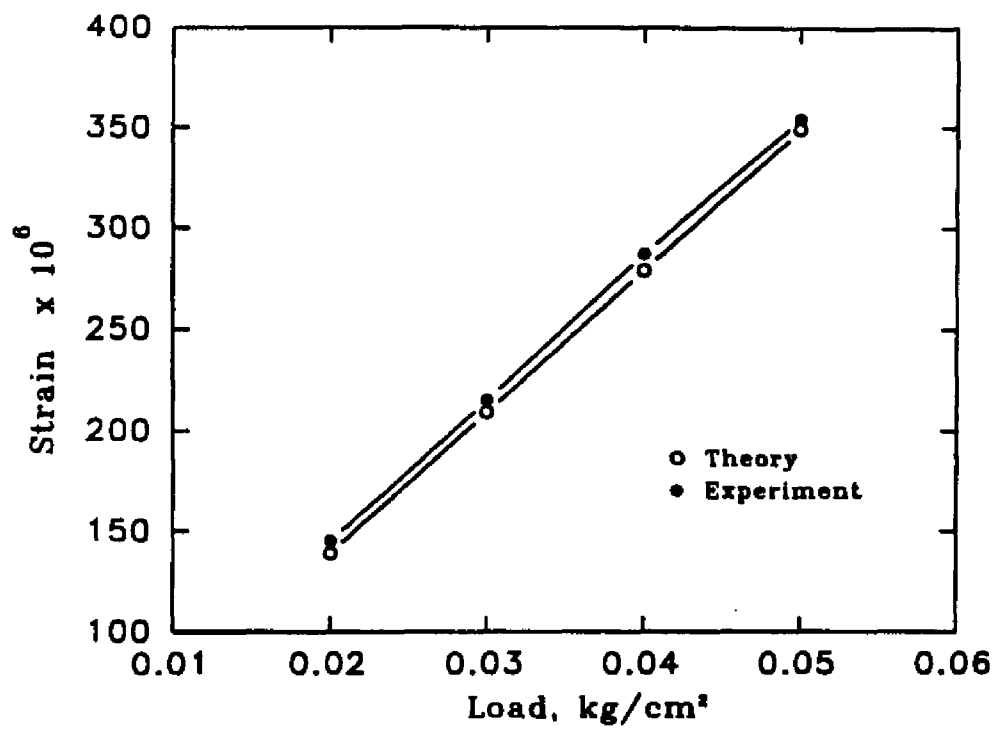
Fig. 19 Maximum Strains of Simply Supported Aluminum Plate

percent higher than the theoretical values. This excess may be due to various experimental set-up defects, such as non-uniformity of the applied load, machining difficulties in achieving uniform thickness, and the roundness of the grooves at the edges, and the full integration used in FEA.

The analysis has been done for two types of boundary conditions, cantilever and simply supported at all the four edges, and results have been given for variations of deflections and stresses with different angles of stiffeners and plate. It has been observed that, for a cantilever plate with any skew angle, as the stiffener angle increases, the deflection reaches a minimum value at a certain angle θ, and then increases. As shown in Fig. 20, the optimized stiffener angle for minimum deflection is different for leading and trailing edge corners. This angle keeps moving towards the left as the skew angle of plate increases (Fig. 21). For skew angle $\gamma = 0°$, the minimum deflection occurs at stiffener angle θ near about 30°. For $\gamma = 10°$, this minimum deflection occurs at 25°, for skew angle $\gamma = 20°$, it occurs at about 20 degrees, and so on. Figure 22 shows the optimum stiffener angles for leading and trailing edge free corners of the cantilever plate for different plate skew angles. The non-dimensional stress variations ($\sigma_x/q \times 10^4$) along the fixed edge and at the root of the cantilever plate, for different skew angle γ and stiffener angle θ, are given in Tables 5 and 6. This analysis has only been done up to and including 60° skew angle, as the accuracy diminishes with further increase.
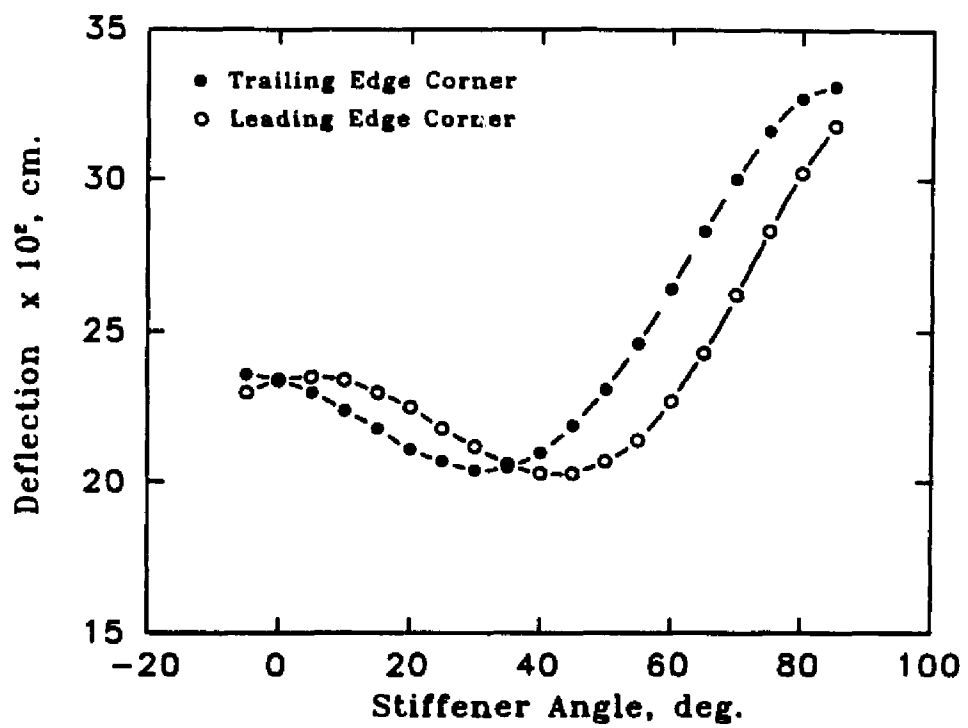
Fig. 20   **Deflections with Stiffener Angles for Square Cantilever Aluminum Plate**
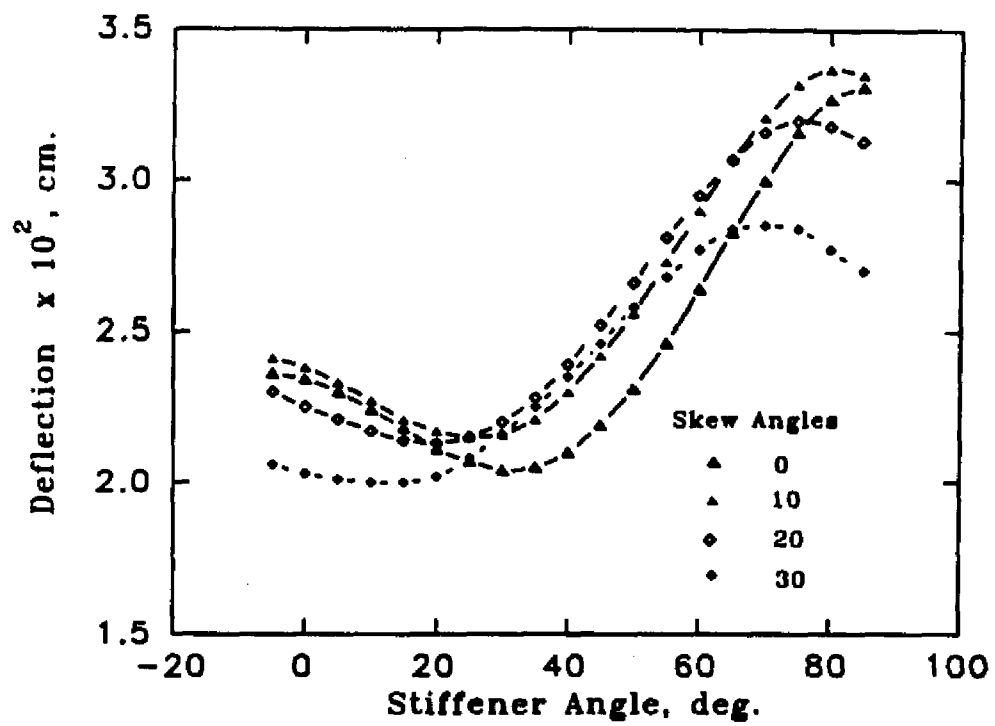
Fig. 21   Rear Tip Deflections for Skew Cantilever Aluminum Plate
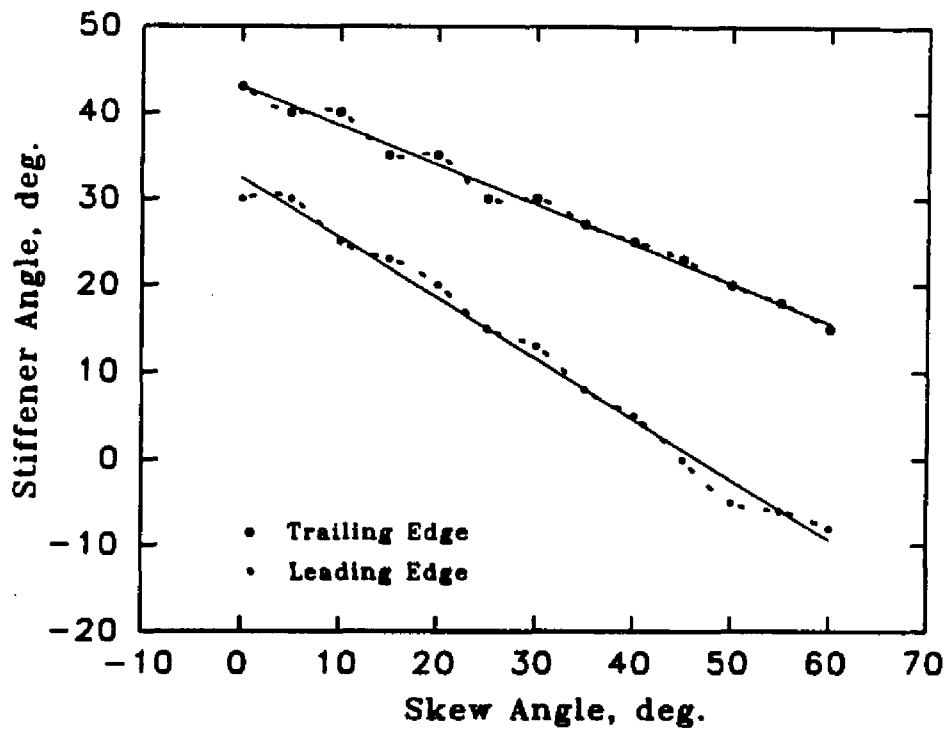
Fig. 22   Optimum Stiffener Angle for Minimum Deflection of Skew Cantilever Aluminum Plate

When the stiffener angle θ (Fig. 11) is zero, the length of the effective stiffener (s_1) is at a minimum, but s_2 will still be large. As θ increases, s_1 will also increase, but s_2 will decrease. Hence for a specific plate and stiffener material, there exists an optimized s_1 and s_2 (or θ), such that the deflection at point A reaches a minimum value. It is obvious that a simply supported plate will have its maximum deflection at the center. For a square plate, the maximum deflection occurs at the stiffener angle $\theta = 45°$ and minimum at $0°$, as shown in Fig. 23. But as the skew angle γ increases, the optimized stiffener angle θ moves towards the left. Because of the dependance of the stress on deflection, the stress variations are also of the same form as those of the deflections, shown by Fig. 24. A comparison has been given in Fig. 25 for two plates of same aspect ratio, weight, and surface area, but one with stiffeners, and the other without. Obviously, the one with stiffeners has minimum deflection, and hence minimum stress. But the effectiveness of the stiffened plate over unstiffened diminishes as the skew angle increases above about $20°$.

An investigation has been done for cross-ply and angle-ply composites. For a plate of uniform thickness, the dependance of maximum tip deflections of a cantilever plate on fiber angle is of the same form as that of an isotropic plate on stiffener angle (Fig. 26). Figures 27 and 28 show the variation of tip deflections of stiffened plates (plate with 8-ply total thickness and a 5-ply stiffener thickness), and Fig. 29 provides the deflection variations for a simply supported cross-ply and angle-ply plates with the angle of sweep, γ.
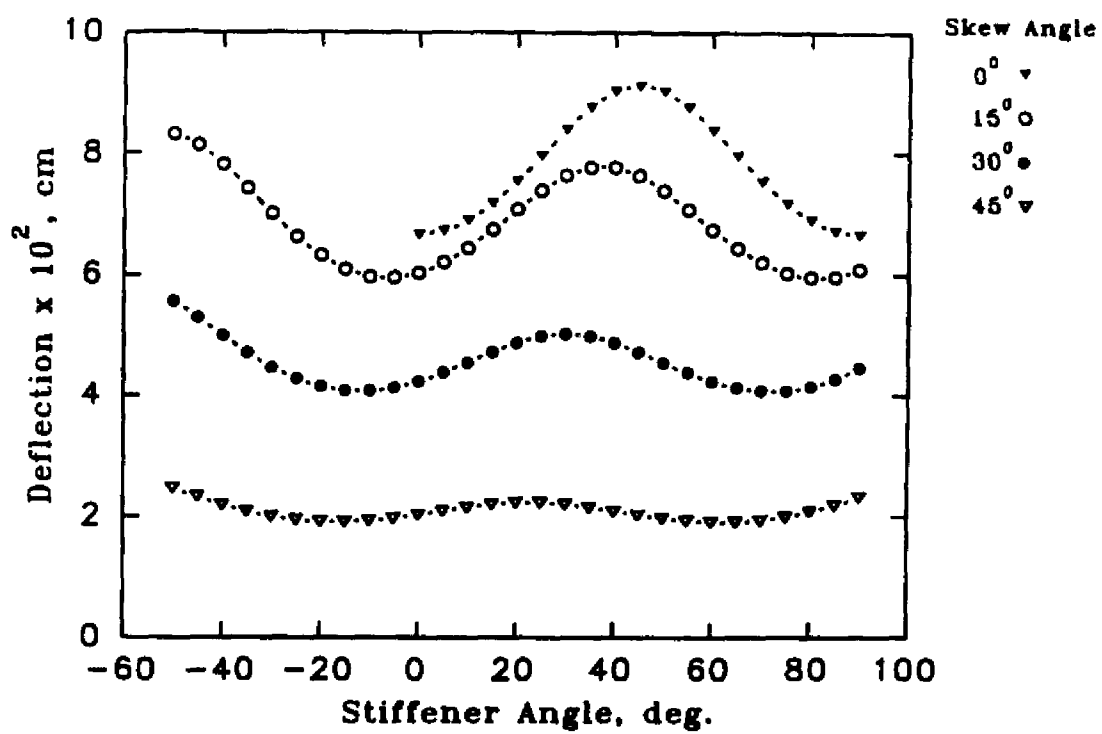
Fig. 23   Deflections with Skew Angles for Simply Supported Aluminum Plate
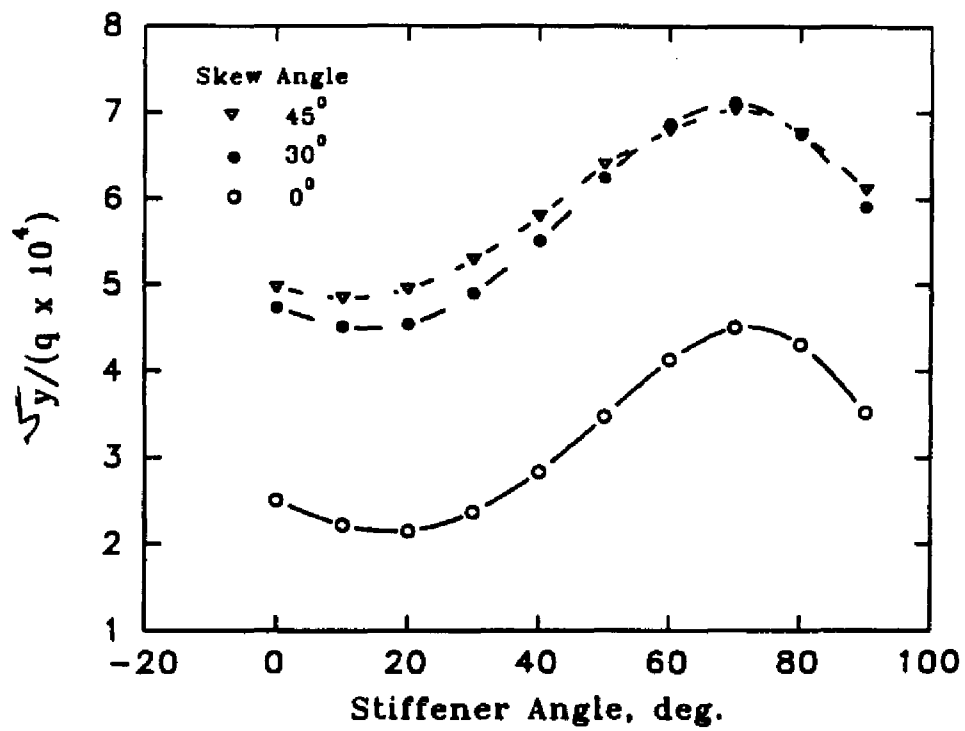
Fig. 24 Non-dimensional Stresses with Stiffener Angles for Cantilever Aluminum Plate
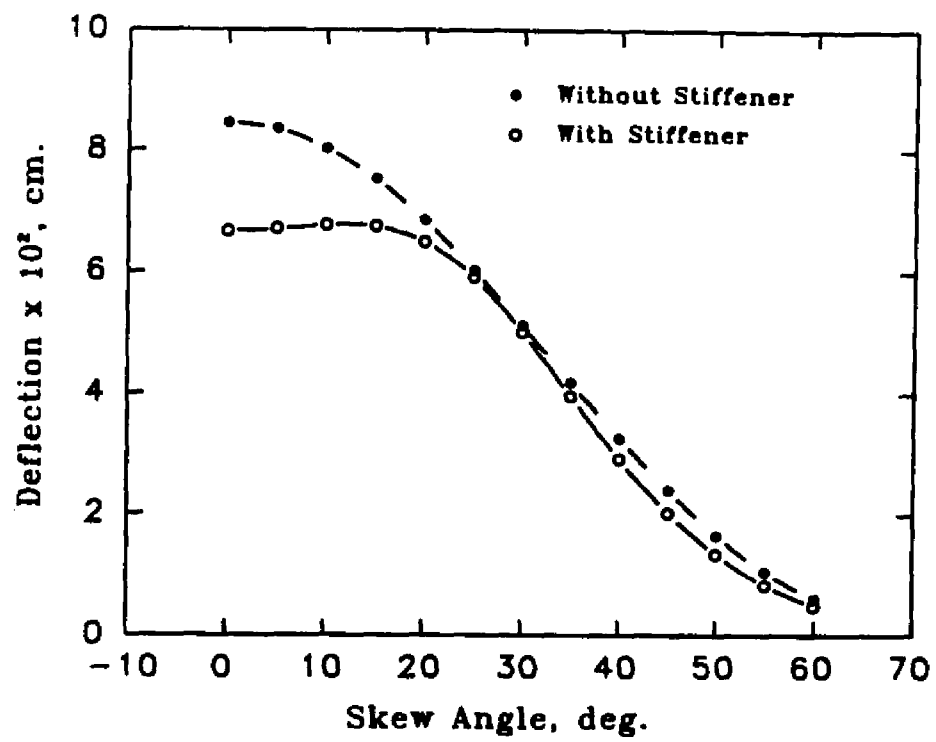
Fig. 25   **Maximum Deflections with Skew Angles for Simply Supported Aluminum Plate**
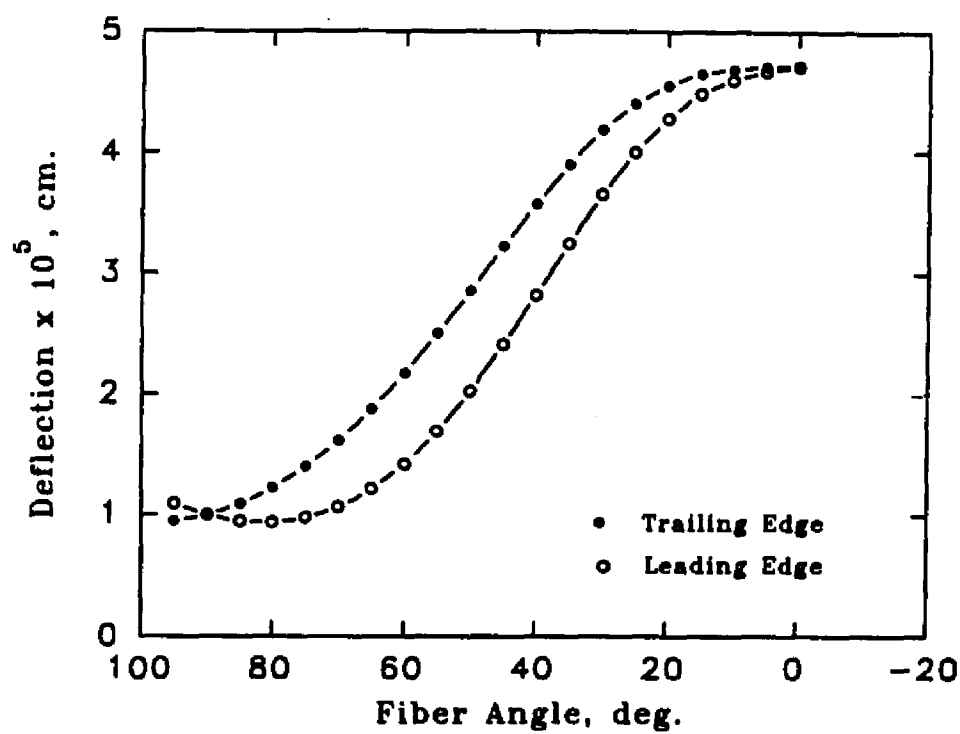
Fig. 26 Deflections with Fiber Angles for Unidirectional Square Cantilever Composite Plate
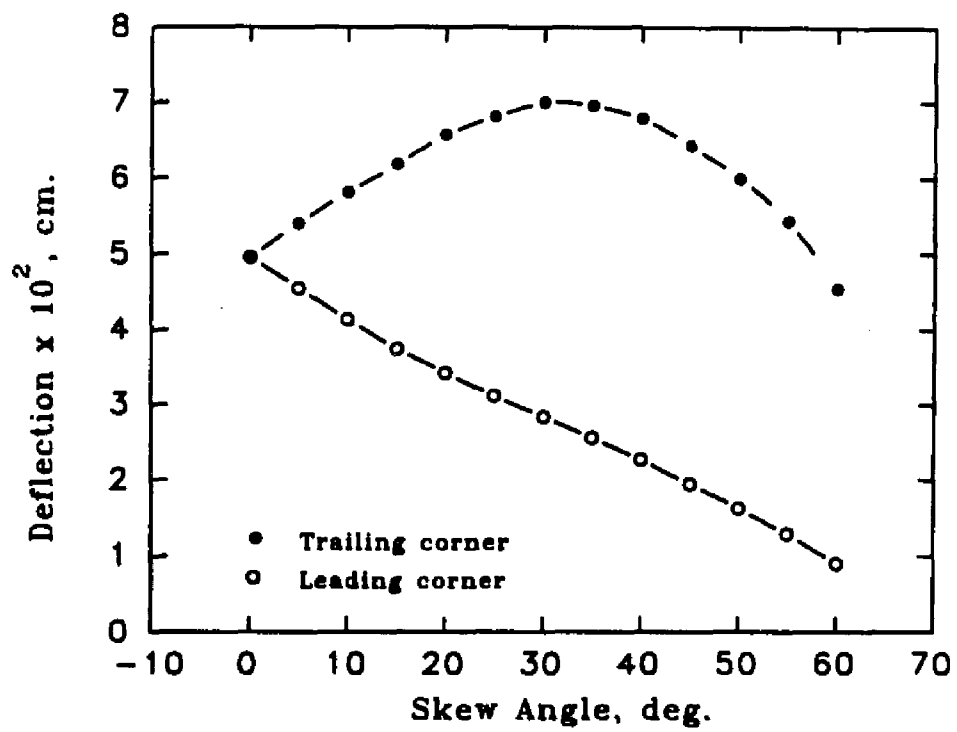
Fig. 27   **Deflections with Skew Angles for Stiffened Cantilever Composite Plate,(Fibers at 0°/90°)**
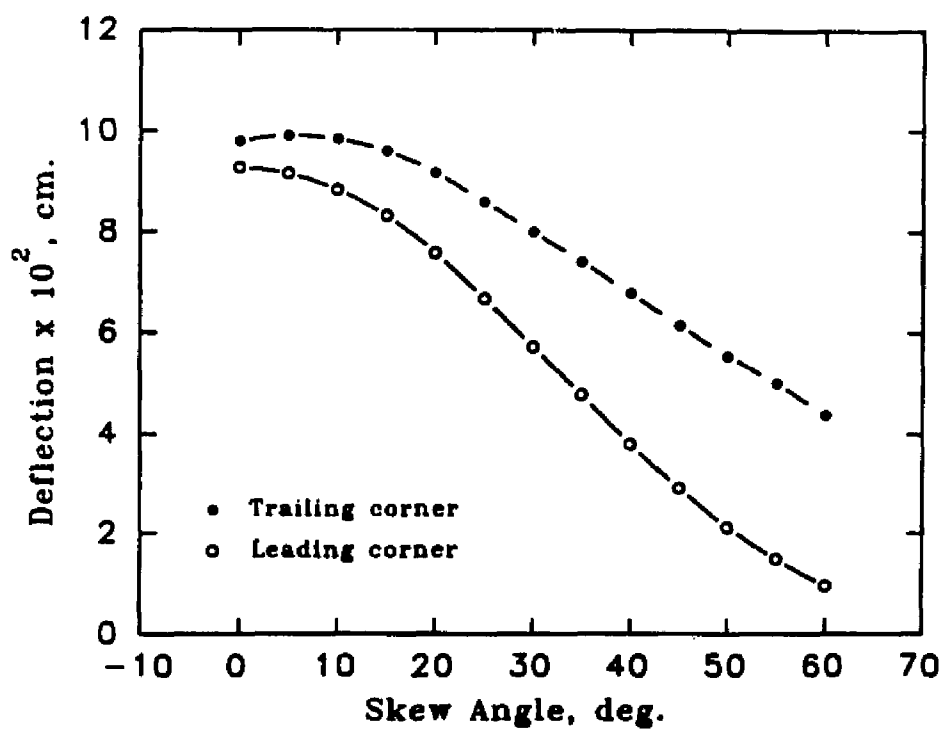
Fig. 28   Deflections with Skew Angles for Stiffened Cantilever Composite Plate,(Fibers at +45°/-45°)
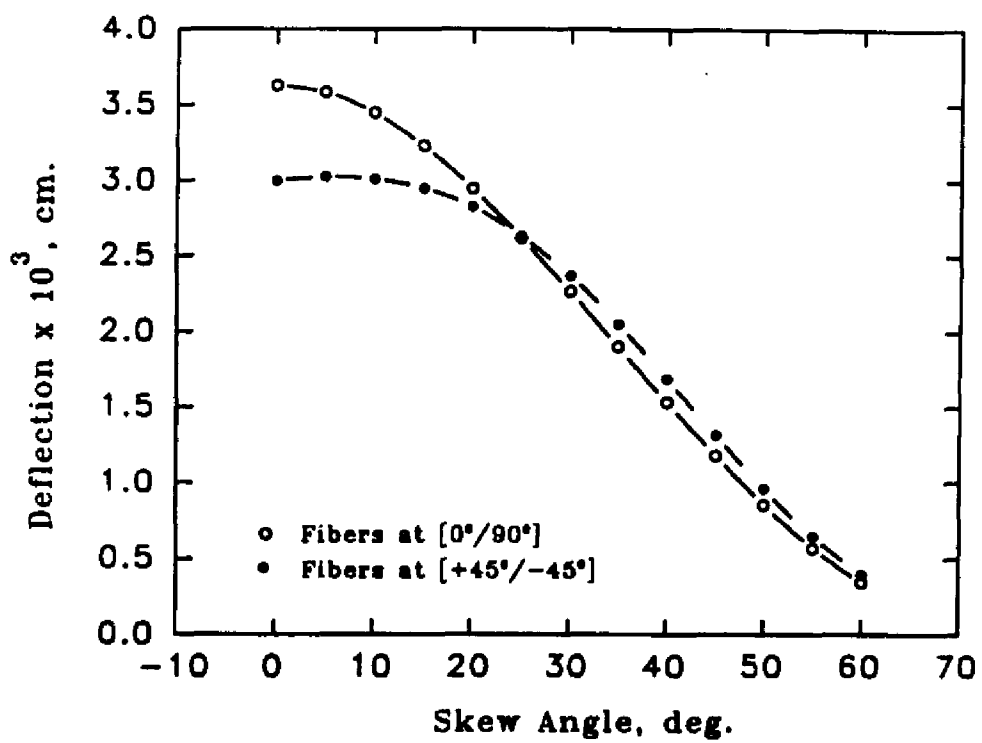
Fig. 29   Maximum Deflections with Skew Angles for Stiffened Simply Supported Composite Plate

The effect of load on the deflection has been analyzed for an isotropic square plate with different pressure loads. Actually as per Fig. 55 of PANDA2 (Bushnell, [21]), the stiffened isotropic plate becomes stiffer and stiffer as the pressure load increases. But in the present case, as the plate is presumed to be an equivalent homogeneous plate of equal thickness, the deflection is directly proportional to the pressure load as shown in Fig. 30.

Table 3. Theoretical and Experimental Deflections

Load (kg/cm²)	w_c x10² (FEM)	w_B x 10² (FEM)	w_B x 10² Naiver's	w_A x 10² (FEM)	w_c x 10² Test	w_B x 10² Test	w_a x 10² Test
0.02 (Isotropic)	0.721	1.231	1.291	0.917	-	-	-
0.03 (Isotropic)	1.081	1.846	1.935	1.375	1.347	2.043	1.764
0.04 (Isotropic)	1.442	2.461	2.580	1.834	1.513	2.640	2.120
0.05 (Isotropic)	1.802	3.007	3.226	2.292	2.042	3.247	2.315
0.03 (Cross-ply)	0.179	0.363	-	0.252	0.204	0.385	0.271
0.03 (Angle-ply)	0.148	0.300	-	0.209	0.174	0.337	0.243

Table 4.   Comparison of Theoretical and Experimental Strains For Isotropic Plate

Load (kg/cm²)	ε_2 (Theory)	ε_7 (Theory)	ε_6 (Theory)	ε_2 (Test)	ε_7 (Test)	ε_6 (Test)
0.02	-139.6	134.9	135.7	-145	141	142
0.03	-209.4	202.3	202.4	-215	210	213
0.04	-279.2	265.9	269.7	-287	274	281
0.05	-349.0	332.3	337.2	-354	344	348

Table 5. **Non-Dimensional Stress Variation [σ_y / (q x 10^4)] For a Cantilever Plate of Skew Angle = 30 vs. Stiffener Angle**

x	θ= 0	10	20	30	40	50	60	70	80	90
0	4.734	4.514	4.538	4.902	5.506	6.242	6.872	7.122	6.756	5.902
3	3.598	3.450	3.404	3.524	3.792	4.206	4.676	5.042	5.064	4.670
6	2.166	2.068	1.929	1.846	1.843	1.952	2.198	2.574	2.926	3.012
9	1.806	1.737	1.601	1.492	1.441	1.472	1.621	1.937	2.336	2.550
12	1.562	1.508	1.366	1.225	1.149	1.183	1.327	1.591	1.944	2.200
15	1.243	1.221	1.087	0.918	0.781	0.737	0.830	1.084	1.474	1.818
18	1.074	1.064	0.931	0.749	0.588	0.518	0.588	0.823	1.217	1.603
21	0.648	0.731	0.664	0.504	0.314	0.149	0.078	0.199	0.587	1.091
24	0.107	0.353	0.421	0.327	0.149	-.073	-.306	-.430	-.204	0.402
27	-.099	0.194	0.295	0.211	0.023	-.226	-.510	-.699	-.505	0.145
30	-.943	-.329	0.089	0.155	-.036	-.357	-.796	-1.33	-1.55	-.858
33	-2.19	-1.04	-.013	0.259	-.334	-1.37	-2.31	-2.96	-3.14	-1.88
36	-2.55	-1.27	-.099	0.218	-.453	-1.64	-2.69	-3.41	-3.61	-2.23

x - The Distances Along the Fixed Edge With Origin at rear Fixed Corner

Table 6. Non Dimensional Parameter (σ_y / q x 10^4) at Origin (θ vs. γ)

Stiffener Angleθ	0 Skew	15 Skew	30 Skew	45 Skew	60 Skew
0	2.508	3.722	4.734	4.966	3.812
10	2.218	3.442	4.514	4.842	3.778
20	2.150	3.420	4.538	4.946	3.880
30	2.370	3.712	4.902	5.292	4.144
40	2.834	4.290	5.506	5.786	4.482
50	3.474	5.030	6.242	6.392	4.820
60	4.126	5.734	6.872	6.798	5.066
70	4.502	6.078	7.122	7.038	5.246
80	4.306	5.766	6.756	6.764	5.214
90	3.516	4.882	5.902	6. 106	4.858
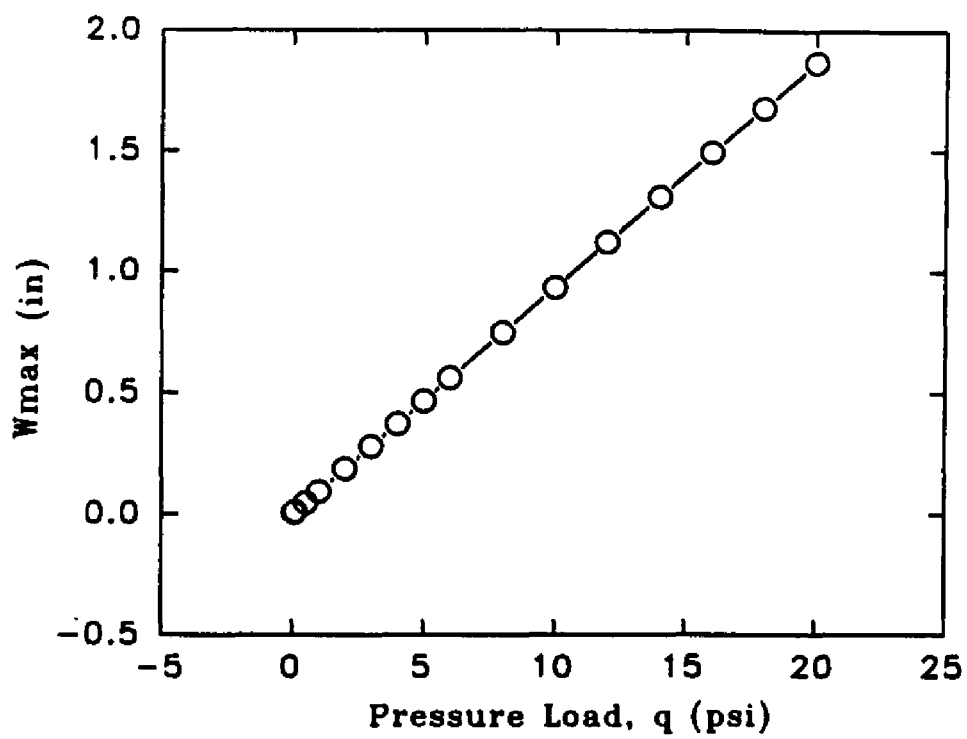
Fig. 30 **Dependance of Deflection on Pressure for Stiffened Square Simply Supported Aluminum Plate**

CHAPTER 5. VIBRATION ANALYSIS OF STIFFENED PLATE

As a second part of the research, the natural frequency and mode shapes of the laminated composite plates are studied. A finite element model has been developed for the analysis of the stiffened plate. This formulation consists of a nine noded plate element with a three noded beam element for the stiffener. The plate and the beam elements are formulated separately and then transformed to a single set of degrees of freedom and then analyzed for the natural frequency. The details of the formulation are as follows:

5.1 Plate Element Formulation

A Lagrange Quadratic plate element with nine nodes having five degrees of freedom at each node has been considered. Along with the vertical deflection w and the two rotations α about x axis and β about y axis, the x displacement u and y displacement v have considered as the neutral axis of the stiffened plate does not lie in a single plane, the use of $u = z\,\alpha$ and $v = z\,\beta$ are not valid any more. The five degrees of freedom per node are:

u_p = the displacement along x axis

v_p = the displacement along y axis

w_p = the vertical displacement along the z axis

α_p = the rotation about x axis

β_p = the rotation about y axis

63
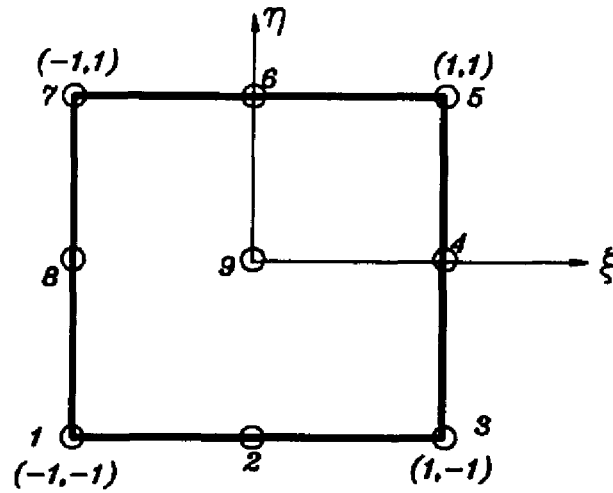
Fig. 31 Plate Element

The shape functions with quadratic variation for nine node plate element are:

$$N_1 = \frac{1}{4}(1-\xi)(1-\eta) - \frac{1}{2}N_5 - \frac{1}{2}N_8 - \frac{1}{4}N_9$$

$$N_2 = \frac{1}{4}(1+\xi)(1-\eta) - \frac{1}{2}N_5 - \frac{1}{2}N_6 - \frac{1}{4}N_9$$

$$N_3 = \frac{1}{4}(1+\xi)(1+\eta) - \frac{1}{2}N_6 - \frac{1}{2}N_7 - \frac{1}{4}N_9$$

$$N_4 = \frac{1}{4}(1-\xi)(1+\eta) - \frac{1}{2}N_7 - \frac{1}{2}N_8 - \frac{1}{4}N_9$$

$$N_5 = \frac{1}{2}(1-\xi^2)(1-\eta) - \frac{1}{2}N_9 \qquad\qquad (39)$$

$$N_6 = \frac{1}{2}(1+\xi)(1-\eta^2) - \frac{1}{2}N_9$$

$$N_7 = \frac{1}{2}(1-\xi^2)(1+\eta) - \frac{1}{2}N_9$$

$$N_8 = \frac{1}{2}(1-\xi)(1-\eta^2) - \frac{1}{2}N_9$$

$$N_9 = (1-\xi^2)(1-\eta^2)$$

Using these shape functions, the displacements at a point on the element can

be represented in terms of the displacements at the elemental nodal points as:

$$u_p = N_1 u_1 + N_2 u_2 + N_3 u_3 + \ldots = \sum_{i=1}^{9} N_i u_i$$

$$v_p = N_1 v_1 + N_2 v_2 + N_3 v_3 + \ldots = \sum_{i=1}^{9} N_i v_i \qquad (40)$$

$$w_p = N_1 w_1 + N_2 w_2 + N_3 w_3 + \ldots = \sum_{i=1}^{9} N_i w_i$$

and hence the displacement vector at any point of the element is given as

$$\delta_p = \begin{Bmatrix} u_p \\ v_p \\ w_p \\ \alpha_p \\ \beta_p \end{Bmatrix} = \sum_{i=1}^{9} N(\xi,\eta)_i \begin{Bmatrix} u_{pi} \\ v_{pi} \\ w_{pi} \\ \alpha_{pi} \\ \beta_{pi} \end{Bmatrix} = \sum_{i=1}^{9} N(\xi,\eta)_i \delta_{pi} \qquad (41)$$

Now the strains of the plate element can be derived from the elemental

displacements. This strain displacement functions for the plate are:

$$\begin{Bmatrix} \epsilon_x \\ \epsilon_y \\ \epsilon_{xy} \\ k_x \\ k_y \\ k_{xy} \\ \epsilon_{xz} \\ \epsilon_{yz} \end{Bmatrix} = \begin{Bmatrix} u_{,x} \\ v_{,y} \\ (u_{,y}+v_{,x}) \\ \alpha_{,x} \\ \beta_{,y} \\ (\alpha_{,y}+\beta_{,x}) \\ (\alpha+w_{,x}) \\ (\beta+w_{,y}) \end{Bmatrix} = \sum_{i=1}^{9} B_i \delta_{pi} \qquad (42)$$

where

$$B_i = \begin{bmatrix} N_{i,x} & 0 & 0 & 0 & 0 \\ 0 & N_{i,y} & 0 & 0 & 0 \\ N_{i,y} & N_{i,x} & 0 & 0 & 0 \\ 0 & 0 & 0 & N_{i,x} & 0 \\ 0 & 0 & 0 & 0 & N_{i,y} \\ 0 & 0 & 0 & N_{i,y} & N_{i,x} \\ 0 & 0 & N_{i,x} & N_i & 0 \\ 0 & 0 & N_{i,y} & 0 & N_i \end{bmatrix} \qquad (43)$$

or in compact form

$$\epsilon_p = B_p \delta_p \qquad (44)$$

The generalized stress strain relationship for a single composite lamina in its principal fiber direction are given as

$$\begin{Bmatrix} \sigma_1 \\ \sigma_2 \\ \sigma_3 \\ \sigma_4 \\ \sigma_5 \\ \sigma_6 \end{Bmatrix} = \begin{bmatrix} Q_{11} & Q_{12} & Q_{13} & 0 & 0 & 0 \\ Q_{12} & Q_{22} & Q_{23} & 0 & 0 & 0 \\ Q_{13} & Q_{23} & Q_{33} & 0 & 0 & 0 \\ 0 & 0 & 0 & 2Q_{44} & 0 & 0 \\ 0 & 0 & 0 & 0 & 2Q_{55} & 0 \\ 0 & 0 & 0 & 0 & 0 & 2Q_{66} \end{bmatrix} \begin{Bmatrix} \epsilon_1 \\ \epsilon_2 \\ \epsilon_3 \\ \epsilon_{23} \\ \epsilon_{31} \\ \epsilon_{12} \end{Bmatrix} \qquad (45)$$

where for a two dimensional transversely isotropic lamina

$$Q_{11} = \frac{E_{11}}{(1 - v_{12}v_{21})}, \qquad Q_{22} = \frac{E_{22}}{(1 - v_{12}v_{21})},$$

$$Q_{12} = Q_{21} = v_{21}Q_{11}, \qquad Q_{44} = G_{23}, \qquad (46)$$

$$Q_{55} = G_{13}, \qquad Q_{66} = G_{12}$$

Now transforming these stress strain relations to the x-y-z coordinate system, we have

$$\begin{Bmatrix} \sigma_x \\ \sigma_y \\ \sigma_z \\ \sigma_{yz} \\ \sigma_{xz} \\ \sigma_{xy} \end{Bmatrix} = \begin{bmatrix} \overline{Q}_{11} & \overline{Q}_{12} & \overline{Q}_{13} & 0 & 0 & \overline{Q}_{16} \\ \overline{Q}_{12} & \overline{Q}_{22} & \overline{Q}_{23} & 0 & 0 & \overline{Q}_{26} \\ \overline{Q}_{13} & \overline{Q}_{23} & \overline{Q}_{33} & 0 & 0 & \overline{Q}_{36} \\ 0 & 0 & 0 & \overline{Q}_{44} & \overline{Q}_{45} & 0 \\ 0 & 0 & 0 & \overline{Q}_{45} & \overline{Q}_{55} & 0 \\ \overline{Q}_{16} & \overline{Q}_{26} & \overline{Q}_{36} & 0 & 0 & \overline{Q}_{66} \end{bmatrix} \begin{Bmatrix} \epsilon_x \\ \epsilon_y \\ \epsilon_z \\ \epsilon_{yz} \\ \epsilon_{xz} \\ \epsilon_{xy} \end{Bmatrix} \tag{47}$$

where

$$[\overline{Q}] = [T]^{-1}[Q][T]. \tag{48}$$

$[T]$ is the coordinate transformation matrix from principal coordinate system to the x-y-z coordinate system.

For such a thin walled composite laminate of plane stress, $\epsilon_z = 0$ and σ_z is negligible. The overall plate forces are then

$$\begin{Bmatrix} N_x \\ N_y \\ N_{xy} \\ Q_x \\ Q_y \end{Bmatrix} = \int_{-h/2}^{+h/2} \begin{Bmatrix} \sigma_x \\ \sigma_y \\ \sigma_{xy} \\ \sigma_{xz} \\ \sigma_{yz} \end{Bmatrix} dz = \sum_{k=1}^{N} \int_{h_{k-1}}^{h_k} \begin{Bmatrix} \sigma_x \\ \sigma_y \\ \sigma_{xy} \\ \sigma_{xz} \\ \sigma_{yz} \end{Bmatrix} dz_k . \tag{49}$$

and the moments are

$$\begin{Bmatrix} M_x \\ M_y \\ M_{xy} \end{Bmatrix} = \int_{-h/2}^{+h/2} \begin{Bmatrix} \sigma_x \\ \sigma_y \\ \sigma_{xy} \end{Bmatrix} z\, dz = \sum_{k=1}^{N} \int_{h_{k-1}}^{h_k} \begin{Bmatrix} \sigma_x \\ \sigma_y \\ \sigma_{xy} \end{Bmatrix} z_k\, dz_k . \tag{50}$$

Hence the normal forces and the bending moments reduces to

$$\begin{Bmatrix} N \\ M \end{Bmatrix} = \begin{bmatrix} [A] & [B] \\ [B] & [D] \end{bmatrix} \begin{Bmatrix} \epsilon \\ k \end{Bmatrix} . \qquad (51)$$

where

$$(A_{ij}, B_{ij}, D_{ij}) = \int_{-h/2}^{h/2} Q_{ij}^{-}(1, z, z^2)dz \qquad (52)$$

It is well known that the transverse shear deformation effects are important in composite material plates in determining vibration natural frequency. To determine these forces, Q_x and Q_y, it is assumed that the transverse shear stresses vary parabolically across the laminate thickness. A continuous functional variation is used with a weighting function as

$$f(z) = W_s [1-(\frac{z}{h/2})^2] \qquad (53)$$

where W_s is the weighting function for shear.

Now to obtain the shear force and shear stress relation, from eqn. 49

$$\begin{aligned} Q_x &= \int_{-h/2}^{h/2} \sigma_{xz} dz \\ &= \sum_{k=1}^{N} \int_{h_{k-1}}^{h_k} (\overline{Q_{45}}f(z)\epsilon_{yz} + \overline{Q_{55}}f(z)\epsilon_{xz})dz \\ &= (A_{55}\epsilon_{xz} + A_{45}\epsilon_{yz}) \end{aligned} \qquad (54)$$

where

$$A_{ij} = \sum_{k=1}^{N} \int_{h_{k-1}}^{h_k} \overline{Q_{ij_k}} f(z) \, dz$$

$$= \sum_{k=1}^{N} \overline{Q_{ij_k}} W_s \int_{h_{k-1}}^{h_k} [1-(\frac{z}{h/2})^2] dz \tag{55}$$

$$= W_s \sum_{k=1}^{N} \overline{Q_{ij_k}} [h_k - h_{k-1} - \frac{4}{3} \frac{(h^3_k - h^3_{k-1})}{h^2}]$$

i,j = 4, 5 only. In a similar way Q_y can also be derived. Hence the shear stress to strain relation is now

$$\begin{Bmatrix} Q_x \\ Q_y \end{Bmatrix} = \begin{bmatrix} A_{55} & A_{45} \\ A_{45} & A_{55} \end{bmatrix} \begin{Bmatrix} \sigma_{xz} \\ \sigma_{yz} \end{Bmatrix} \tag{56}$$

Hence the generalized stress strain relationship for the plate element is given as

$$\begin{Bmatrix} N_x \\ N_y \\ N_{xy} \\ M_x \\ M_y \\ M_{xy} \\ Q_x \\ Q_y \end{Bmatrix} = \begin{bmatrix} A_{11} & A_{12} & A_{16} & B_{11} & B_{12} & B_{16} & 0 & 0 \\ A_{12} & A_{22} & A_{26} & B_{21} & B_{22} & B_{26} & 0 & 0 \\ A_{16} & A_{26} & A_{66} & B_{16} & B_{26} & B_{66} & 0 & 0 \\ 0 & 0 & 0 & D_{11} & D_{12} & D_{16} & 0 & 0 \\ 0 & 0 & 0 & D_{12} & D_{22} & D_{26} & 0 & 0 \\ 0 & 0 & 0 & D_{16} & D_{26} & D_{66} & 0 & 0 \\ 0 & 0 & 0 & 0 & 0 & 0 & A_{55} & A_{45} \\ 0 & 0 & 0 & 0 & 0 & 0 & A_{45} & A_{44} \end{bmatrix} \begin{Bmatrix} u_{,x} \\ v_{,y} \\ (u_{,y}+v_{,x}) \\ \alpha_{,x} \\ \beta_{,y} \\ (\alpha_{,y}+\beta_{,x}) \\ (\alpha+w_{,x}) \\ (\beta+w_{,y}) \end{Bmatrix} \tag{57}$$

or in compact form

$$\sigma_p = [D_p] \, \epsilon_p \tag{58}$$

Having obtained the strain displacement matrix B_p and the stress strain matrix D_p, the principle of strain energy derivation yields the stiffness matrix for the plate element as

$$[K_p]^e = \int_A [B_p] [D_p] [B_p] dA \qquad (59)$$

The element stiffness matrix for the element are computed by numerical integration by a two point Gaussian Quadrature rule.

5.2 Beam Element Formulation

The stiffener(s) of the plate are considered as beams running from one edge to the other. The plane of each lamina in the stiffener is perpendicular to the mid plane surface of the plate. Hence bending of the stiffener is in a plane perpendicular to the thickness of laminate. Fibers in the stiffener are all unidirectional running along the length of the stiffener. Hence the effect of laminate can be neglected and the whole thickness can be considered as made of single layer.

Fig. 32 The Beam Element

The beam element is formulated with three node, each node having four degrees of freedom. The transverse deflection of the stiffener in a direction perpendicular to its length and parallel to the plate mid surface is neglected. The degrees of freedom are then

u_s = the displacement along the length of stiffener

w_s = the vertical deflection along the z axis

α_s = the rotation about the length of stiffener (twisting of stiffener)

B_s = the rotation about an axis perpendicular to the stiffener

The shape functions for this beam element with quadratic variation are

$$N_i = \frac{\xi \xi_i}{2}(1+\xi\xi_i) \qquad i = 1,3$$
$$N_2 = (1-\xi^2)$$

(60)

Representing the degrees of freedom in terms of shape functions as

$$\delta_s = \begin{Bmatrix} u_s \\ w_s \\ \alpha_s \\ \beta_s \end{Bmatrix} = \sum_{i=1}^{3} N_i(\xi) \begin{Bmatrix} u_{si} \\ w_{si} \\ \alpha_{si} \\ \beta_{si} \end{Bmatrix} = \sum_{i=1}^{3} N_i(\xi)\, \delta_{si}$$

(61)

Now the generalized strain displacement relation for the beam element is related as

$$\epsilon_s = \begin{Bmatrix} \epsilon_{sx} \\ k_{sx} \\ k_{sy} \\ \epsilon_{xz} \end{Bmatrix} - \sum_{i=1}^{3} B_i \delta_{si} = B_s \delta_s \qquad (62)$$

where

$$B_i = \begin{bmatrix} N_{i,x'} & 0 & 0 & 0 \\ 0 & 0 & N_{i,x'} & 0 \\ 0 & 0 & 0 & N_{i,x'} \\ 0 & N_{i,x'} & N_i & 0 \end{bmatrix} \qquad (63)$$

It being a beam element, the transverse forces
$N_y = N_{xy} = M_y = M_{xy} = 0$
The generalized stress strain relation for this beam element is

$$\sigma_s = \begin{Bmatrix} N_{sx} \\ M_{sx} \\ T_{sx} \\ Q_{sxz} \end{Bmatrix} = \begin{bmatrix} A_{11} & 0 & 0 & 0 \\ 0 & D_{11} & 0 & 0 \\ 0 & 0 & T_s & 0 \\ 0 & 0 & 0 & A_{55} \end{bmatrix} \begin{Bmatrix} u_{s,x} \\ \alpha_{s,x} \\ \beta_{s,x} \\ \alpha - w_{s,x} \end{Bmatrix} \qquad (64)$$

where

$$A_{11}, D_{11} = \sum_{k=1}^{N} E_x b_k \{ h_k - h_{k-1}, \ \frac{1}{3}(h_k^3 - h_{k-1}^3) \}$$
$$= E_x A, \ E_x I_x$$
$$T_s = G_{12} \frac{bh}{12} (h^2 + b^2) \qquad (65)$$
$$A_{55} = \frac{1}{W_s} \sum_{k=1}^{N} G_{12} b_k (h_k - h_{k-1})$$

or in a compact form

$$\sigma_s = [D_s] \ \epsilon_s \qquad (66)$$

Although the strain displacement matrix B_s and stress strain matrix D_s are formulated, they are in a plane below the plate mid-surface. Also the axis of the stiffener may be oriented in any direction making an angle Θ with the plate coordinate system. Hence before assembling the plate and beam element stiffness matrices, the beam element matrix should be transferred properly.
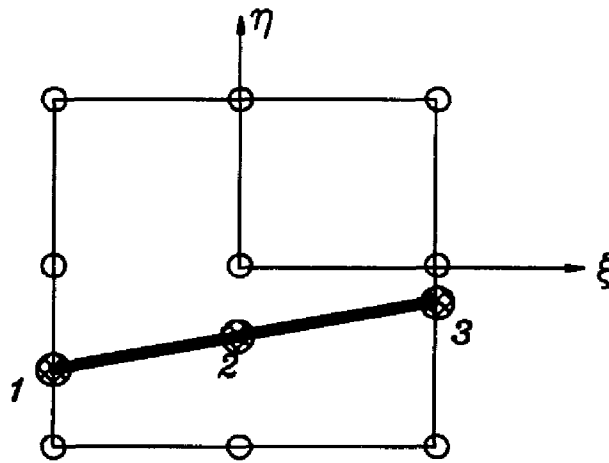
Fig. 33 Plate Element with Inclined Stiffener

The Rotational Transformation for a stiffener angle ϕ:

$$\begin{Bmatrix} u_s \\ w_s \\ \theta_{xsi} \\ \theta_{ys} \end{Bmatrix}_i = \begin{bmatrix} \cos\phi & \sin\phi & 0 & 0 & 0 \\ 0 & 0 & 1 & 0 & 0 \\ 0 & 0 & 0 & \cos\phi & \sin\phi \\ 0 & 0 & 0 & -\sin\phi & \cos\phi \end{bmatrix} \begin{Bmatrix} u_{sp} \\ v_{sp} \\ w_{sp} \\ \theta_{sxp} \\ \theta_{syp} \end{Bmatrix}_i , \quad i = 1,2,3 . \tag{67}$$
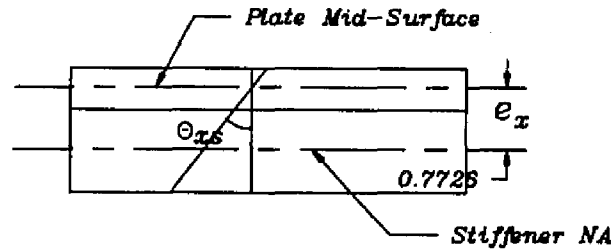
Fig. 34 Stiffened Plate

For eccentrical transformation

$$
\begin{aligned}
u_s &= u_p - e_x \theta_{xp} \\
w_s &= w_p \\
\theta_{xs} &= \theta_{xp} \\
\theta_{ys} &= \theta_{yp}
\end{aligned}
$$

(68)

For the stiffener

$$
\epsilon_s = B_s \delta_s \quad and \quad \sigma_s = D_s B_s \delta_s
$$

(69)

Hence the stiffness matrices for the stiffener is

$$
[K] = T_e^T T_r^T [\int_L B_s^T D_s B_s dx] T_r T_e
$$

(70)

The stiffness matrices for the plate and the stiffeners are then added to obtain the stiffness matrix for the stiffened plate element. The elemental stiffness matrices are then assembled for all the elements to obtain the global stiffness matrix [K]. This matrix size is equal to the number of nodes times the number of degrees of freedom per node (5). The mass matrix [M] is then formulated by lumping the distributed mass of the plate at the connecting nodes.

Now the equilibrium equation of an elastic system in motion is given as

$$[M]\{\delta''\} + [C]\{\delta'\} + [K]\{\delta\} = \{F(t)\}. \tag{71}$$

For the calculation of natural frequency in the present work, the damping effect is neglected. Hence the governing equation to be solved is reduced to

$$([K] - \omega^2[M])\{\lambda\} = \{0\}. \tag{72}$$

Equation 72 is formulated by using the global stiffness [K] and mass matrices [M] and then solved for the natural frequencies by using the available subroutine LOW [31]. The results obtained are discussed in the 'Results and Discussion' section.

5.3 Experimental Modal Analysis

Several experimental configurations and testing procedures are available for characterizing the modal behavior of a linear elastic structure. Many measurement techniques for experimental modal analysis (EMA) are described in detail in references by Ewing [56] and Allemang, et al.[57]. The experimental modal analysis (EMA) technique was adopted in this work for exciting the plate at a single point, however, this point was varied from one point to another for plates with different boundary conditions. To execute the modal tests a series of individual tasks should be performed. The test configuration, the basic measurement system, and post processing are the three major steps for modal testing.

For this investigation the composite plates were supported both in "free" and "clamped" conditions. In the first case the plate is freely suspended in space ensuring the detachment of all the coordinates to ground. The test piece is supported with ultra-light elastic bands in such a way that the rigid body modes no longer exhibit zero natural frequencies but are very small relative to the bending modes, and the elastic modes of interest are not disturbed. The second condition is when the test object is mounted to a rigid clamp (i.e. "grounded").

The clamping device shown in Fig. 35 ensured zero displacement of the structure at the supported edges. Difficulties of grounded structures are reported in great extent by Ewing [56]. The interference of foundation and environmental interactions are minimized by attaching the plates to a thick beam, which itself is mounted to a solid plate placed on a vibration isolation platform. To preclude local stiffening, confirm repeatability and increase the level of confidence in the experimental data, simple tests were performed with the structural configurations dismantled and re-assembled again.

To conduct mobility measurements on the structures, a basic measurement chain consisting of excitation instruments, transducers, amplifiers and a Fast Fuorier Transform (FFT) Analyzer was configured, as shown in Fig. 36. In this study the plate was excited by one of the most common and successfully used methods, i.e., instrumented impact hammer.
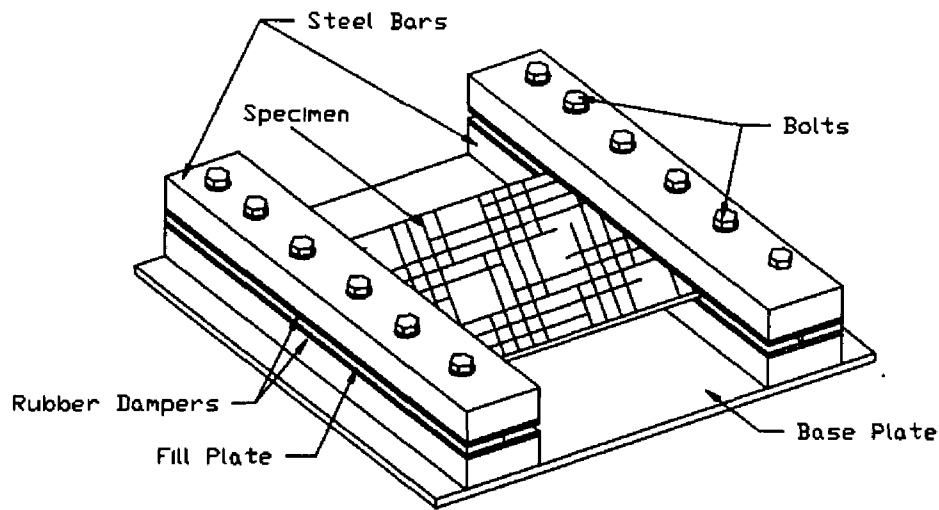
Fig. 35 Clamping Device of Experiment

The response of the plates were sensed by attaching a miniature accelerometer to a predetermined DOF on the plate using bees-wax. According to the change of behavior on the plates due to various boundary conditions, the driving points were selected to respond to the major modes of interest. The excitation force input to the structure and the associated response was measured and the FRFs containing the modal properties generated within the FFT analyzer were recorded.

To identify the frequency response functions, each plate was initially simulated by a controlled and measurable dynamic force with a flat spectral density over the frequency range of interest. The associated response was simultaneously measured with the aid of an appropriate accelerometer,
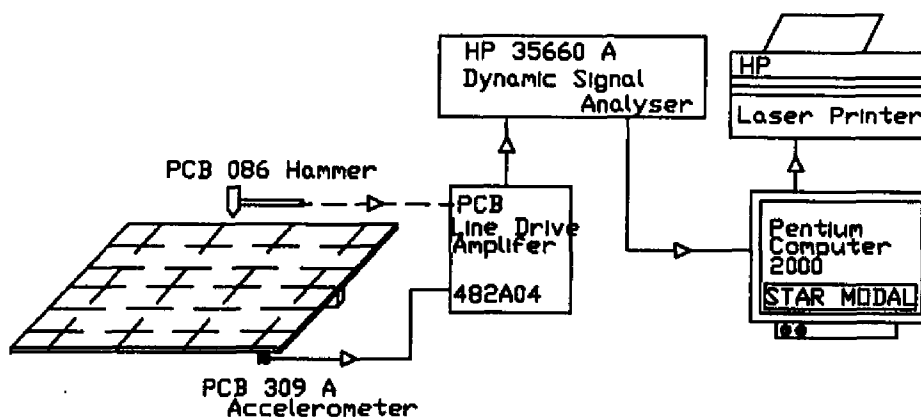
Fig. 36 Experimental Set-up for Modal Test

which did not significantly influence the dynamic behavior of the plates. Based on the excitation auto-spectrum, the response auto-spectrum, and the cross-spectrum relating these two, the individual FRFs were accordingly evaluated. Fig. 37 shows the discretised plate along with its corresponding mesh and the selected locations for the reference degree of freedom.

The frequency range that comprises the major modes of interest for each configuration were then identified. Frequency spans of 1.6 khz, 0.8 khz, and 0.8 khz were selected for the free, clamped-free and the clamped-clamped configurations, respectively. These spans were maintained constant throughout the experiments when various types of stiffeners were connected to the plates. For generating a complete set of data, FRFs were estimated

between a reference DOF and a collection of representative DOFs on the overall structure. The response DOFs were used as the driving points with the modal hammer as the excitation source.
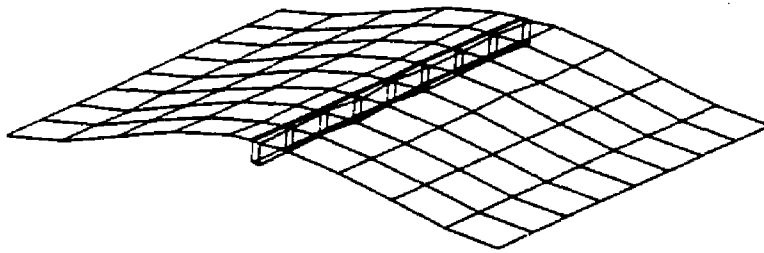
Fig. 37 Experimental Plate Discretization in 1st Mode

Prior to conducting preliminary mobility tests and at the end of each experiment, the measurement chain was calibrated for furnishing the overall sensitivity of the system over the test frequency range. The frequency response functions for each DOF were averaged 3 times before transferring to the computer for modal parameter identification and the quality of each and every function was controlled by maintaining an acceptable coherence function value.

The principle upon which the FRF is determined using transient excitations has been covered in detail by Ewing [56], Allemang, et al [57], Randall [58], Halvorsen, et al [59], and Ramsey [60, 61].

The final stage of the EMA parameter identification process is concerned with the estimation of unknown modal parameters from the measured FRFs. The concepts, advantages and classifications of various modal identification techniques are given by Leuridan, et al. [62] and Lembregts (1990). Appropriate curve fitting routines were employed to estimate the natural frequencies, damping and mode shapes of the plates, depending on the intensity of coupling modes. The single degree of freedom (SDOF) method was used for the well separated modes of some configuration and the multiple degree of freedom (MDOF) routines were adopted to identify the modal properties of heavily coupled spectrums. The natural frequencies and mode shapes obtained from experiment are presented in the results and discussion section along with the theoretical results.

5.4 Results and Discussion for Vibration Analysis

The present finite element model is first being validated by running a few existing cases of frequency analysis and comparing the results with some published values. One of these analyses was the frequency evaluation of a single stiffened isotropic plate with simply supported boundary conditions as

used by B.R. Long [41] and Aksu and Ali [40]. The dimensions of the plate used was (24" x 16" x 0.25") and that of the stiffener was (0.875" x 0.5"). The details of the plate and stiffener are shown in the Fig. 38. Table 7 shows a comparison of the first few frequencies of the present model and those of published results and NASTRAN results are presented. Another analysis was made for unstiffened laminated crossply composite plate with simply supported boundary conditions. The compared values are shown in detail in Table 8.

Isotropic Stiffened Plate.

*Stiffener Size 0.875" * 0.5"*
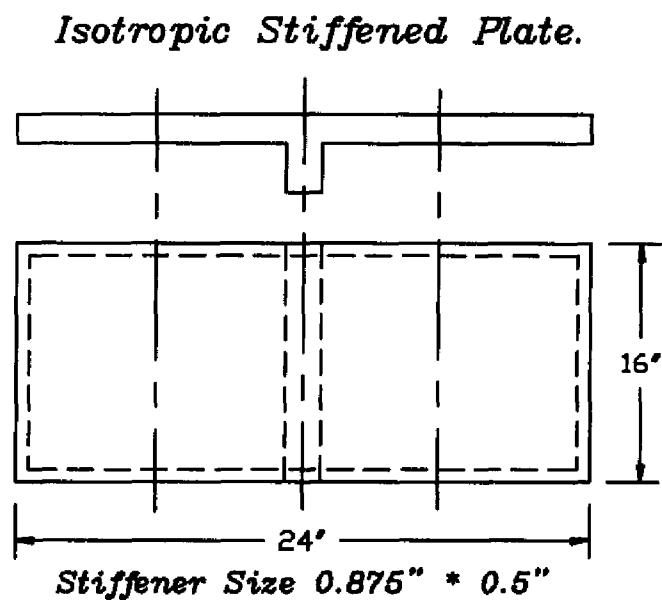
Fig. 38 Simply Supported Plate From Ref. [40]

Table 7. Comparison of Frequencies (Hz) For Isotropic Stiffened Plate

Mode Shape #	Present	Ref. [40, 41]*	NASTRAN
1	231.5	224.0	234.6
2	275.2	273.6	275.8
3	487.7	484.9	492.7
4	781.3	777.4	776.8
5	1112.2	1098.6	1082.3

*: Ref. [41]- Long, B.R., Ref. [40]- Aksu, G. and Ali, R.

Table 8. Laminated Composite (0/90/0) SSSS Plate

Frequency Parameter	Mode #	Present	Reference	Reference
Square Plate Ω	1 2	15.267 22.786	14.697 22.132 Ref. [37]	14.725 22.055 Ref. [38]
Skew (30) Plate $\sqrt{\lambda}$	1	22.27	23.64 Ref. [29]	22.73 NASTRAN

$\bar{\Omega} = (\omega a^2/h)\sqrt{\rho/E_2}$, $\sqrt{\lambda} = \sqrt{(\rho t \omega^2 a^4/\sqrt{D_1 D_2})}$, fibers at $0°$.

With proper validation of the present model with stiffened isotropic and composite plates, sixteen cases have been considered for further study. Out of them ten were for rectangular composite plates and six were for the 30° skew composite plates. The four stiffening conditions used are

      i) Unstiffened

      ii) Single stiffened

      iii) Single stiffened across

and   iv) Double stiffened.

For all the cases, the two opposite long edges were free. The three different boundary conditions applied to the other two opposite short edges were

      i) Clamped-clamped

      ii) Clamped-free (Cantilever)

      iii) Free-free

The plates used were composed of thirteen layers of crossply (0°/90°) laminates. Each lamina being 0.015" thick with a total plate thickness of 0.195". The top and the bottom laminae have the fiber direction along the longer edge of the plate. The stiffeners were composed of twenty-five layers of unidirectional (0°/0°) with fibers along the length of the stiffener. Each lamina had a thickness of 0.01" with a total stiffener thickness of 0.25". The depth of the stiffeners was 0.75" in all of the above cases. The material used for this analysis was Scotchply composites for which the material properties are listed in the Table 1. In each case considered, the experimental results were compared with those of NASTRAN and the present theoretical values. The first ten natural frequencies for each composite plate along with their first few mode shapes are presented in the following pages from case 1 to case 16. An example of a typical theoretical model finite element meshing and NASTRAN meshing for a single stiffened clamped-clamped plate are shown in the Fig. 39 and Fig. 40, respectively. The damping presented in the following cases is (*C/2M*) for the critical damp and hence its units are in Hz.
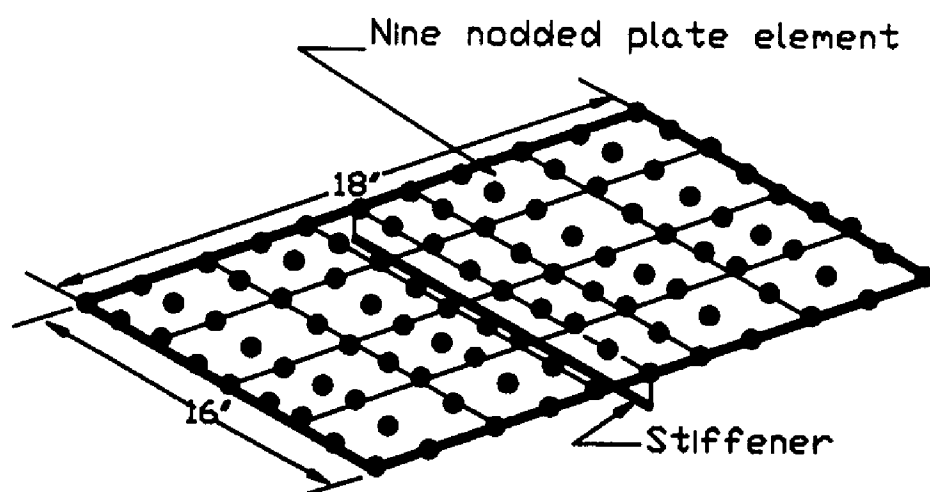
Fig. 39 Theoretical Model Meshing

Number of elements   = 20

Number of nodes   = 99

Total number of DOF   = 495
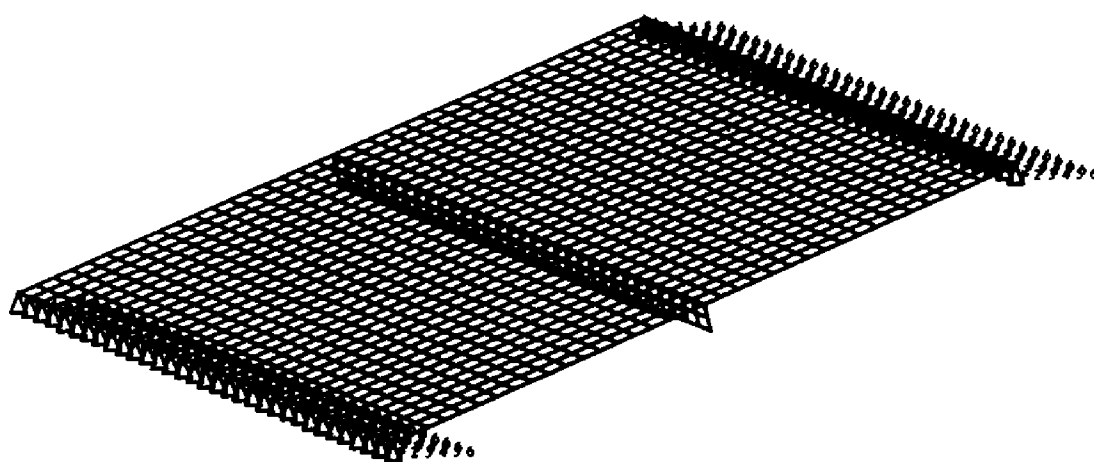
Fig. 40 Typical NASTRAN Meshing

Case: 1

Plate:	Crossply composite plate (18" x 16").
Stiffener:	No stiffener.
B.C.:	Two opposite small edges clamped and other two free.
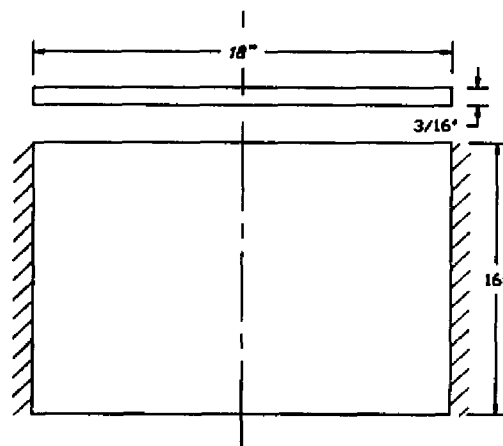
Fig. 41 Clamped-Clamped Unstiffened Plate

Table 9. Frequency in Cycles/sec (Hz.)

Mode No.	Type of Mode	Present (Hz.)	NASTRAN (Hz.)	Expt. (Hz.)	Damp. (Hz.)	Damp. (%)
1	1st Bending	81.22	80.61	80.43	0.385	0.478
2	1st Twisting	92.50	91.71	90.71	0.416	0.458
3	2nd Twisting	173.67	169.41	151.73	0.733	0.483
4	2nd Bending	231.01	222.22	205.32	5.610	2.730
5	Coupled	243.13	237.61	240.29	1.230	0.510
6	Coupled	304.53	299.16	294.77	1.870	0.635
7	Coupled	328.21	323.44	308.56	2.050	0.665
8	3rd Bending	465.04	457.02	447.77	4.810	1.070
9	Coupled	490.00	475.81	459.54	2.700	0.587
10	Coupled	538.52	527.35	515.12	4.060	0.788

Mode # 1

Mode # 2

Mode # 3

Mode # 4

Mode # 5

Fig. 42   **Mode   Shapes   For   Clamped-Clamped   Unstiffened Composite Plate**

Mode # 1

Mode # 2

Mode # 3

Mode # 4

Mode # 5

Mode # 6
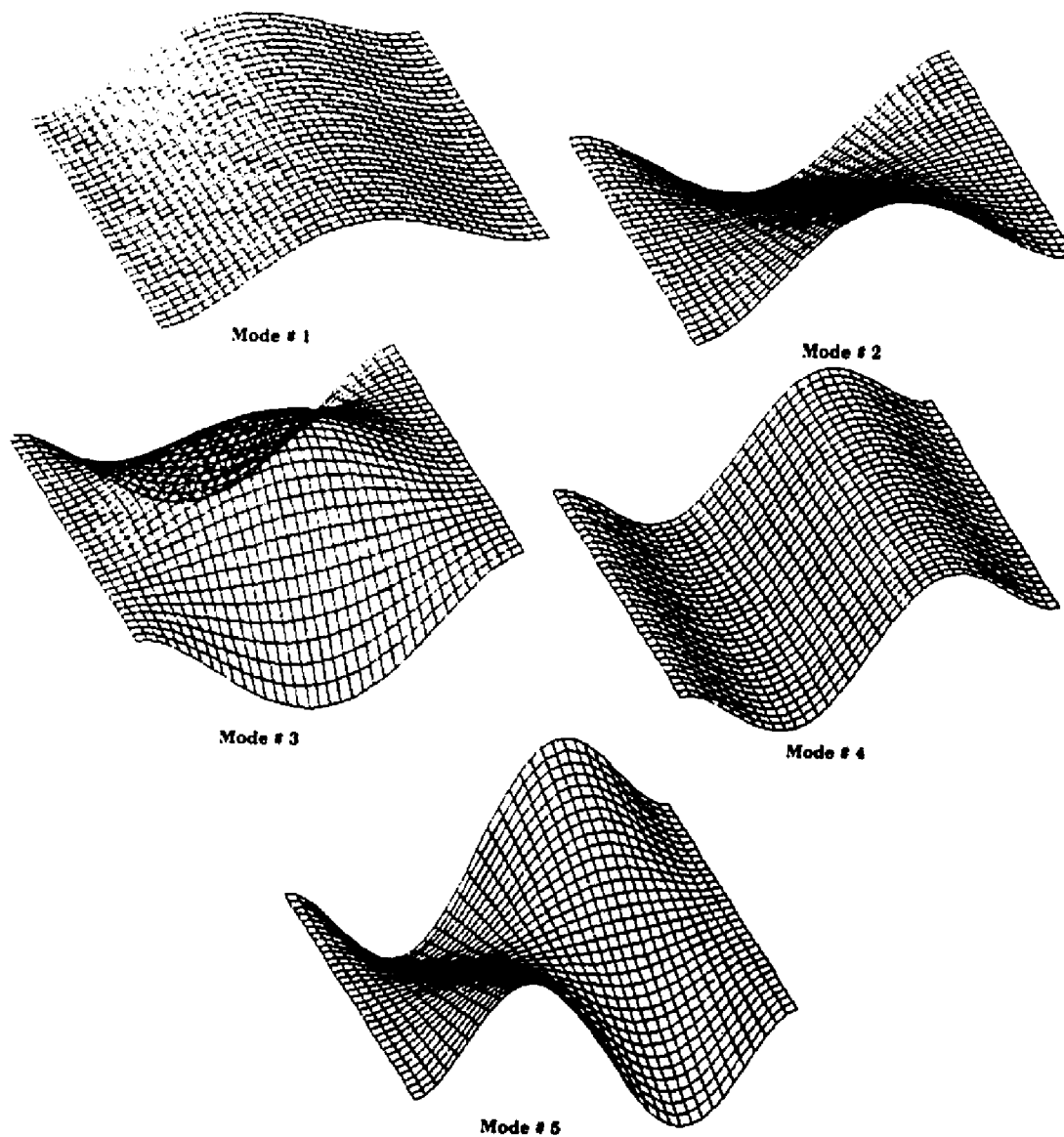
Fig. 43   **Experimental Mode Shapes For Clamped-Clamped Unstiffened Composite Plate**

Case: 2

Plate: Crossply composite plate (18" x 16").
Stiffener: Single stiffener along 16" side symmetrically placed.
B.C.:   Two opposite small edges clamped and other two free.
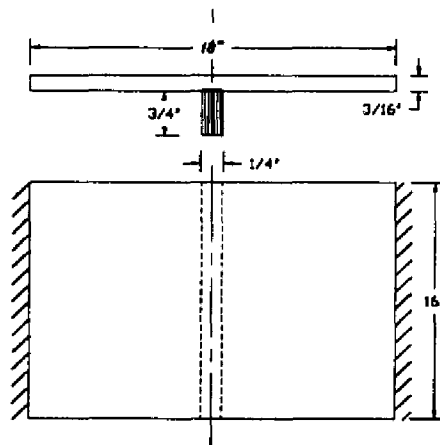
Fig. 44 Clamped-Clamped Single Stiffened Plate

Table 10. Frequency in Cycles/sec (Hz.)

Mode No.	Type of Mode	Present (Hz.)	NASTRAN (Hz.)	Expt. (Hz.)
1	1st Bending	78.13	75.69	76.01
2	1st Twisting	88.60	86.14	86.34
3	2nd Bending	224.09	221.70	223.08
4	2nd Twisting	228.11	222.20	--
5	Coupled	243.42	240.31	240.32
6	Coupled	327.11	314.63	300.00
7	3rd Bending	409.00	416.52	--
8	Coupled	447.31	431.84	440.21
9	3rd Twisting	490.00	471.00	--
10	Coupled	513.89	483.81	594.43

-- Modes missed during the experiment.

Mode # 1

Mode # 2

Mode # 3

Mode # 4

Mode # 5

Mode # 6

Mode # 7

Mode # 8

Fig. 45   Mode Shapes For Clamped-Clamped Single Stiffened Composite Plate

Case: 3

Plate: Crossply composite plate (18" x 16").
Stiffener: Single stiffener along 18" side symmetrically placed.
B.C.:   Two opposite small edges clamped and other two free.
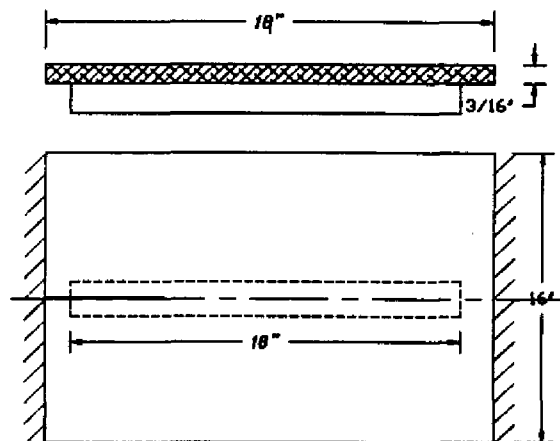
Fig. 46 Clamped-Clamped Single Stiffened Plate

Table 11. Frequency in Cycles/sec (Hz.)

Mode No.	Type of Mode	Present (Hz.)	NASTRAN (Hz.)	Expt. (Hz.)	Damp. (Hz.)	Damp. (%)
1	1st Bending	87.33	92.35	90.98	0.450	0.494
2	1st Twisting	94.12	92.67	101.79	0.474	0.466
3	2nd Twisting	182.70	173.70	188.75	1.090	0.578
4	Coupled	240.11	239.01	238.72	1.590	0.667
5	2nd Bending	246.20	245.53	--	--	--
6	3rd Twisting	323.67	362.73	308.23	1.300	0.422
7	Coupled	357.00	373.20	--	--	--
8	Coupled	440.73	453.94	432.23	3.430	0.794
9	3rd Bending	480.21	460.11	--	--	--
10	Coupled	511.00	478.40	--	--	--

-- Modes missed during the experiment.

Mode # 1

Mode # 2

Mode # 3

Mode # 4

Mode # 5

Mode # 6

Mode # 7

Mode # 8

Fig. 47   **Mode Shapes For Clamped-Clamped Cross Stiffened Composite Plate**

Mode # 1

Mode # 2

Mode # 3

Mode # 4

Mode # 6

Mode # 7
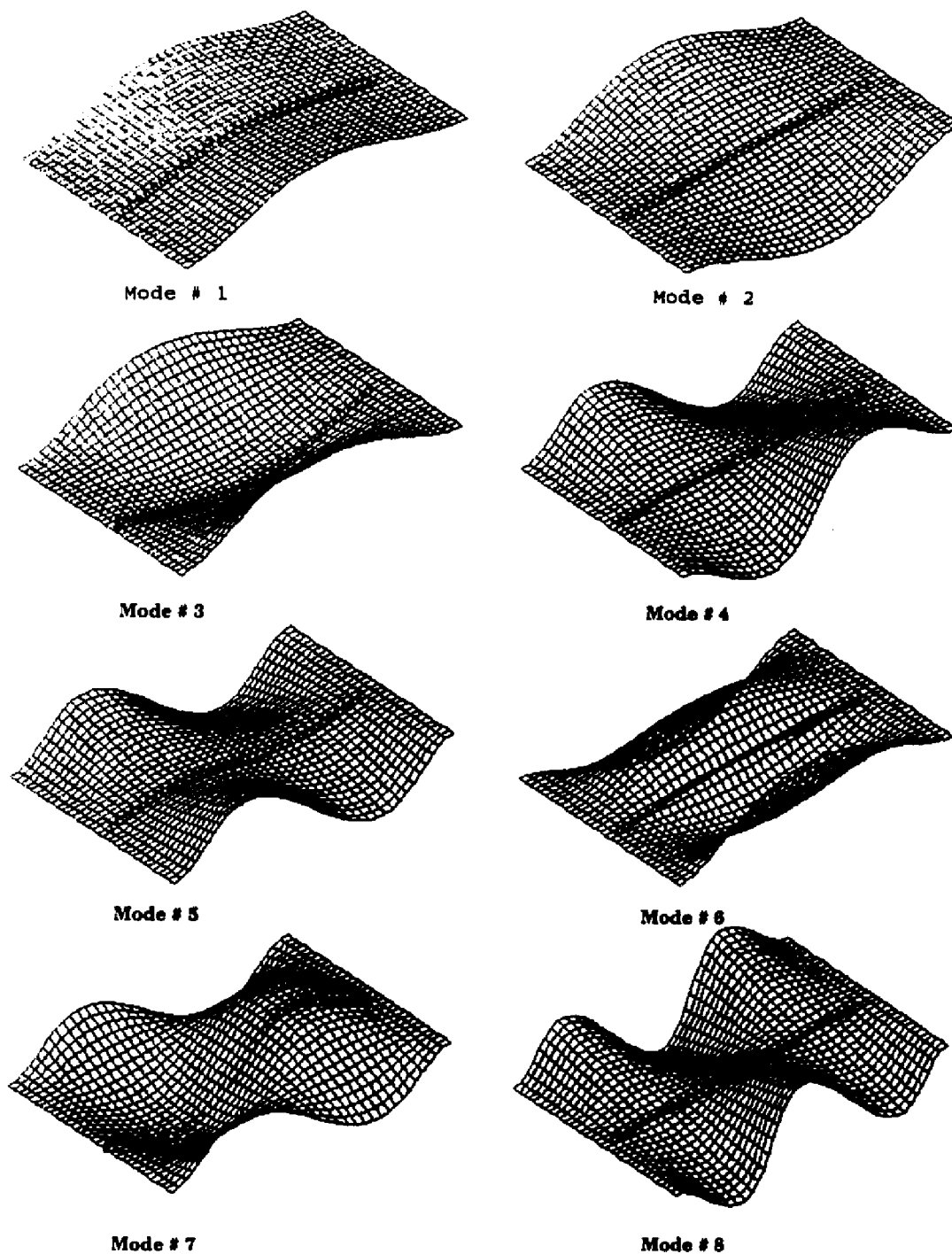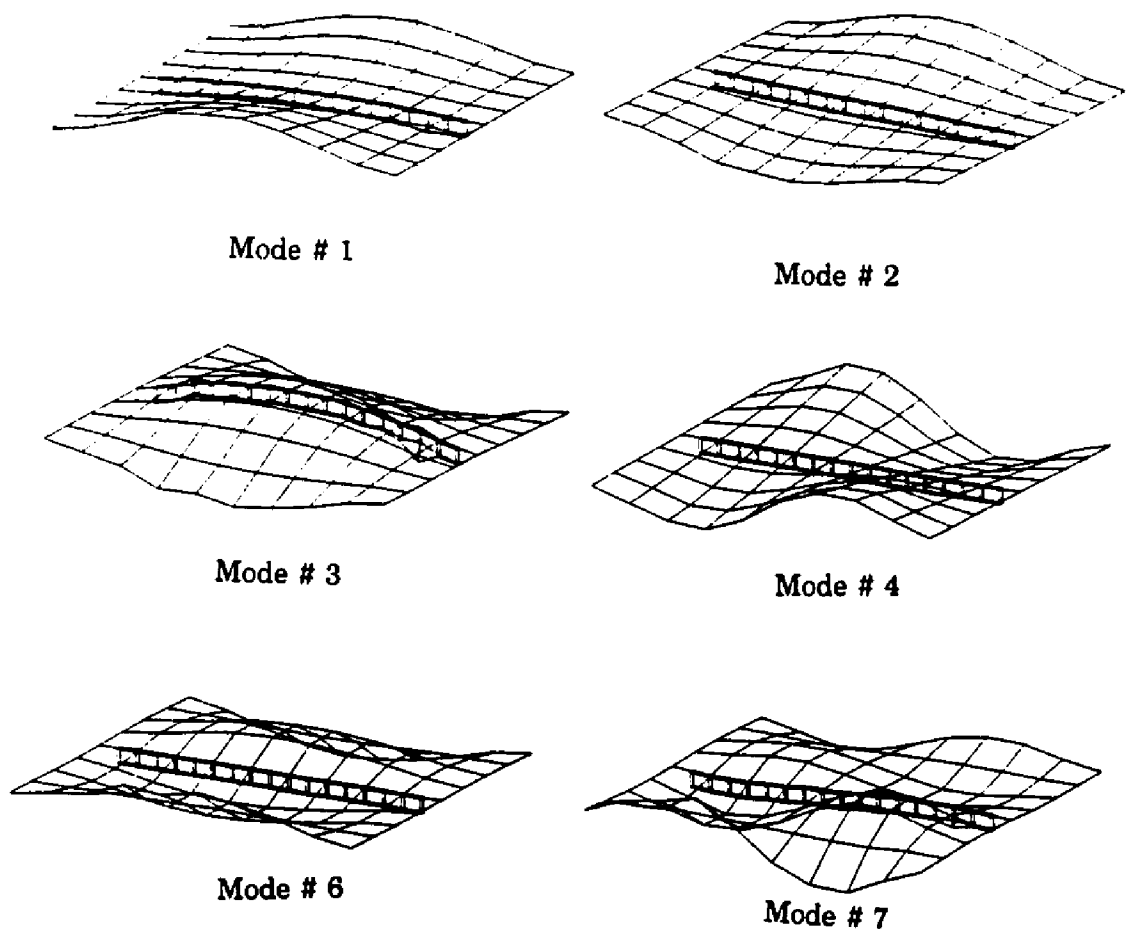
Fig. 48   Experimental Mode Shapes For Clamped-Clamped Cross
Stiffened Composite Plate

Case: 4

Plate: Crossply composite plate (18" x 16").
Stiffener: Double stiffener along 16" side symmetrically placed.
B.C.:   Two opposite small edges clamped and other two free.
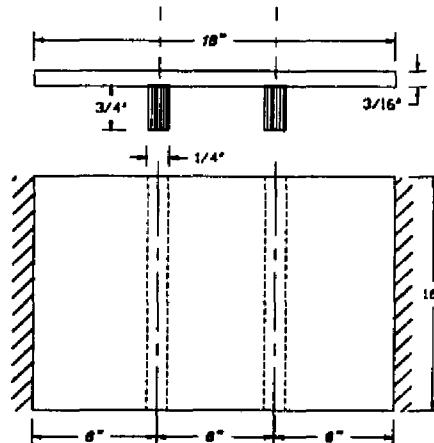
Fig. 49 Clamped-Clamped Double Stiffened Plate

Table 12. Frequency in Cycles/sec (Hz.)

Mode No.	Type of Mode	Present (Hz.)	NASTRAN (Hz.)	Expt. (Hz.)	Damp. (Hz.)	Damp. (%)
1	1st Bending	74.10	74.73	64.69	1.370	2.120
2	1st Twisting	88.27	86.69	74.13	-1.910	-2.570
3	2nd Bending	195.21	201.00	174.01	0.631	0.362
4	Coupled	209.82	215.52	189.84	1.410	0.741
5	2nd Twist	248.44	238.61	375.00	-3.470	-0.924
6	Coupled	319.90	343.23	--	--	--
7	3rd Bending	431.13	429.00	420.45	1.050	0.250
8	Coupled	453.22	451.82	456.93	0.693	-0.151
9	Coupled	491.10	533.26	497.39	1.330	0.267
10	Coupled	573.91	544.89	632.28	0.239	0.037

-- Modes missed during the experiment.
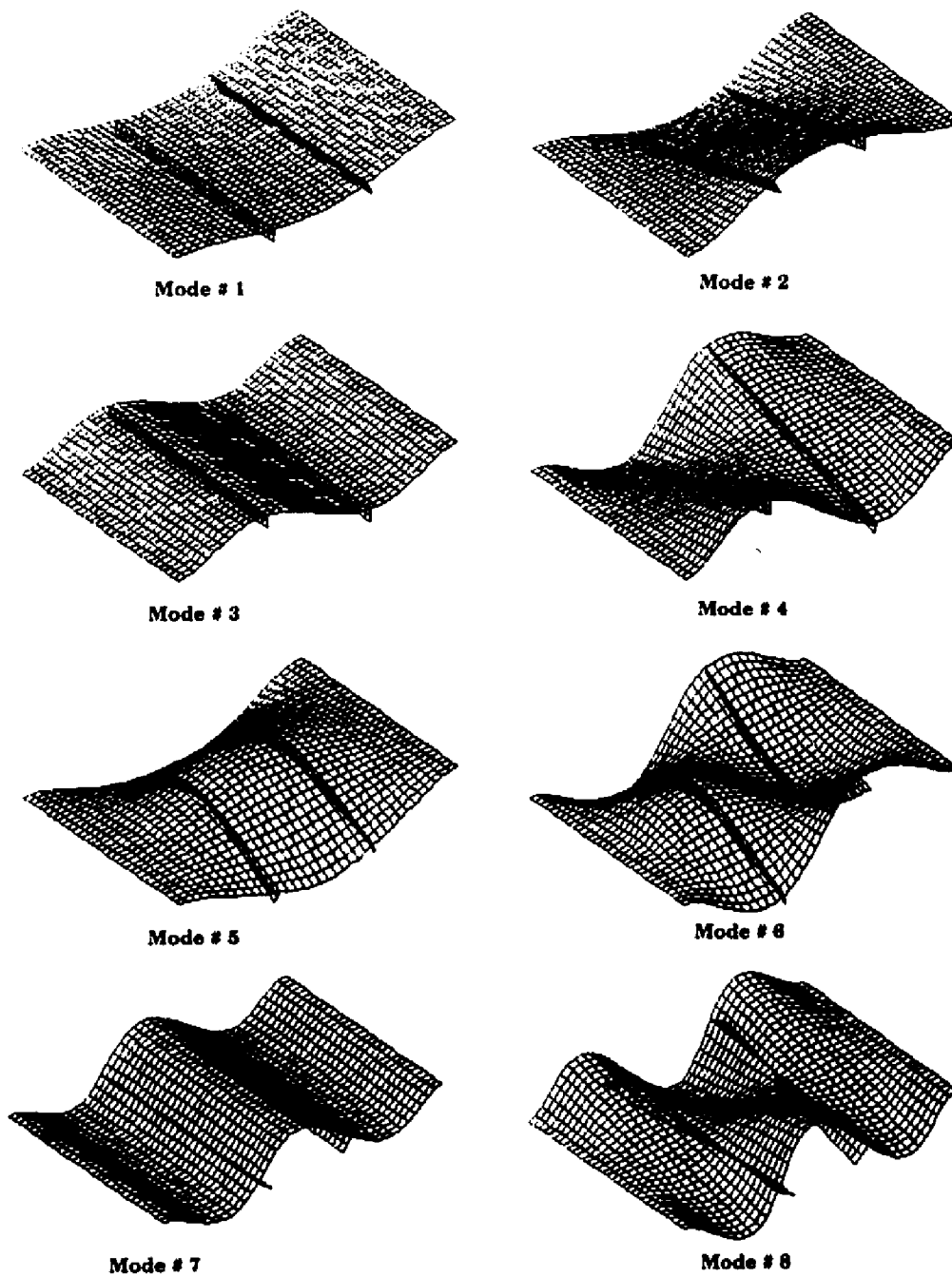
Mode # 1

Mode # 2

Mode # 3

Mode # 4

Mode # 5

Mode # 6

Mode # 7

Mode # 8

Fig. 50   **Mode Shapes For Clamped-Clamped Double Stiffened Composite Plate**

Mode # 1   Mode # 2

Mode # 3   Mode # 4

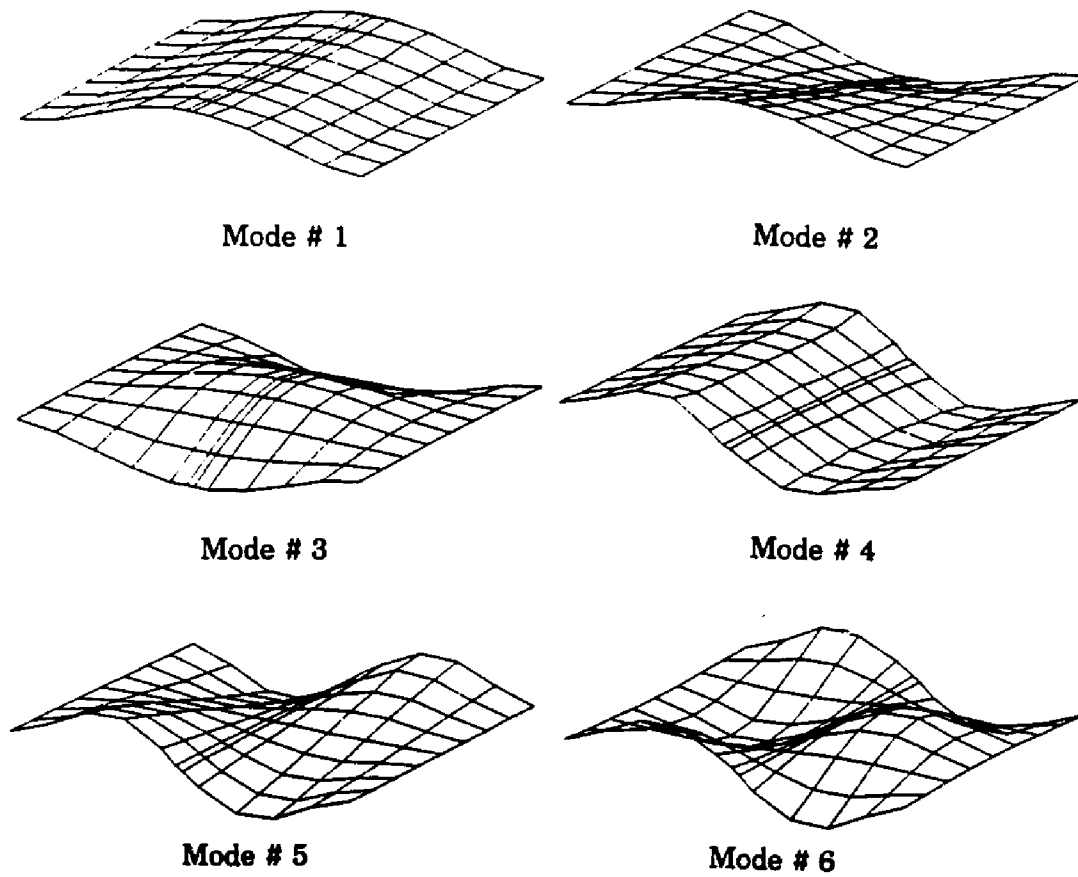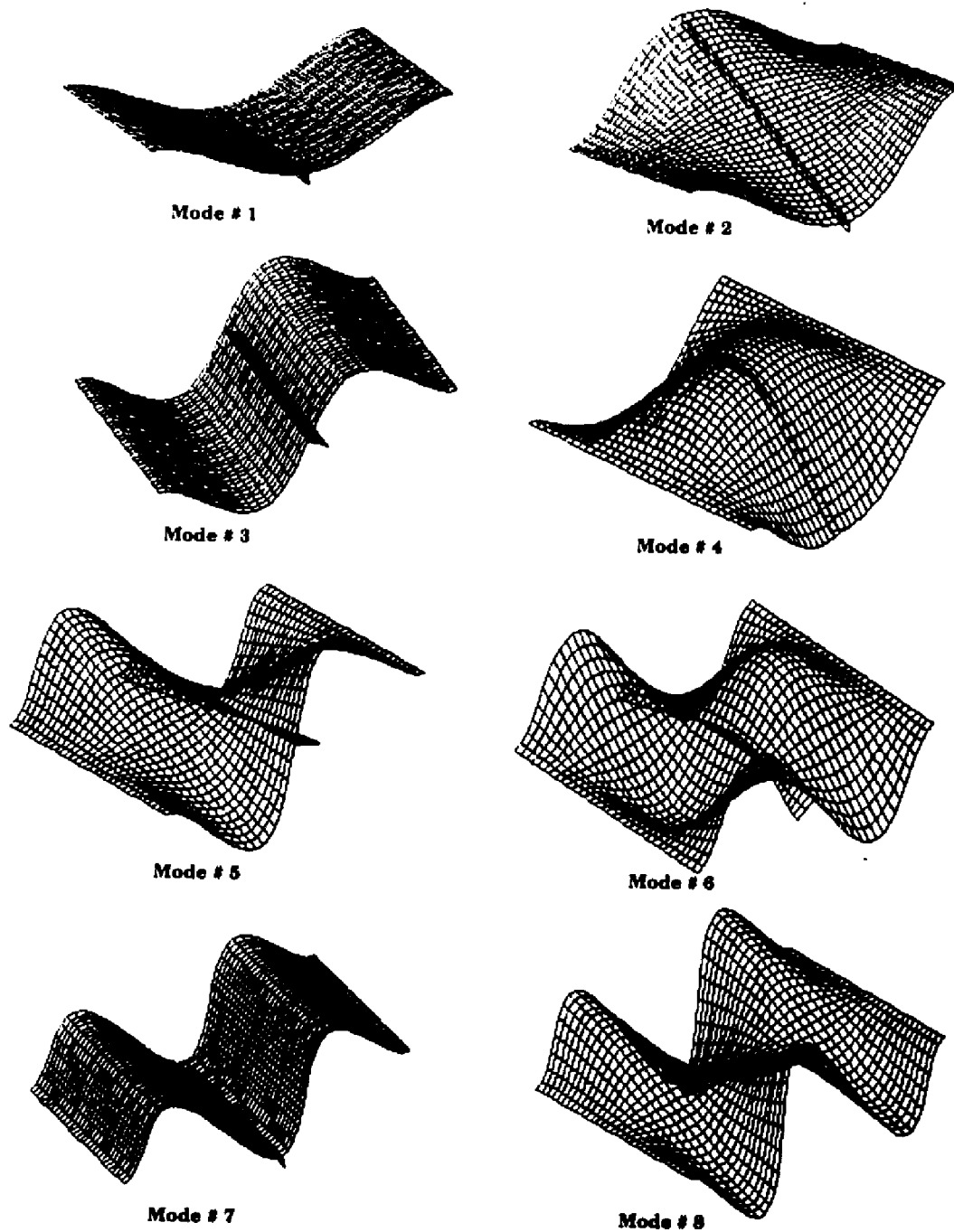Mode # 5   Mode # 6

Fig. 51   Experimental Mode Shapes For Clamped-Clamped Double
            Stiffened Composite Plate

Case: 5

Plate: Crossply composite plate (19" x 16").
Stiffener: No stiffener.
B.C.:   One 16" edge clamped and other three free.
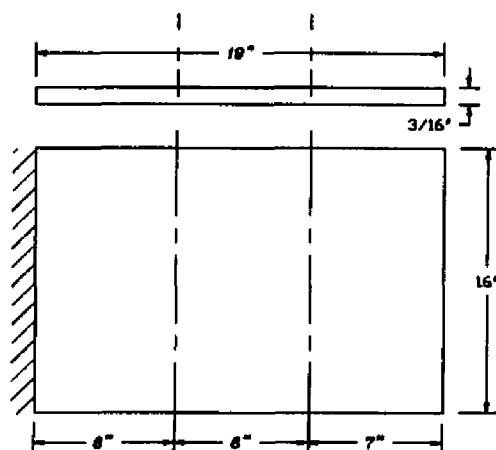
Fig. 52 Cantilever Unstiffened Plate

Table 13. Frequency in Cycles/sec (Hz.)

Mode No.	Type of Mode	Present (Hz.)	NASTRAN (Hz.)	Expt. (Hz.)
1	1st Bending	14.21	11.36	12.00
2	1st Twisting	27.33	25.66	24.00
3	2nd Bending	71.63	71.06	66.00
4	Coupled	95.32	96.48	88.00
5	2nd Twisting	124.70	126.50	122.00
6	Coupled	189.34	189.11	186.00
7	3rd Bending	202.68	199.42	210.00
8	Coupled	243.70	223.32	--
9	Coupled	295.34	311.25	--
10	3rd Twisting	327.85	331.56	--

-- Modes missed during the experiment.

Mode # 1

Mode # 2

Mode # 3

Mode # 4

Mode # 5

Mode # 6

Mode # 7

Mode # 8
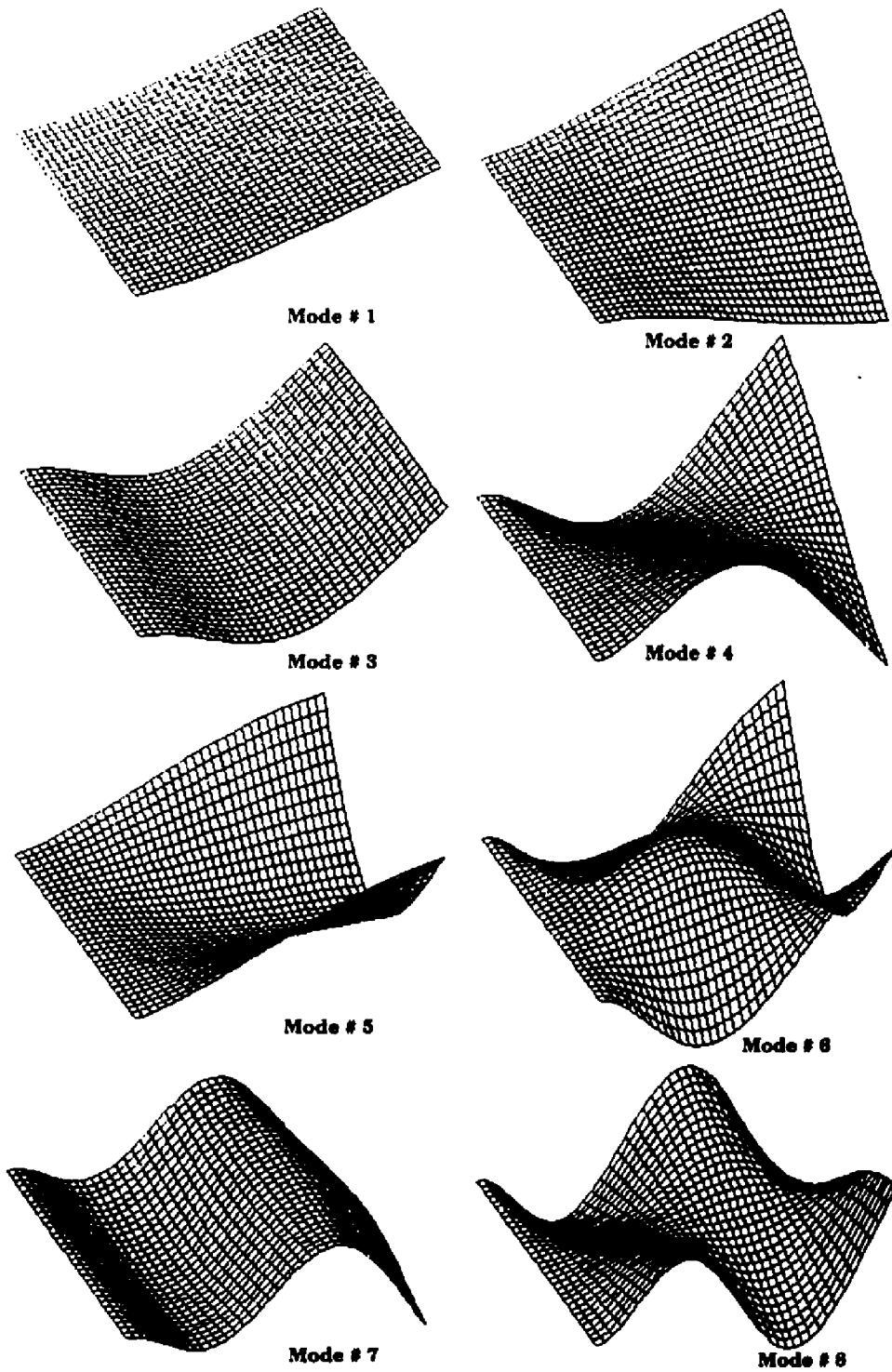
Fig. 53 Mode Shapes For Cantilever Unstiffened Composite Plate

Case: 6

Plate: Crossply composite plate (19" x 16").
Stiffener: Single stiffener along 16" side at 2/3rd position.
B.C.:   One 16" edge clamped and other three free.
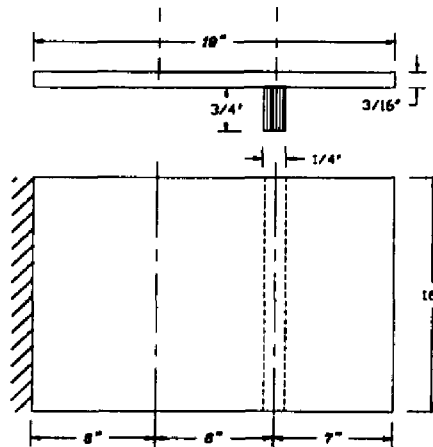
Fig. 54 Cantilever Single Stiffened Plate

Table 14. Frequency in Cycles/sec (Hz.)

Mode No.	Type of Mode	Present (Hz.)	NASTRAN (Hz.)	Expt. (Hz.)
1	1st Bending	13.60	11.08	10.00
2	1st Twisting	26.56	25.69	24.00
3	2nd Bending	72.06	69.34	66.00
4	Coupled	102.35	96.52	90.00
5	2nd Twisting	167.81	157.41	160.00
6	3rd Bending	202.67	193.32	182.00
7	Coupled	213.50	204.53	204.00
8	Coupled	243.93	216.40	--
9	Coupled	319.00	329.72	--
10	3rd Twisting	378.84	367.81	--

-- Modes missed during the experiment.

Mode # 1

Mode # 2

Mode # 3

Mode # 4

Mode # 5

Mode # 6

Mode # 7

Mode # 8

Fig. 55 Mode Shapes For Cantilever Single Stiffened Composite Plate

Case: 7

Plate: Crossply composite plate (19" x 16").
Stiffener: Single stiffener along 19" side symmetrically placed.
B.C.:   One 16" edge clamped and other three free.
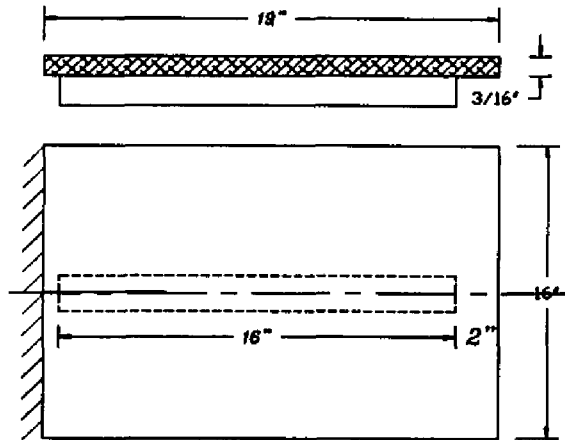
Fig. 56 Cantilever Single Stiffened Plate

Table 15. Frequency in Cycles/sec (Hz.)

Mode No.	Type of Mode	Present (Hz.)	NASTRAN (Hz.)	Expt. (Hz.)
1	1st Bending	16.34	13.79	15.00
2	1st Twisting	26.71	26.48	24.00
3	2nd Bending	93.01	90.50	95.00
4	Coupled	102.62	98.14	103.00
5	2nd Twisting	131.04	122.90	110.00
6	Coupled	206.50	199.00	202.00
7	Coupled	238.55	224.92	227.00
8	3rd Bending	248.00	229.93	242.00
9	3rd Twisting	324.07	331.40	331.00
10	Coupled	378.12	383.32	--

-- Modes missed during the experiment.
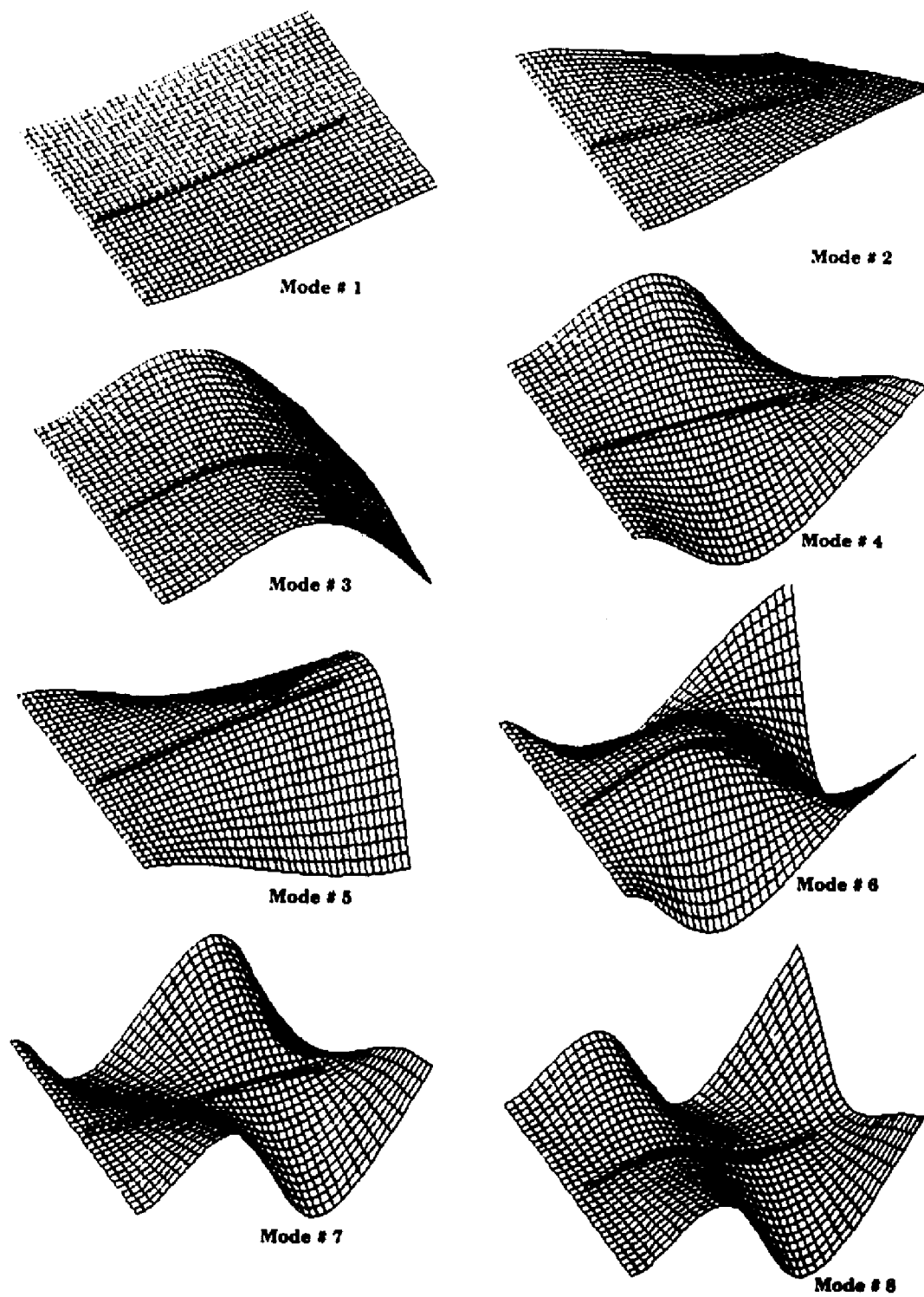
Fig. 57 Mode Shapes For Cantilever Cross Stiffened Composite Plate

Case: 8

Plate: Crossply composite plate (19" x 16").
Stiffener: Double stiffener along 16" side symmetrically placed.
B.C.:   One 16" edge clamped and other three free.
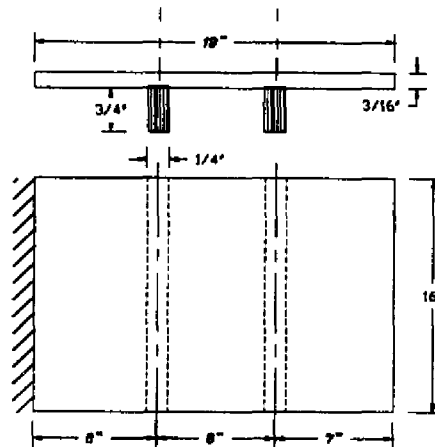
Fig. 58 Cantilever Double Stiffened Plate

Table 16. Frequency in Cycles/sec (Hz.)

Mode No.	Type of Mode	Present (Hz.)	NASTRAN (Hz.)	Expt. (Hz.)	Damp. (Hz.)	Damp. (%)
1	1st Bending	13.71	11.06	9.01	0.503	5.580
2	1st Twisting	28.63	26.46	23.94	0.313	1.310
3	2nd Bending	66.03	67.43	63.16	0.159	0.252
4	Coupled	96.70	94.17	86.37	0.443	0.513
5	2nd Twisting	165.05	158.00	161.97	0.724	0.447
6	3rd Bending	194.11	183.50	174.03	0.954	0.548
7	Coupled	212.48	206.00	194.24	0.870	0.448
8	Coupled	267.07	242.30	251.37	1.170	0.329
9	Coupled	338.16	342.80	354.01	2.240	0.571
10	3rd Twisting	359.27	367.80	391.81	2.200	0.492

Mode # 1

Mode # 2

Mode # 3

Mode # 4

Mode # 5

Mode # 6

Mode # 7

Mode # 8

Fig. 59 Mode Shapes For Cantilever Double Stiffened Composite Plate

Mode # 2

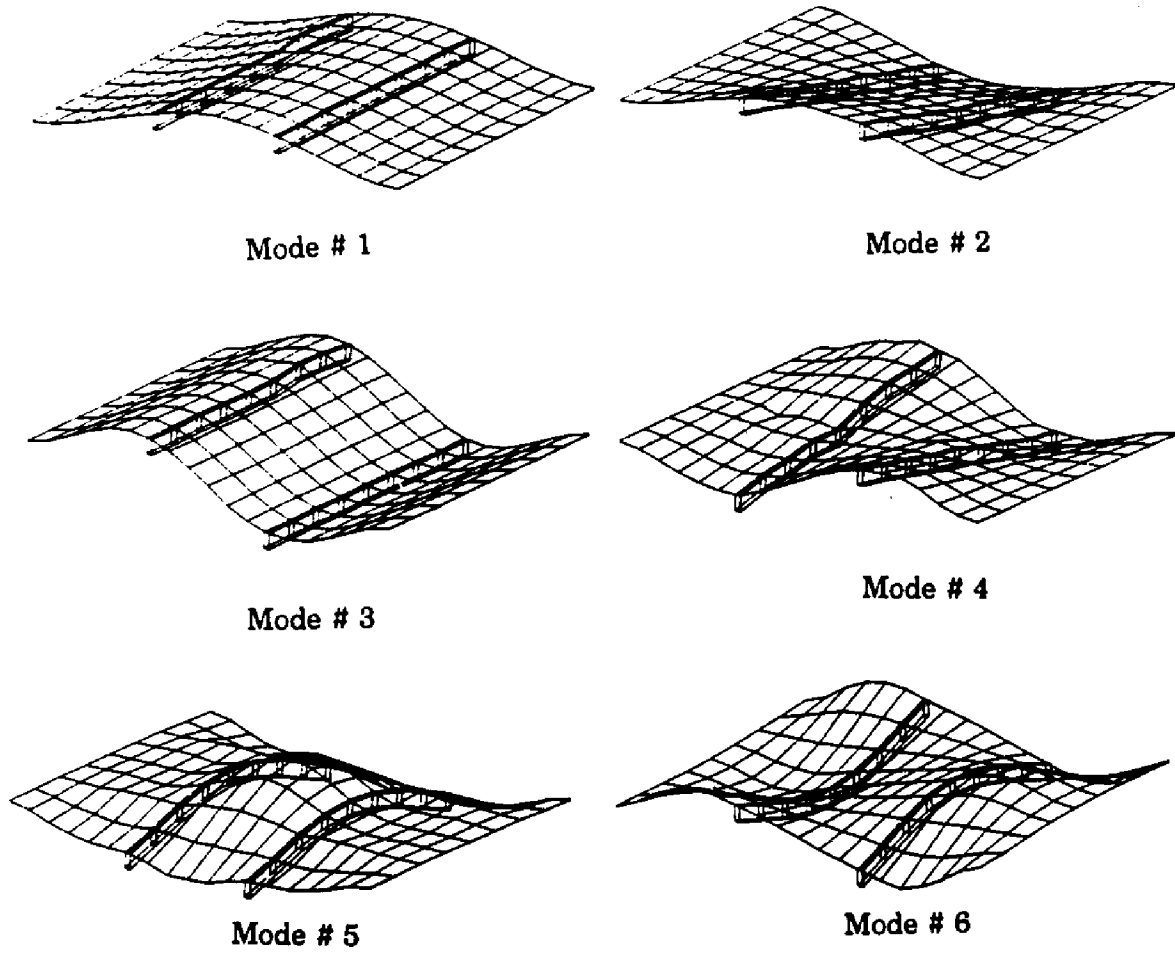Mode # 3

Mode # 4

Mode # 5

Mode # 6

Mode # 7
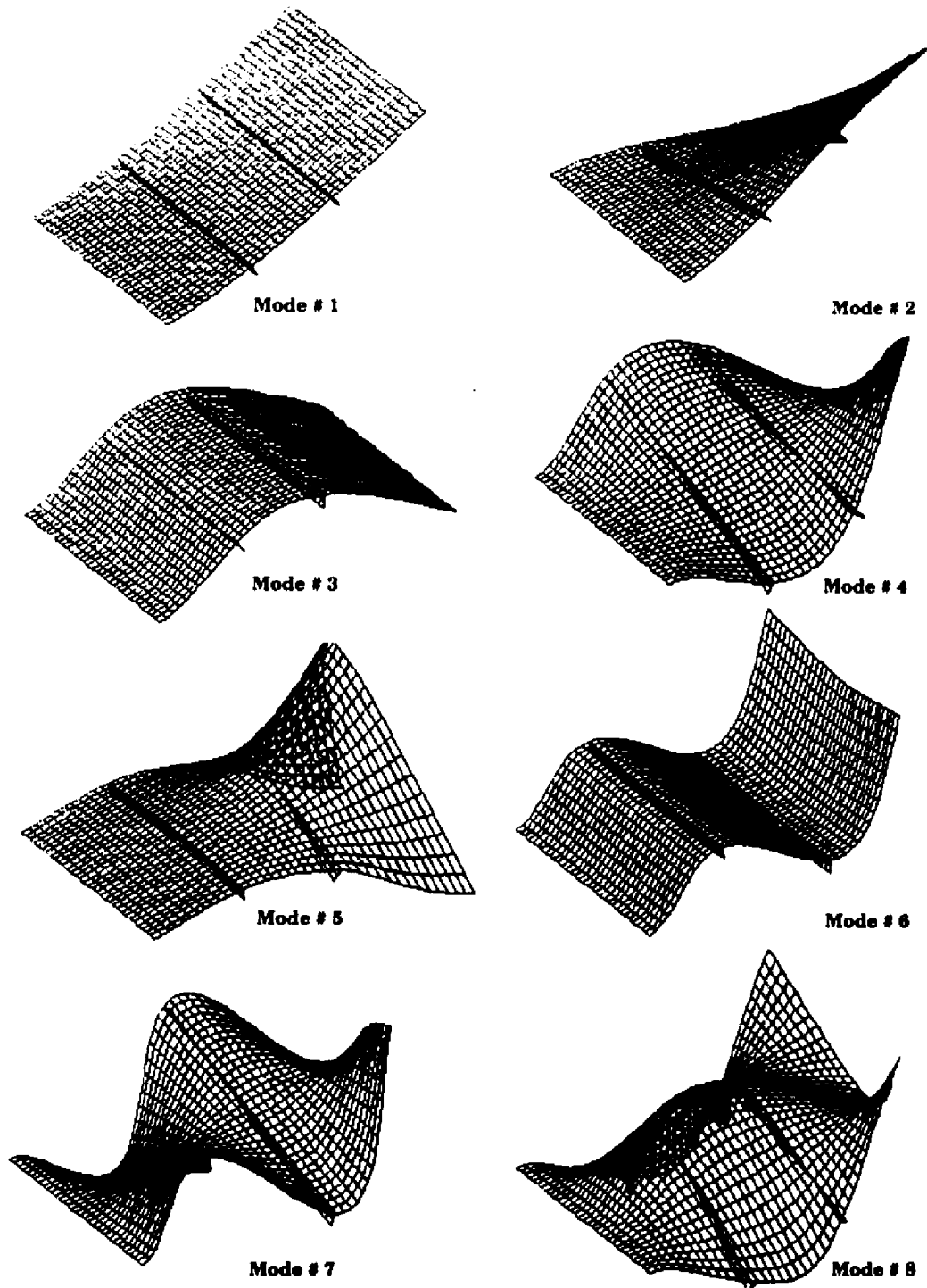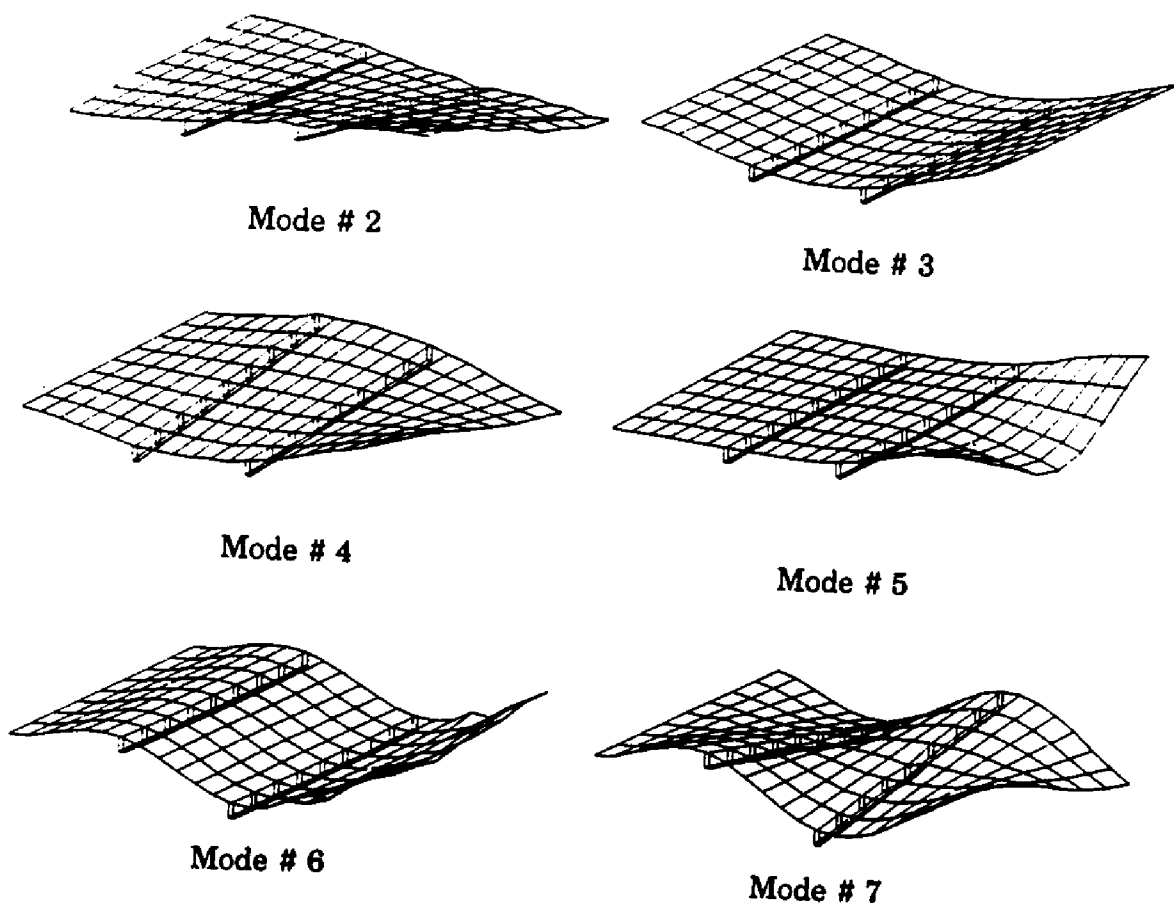
Fig. 60   **Experimental Mode Shapes For Cantilever Double Stiffened Composite Plate**

Case: 9

Plate: Crossply composite plate (20" x 16").
Stiffener: No Stiffener.
B.C.:   All sides free.
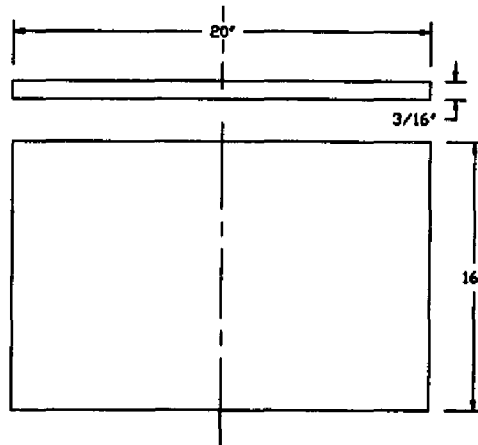
Fig. 61 Free-Free Unstiffened Plate

Table 17. Frequency in Cycles/sec (Hz.)

Mode No.	Type of Mode	Present (Hz.)	NASTRAN (Hz.)	Expt. (Hz.)
1	1st Twisting	36.88	37.83	34.00
2	1st Bending	67.13	64.96	64.00
3	Coupled	107.39	100.42	94.00
4	2nd Bending	126.70	118.40	115.00
5	2nd Twisting	153.06	140.00	133.00
6	3rd Bending	189.77	179.63	177.00
7	Coupled	217.33	204.91	194.00
8	Coupled	235.76	211.83	204.00
9	Coupled	338.00	315.10	301.00
10	Coupled	367.71	325.16	316.00

Mode # 1

Mode # 2

Mode # 3

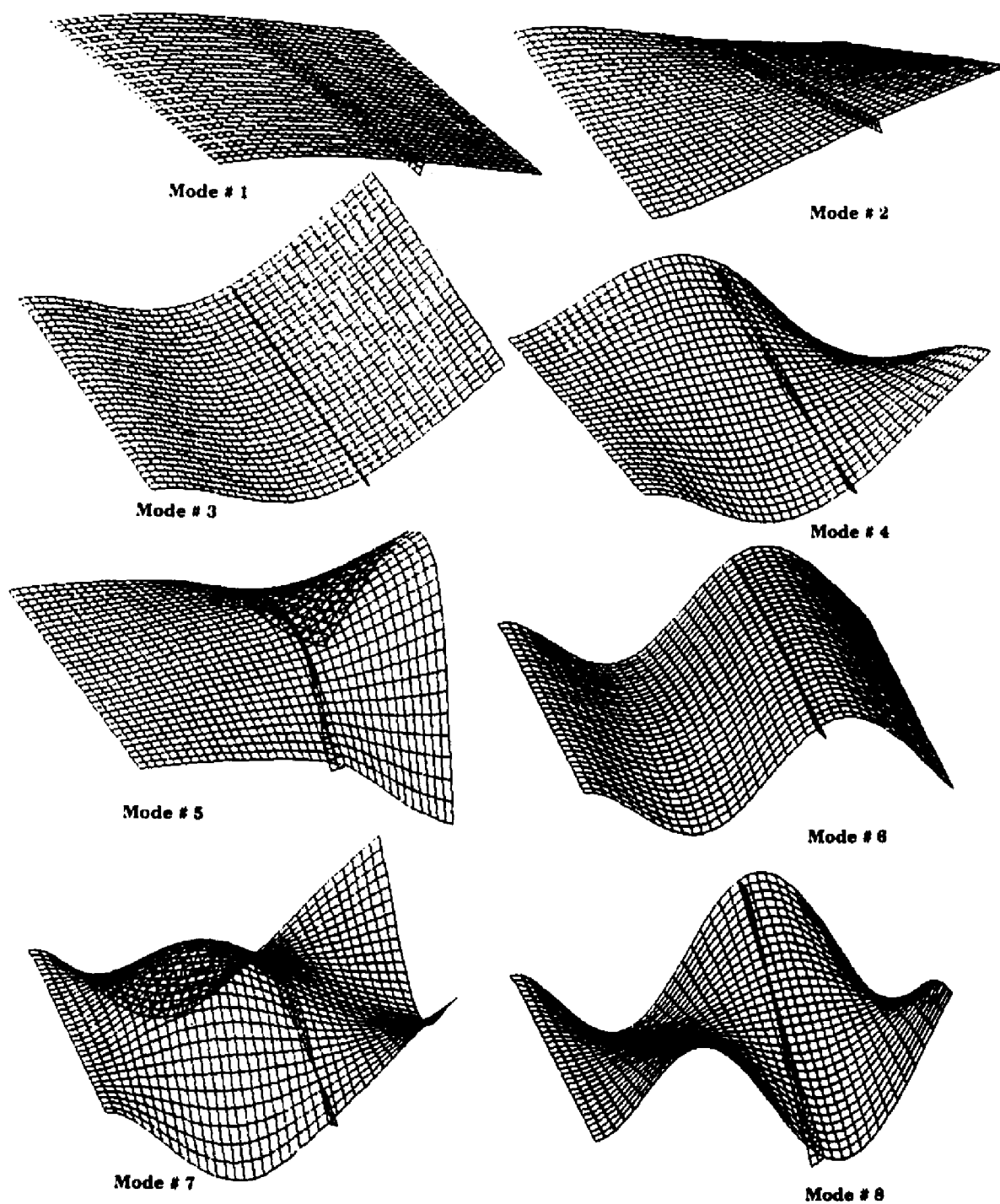Mode # 4

Mode # 5

Mode # 6

Mode # 7

Mode # 8
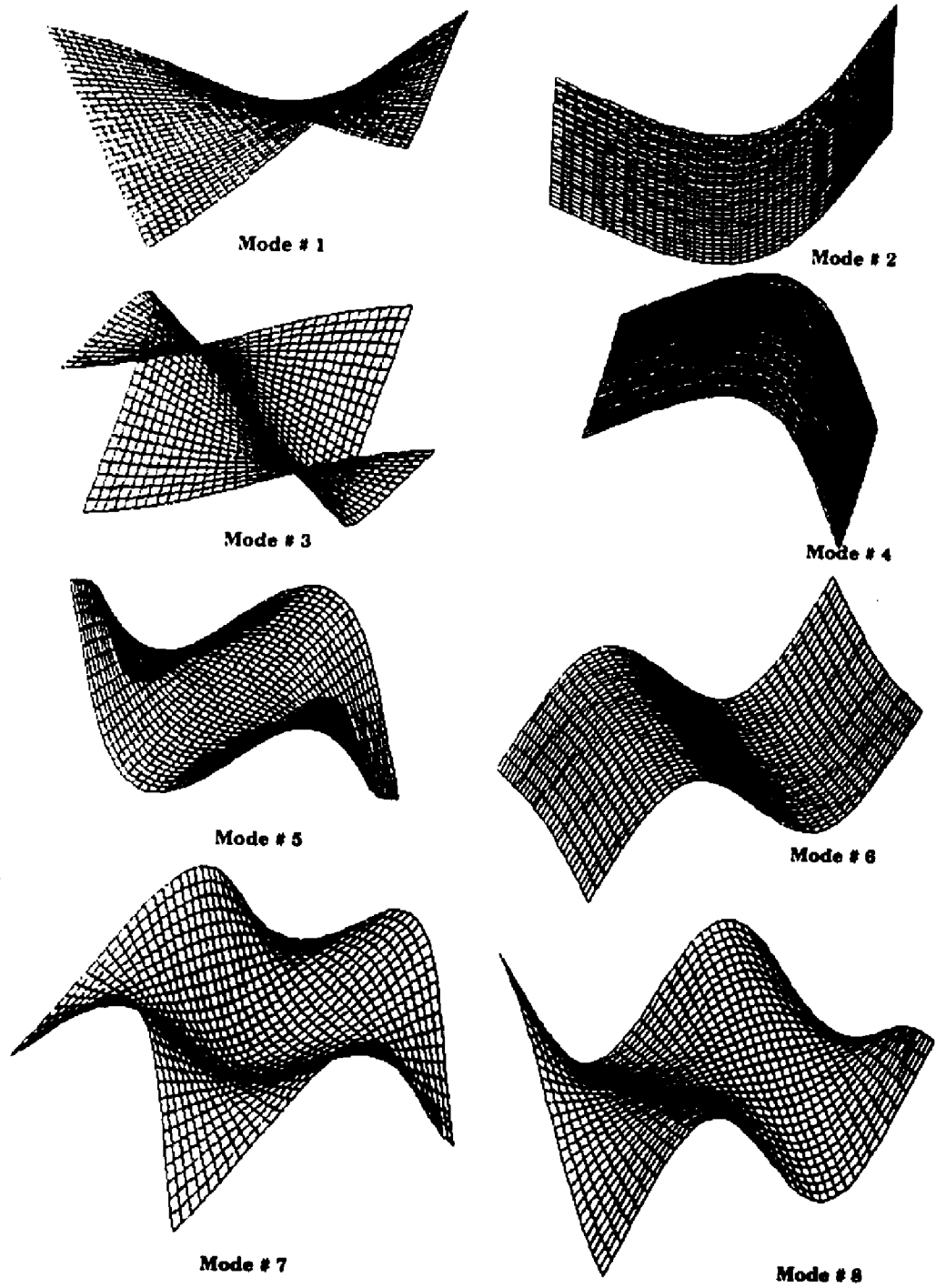
Fig. 62 Mode Shapes For Free-Free Unstiffened Composite Plate

Case: 10

Plate: Crossply composite plate (20" x 16").
Stiffener: Single stiffener along 20" side symmetrically placed.
B.C.:   All sides free.
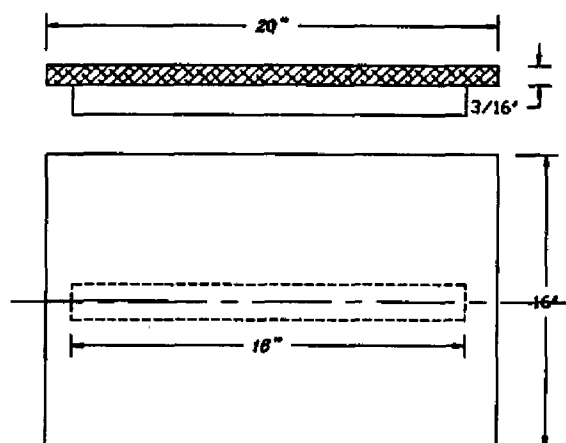
Fig. 63 Free-Free Single Stiffened Plate

Table 18. Frequency in Cycles/sec (Hz.)

Mode No.	Type of Mode	Present (Hz.)	NASTRAN (Hz.)	Expt. (Hz.)
1	1st Twisting	36.23	39.39	34.00
2	1st Bending	77.18	91.20	94.00
3	Coupled	98.56	102.52	101.00
4	2nd Bending	125.06	114.50	114.00
5	2nd Twisting	140.57	136.92	142.00
6	Coupled	193.00	213.61	222.00
7	3rd Bending	223.03	216.10	232.00
8	Coupled	247.44	221.60	268.00
9	3rd Bending	307.71	324.53	290.00
10	Coupled	338.48	345.10	354.00

Mode # 1

Mode # 2

Mode # 3

Mode # 4

Mode # 5

Mode # 6

Mode # 7

Mode # 8
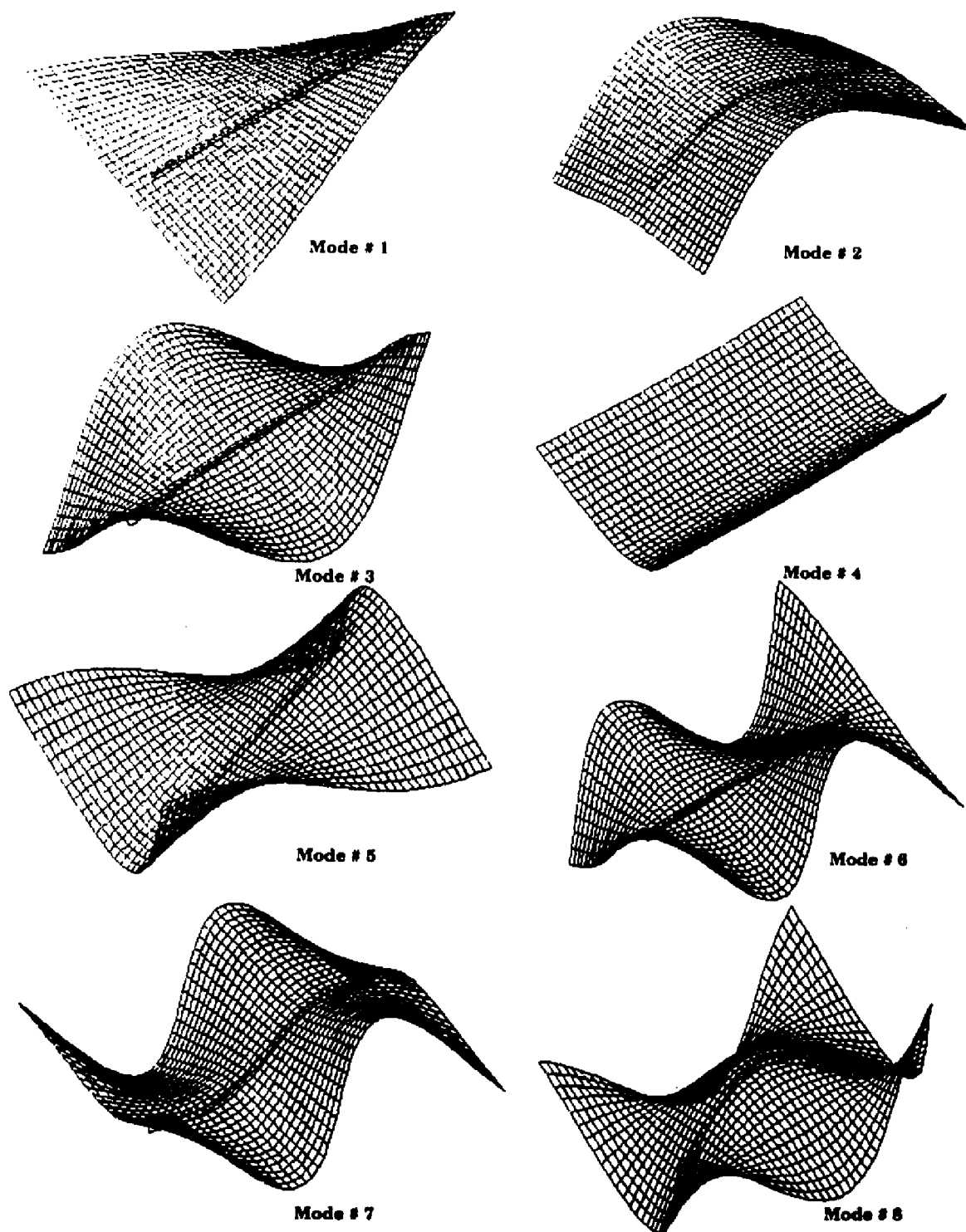
Fig. 64 Mode Shapes For Free-Free Cross Stiffened Composite Plate

Case: 11

Plate: Crossply composite skew plate (18" x 16").
Stiffener: No stiffener.
B.C.:   Two opposite 16" edges clamped and other two free.
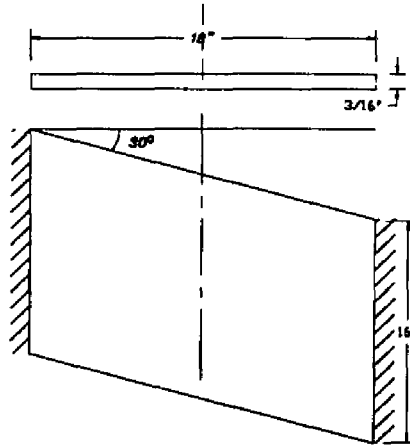
Fig. 65 Clamped-Clamped Unstiffened Skew Plate

Table 19. Frequency in Cycles/sec (Hz.)

Mode No.	Type of Mode	Present (Hz.)	NASTRAN (Hz.)	Expt. (Hz.)
1	1st Bending	79.43	77.86	74.00
2	1st Twisting	93.38	91.34	85.00
3	2nd Twisting	168.11	170.11	155.00
4	2nd Bending	221.00	214.55	207.00
5	Coupled	253.48	242.61	226.00
6	Coupled	294.86	283.19	259.00
7	Coupled	369.71	403.61	356.00
8	Coupled	403.00	407.79	378.00
9	3rd Bending	457.02	436.82	--
10	Coupled	493.51	457.60	--

-- Modes missed during the experiment.

Mode # 1

Mode # 2

Mode # 3

Mode # 4

Mode # 5

Mode # 6

Mode # 7

Mode # 8

Fig. 66   **Mode Shapes For Clamped-Clamped Unstiffened Composite Skew Plate**

Case: 12

Plate: Crossply composite skew plate (18" x 16").
Stiffener: Single stiffener along 16" side symmetrically placed.
B.C.:   Two opposite 16" edges clamped and other two free.
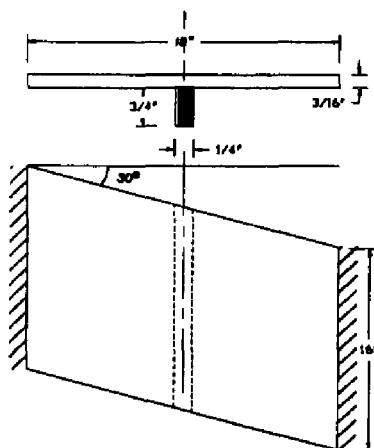
Fig. 67 Clamped-Clamped Single Stiffened Skew Plate

Table 20. Frequency in Cycles/sec (Hz.)

Mode No.	Type of Mode	Present (Hz.)	NASTRAN (Hz.)	Expt. (Hz.)	Damp. (Hz.)	Damp. (%)
1	1st Bending	73.90	73.43	69.73	0.374	0.537
2	1st Twisting	89.31	86.37	76.46	0.128	0.168
3	2nd Bending	198.48	216.10	219.01	1.330	0.608
4	2nd Twisting	215.10	216.62	288.08	1.580	0.549
5	Coupled	243.75	254.22	294.15	2.020	0.685
6	Coupled	358.11	325.31	442.63	3.910	0.882
7	3rd Bending	423.06	402.20	462.95	3.090	0.668
8	Coupled	471.49	431.00	610.64	4.490	0.734
9	Coupled	504.50	459.42	701.46	5.890	0.840
10	3rd Twisting	548.00	487.92	793.28	7.300	0.919

Mode # 1

Mode # 2

Mode # 3

Mode # 4

Mode # 5

Mode # 6

Mode # 7

Mode # 8

Fig. 68   **Mode Shapes For Clamped-Clamped Single Stiffened Composite Skew Plate**

Case: 13

Plate:	Crossply composite skew plate (19" x 16").
Stiffener:	No stiffener.
B.C.:	One 16" edge clamped and other three free.
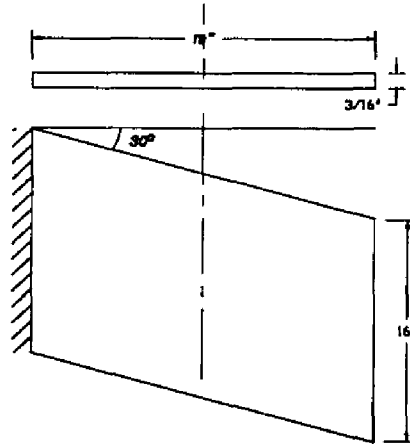
Fig. 69 Cantilever Unstiffened Skew Plate

Table 21. Frequency in Cycles/sec (Hz.)

Mode No.	Type of Mode	Present (Hz.)	NASTRAN (Hz.)	Expt. (Hz.)
1	1st Bending	15.73	10.54	8.00
2	1st Twisting	28.32	25.19	26.00
3	2nd Bending	73.11	67.13	60.00
4	2nd Twisting	89.70	81.79	80.00
5	Coupled	157.56	145.56	131.00
6	Coupled	189.20	162.88	140.00
7	3rd Bending	205.48	193.75	193.00
8	Coupled	248.51	236.86	234.00
9	Coupled	277.93	259.31	243.00
10	Coupled	343.00	345.29	342.00

Mode # 1

Mode # 2

Mode # 3

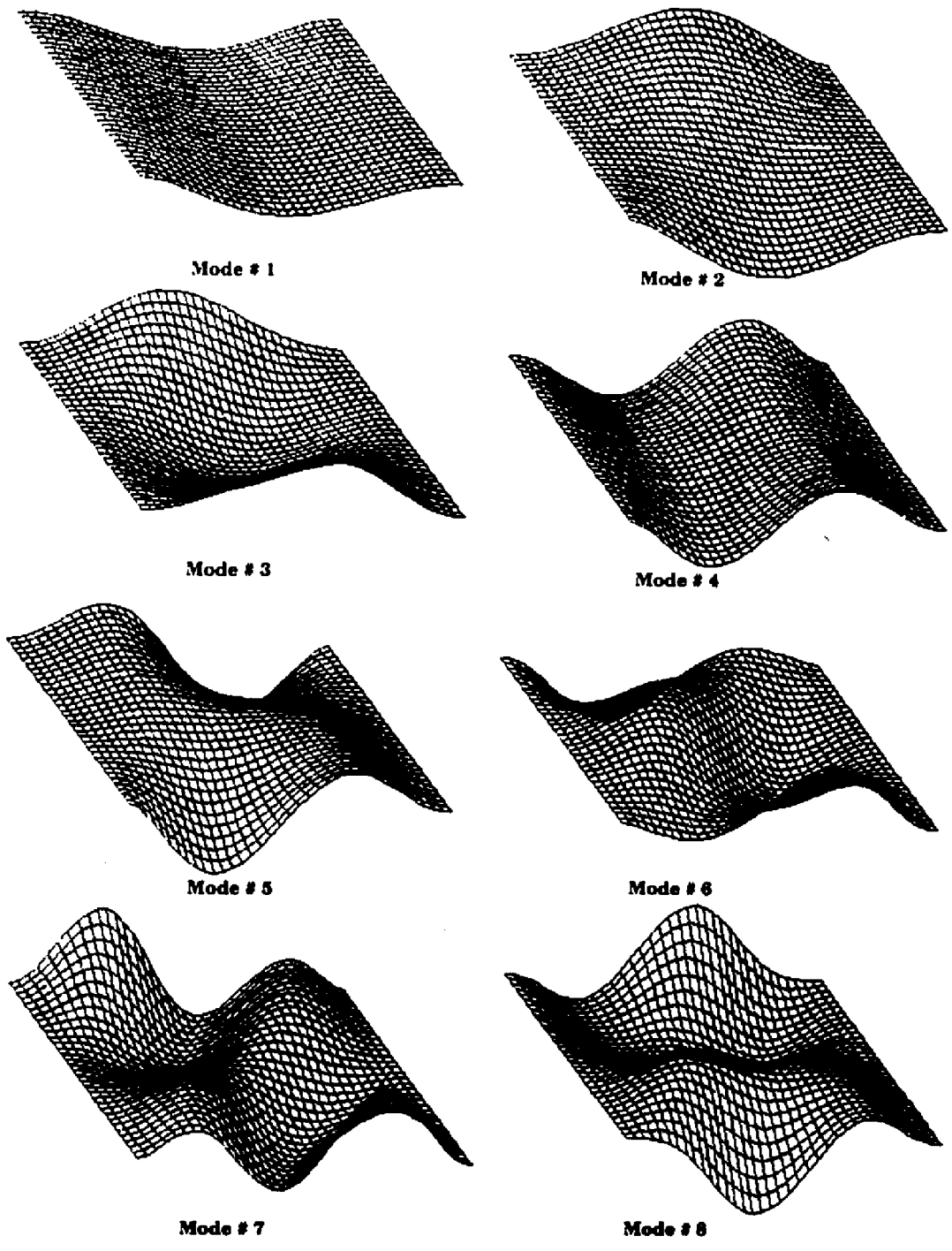Mode # 4

Mode # 5

Mode # 6

Mode # 7

Mode # 8

Fig. 70   Mode Shapes For Cantilever Unstiffened Composite Skew Plate

Case: 14

Plate: Crossply composite skew plate (19" x 16").
Stiffener: Single stiffener along 16" side symmetrically placed.
B.C.:   One 16" edge clamped and other three free.
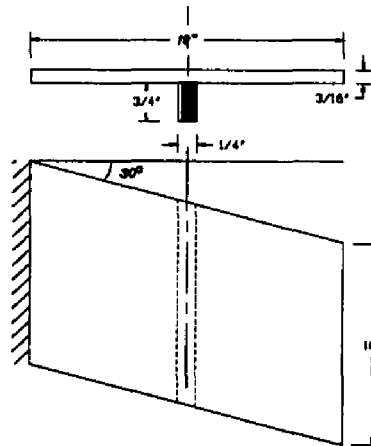
Fig. 71 Cantilever Single Stiffened Skew Plate

Table 22. Frequency in Cycles/sec (Hz.)

Mode No.	Type of Mode	Present (Hz.)	NASTRAN (Hz.)	Expt. (Hz.)	Damp. (Hz.)	Damp. (%)
1	1st Bending	12.51	10.50	8.00	1.680	20.60
2	1st Twisting	29.74	28.98	26.21	0.745	2.840
3	2nd Bending	66.27	64.51	60.00	1.680	2.810
4	Coupled	86.65	82.74	83.42	1.820	2.180
5	2nd Twisting	154.33	146.31	134.45	0.739	0.550
6	3rd Bending	193.26	189.62	189.61	0.766	0.404
7	Coupled	207.64	211.50	228.73	1.080	0.473
8	Coupled	237.50	243.42	244.72	1.130	0.462
9	Coupled	282.00	287.44	293.43	2.080	0.709
10	Coupled	347.21	356.20	335.12	1.680	0.502

Mode # 1

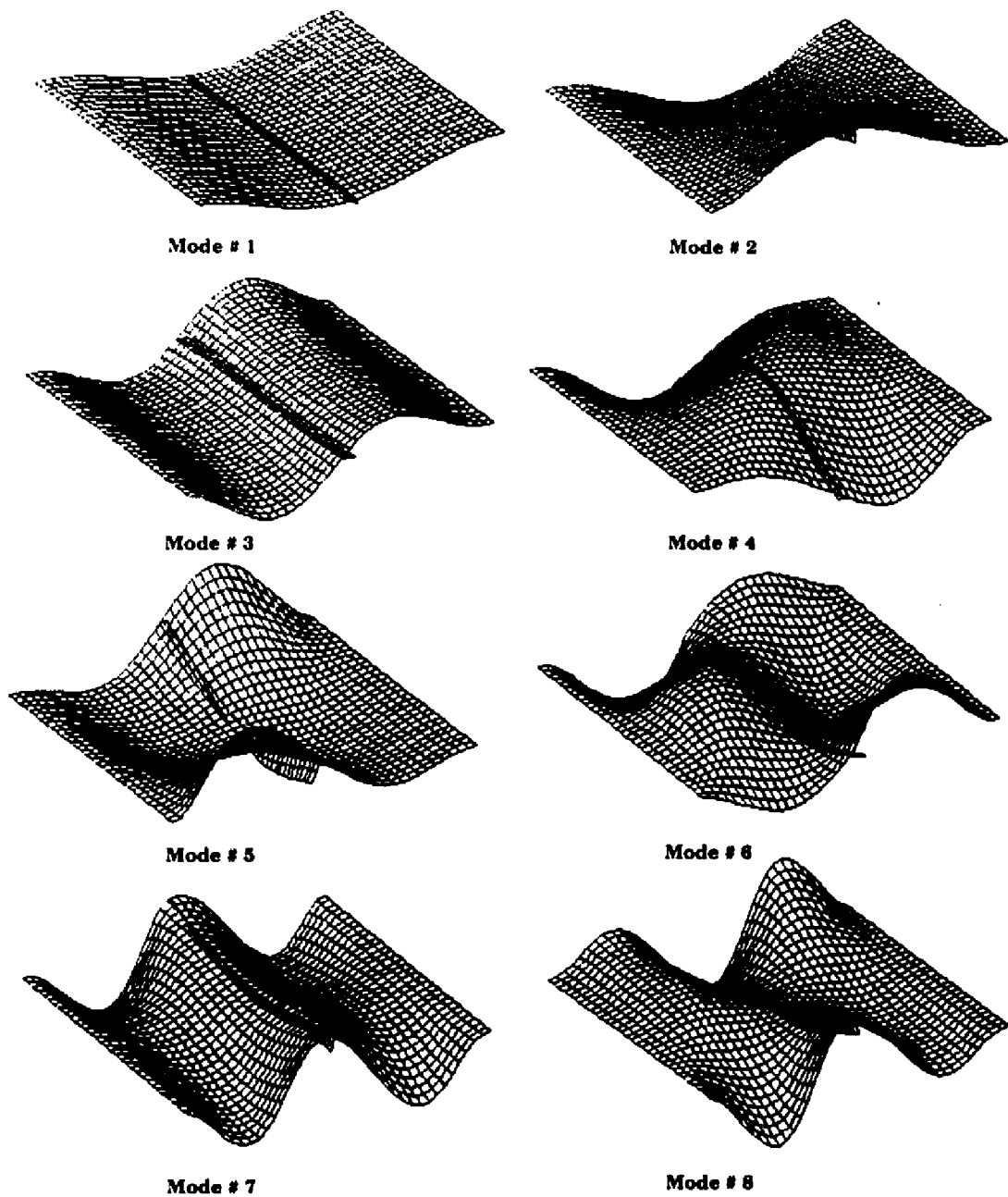Mode # 2

Mode # 3

Mode # 4

Mode # 5

Mode # 6
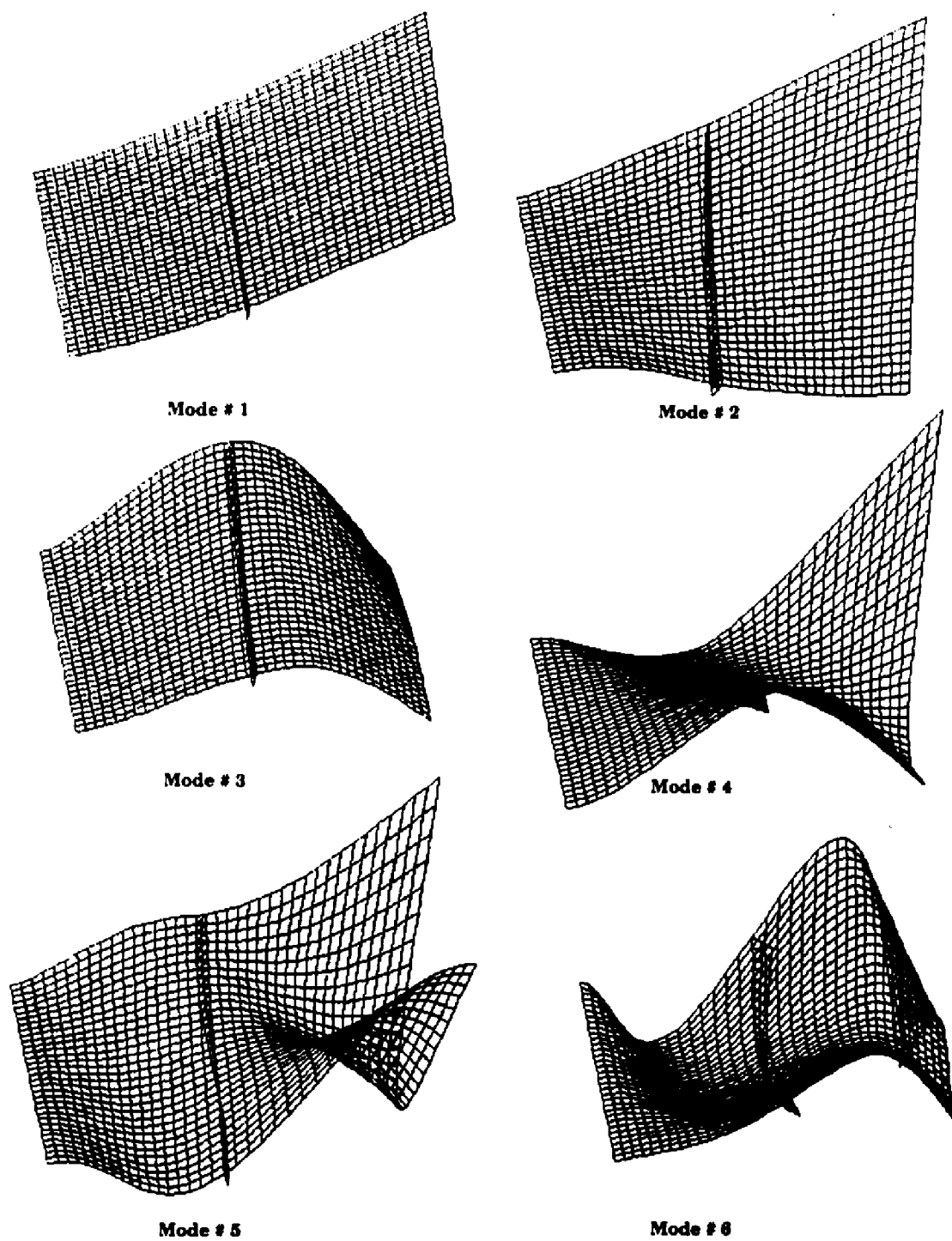
Fig. 72   Mode Shapes For Cantilever Single Stiffened Composite Skew Plate

Case: 15

Plate: Crossply composite skew plate (20" x 16").
Stiffener: No stiffener.
B.C.:   All sides free.
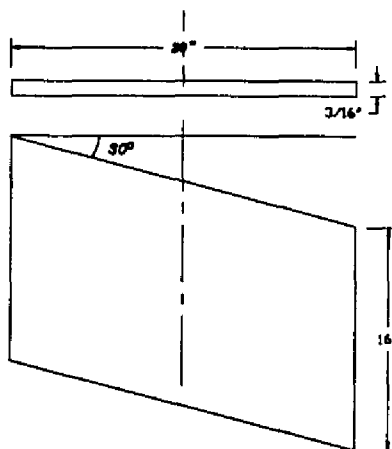
Fig. 73 Free-Free Unstiffened Skew Plate

Table 23. Frequency in Cycles/sec (Hz.)

Mode No.	Type of Mode	Present (Hz.)	NASTRAN (Hz.)	Expt. (Hz.)
1	1st Twisting	35.21	32.20	28.00
2	1st Bending	62.98	62.67	60.00
3	2nd Twisting	84.10	77.21	73.00
4	Coupled	133.00	128.41	117.00
5	2nd Bending	151.54	146.60	134.00
6	Coupled	169.00	159.11	138.00
7	Coupled	194.27	189.30	190.00
8	Coupled	226.76	229.90	233.00
9	Coupled	253.60	240.71	247.00
10	Coupled	317.65	312.52	312.00

Mode # 1

Mode # 2

Mode # 3

Mode # 4

Mode # 5

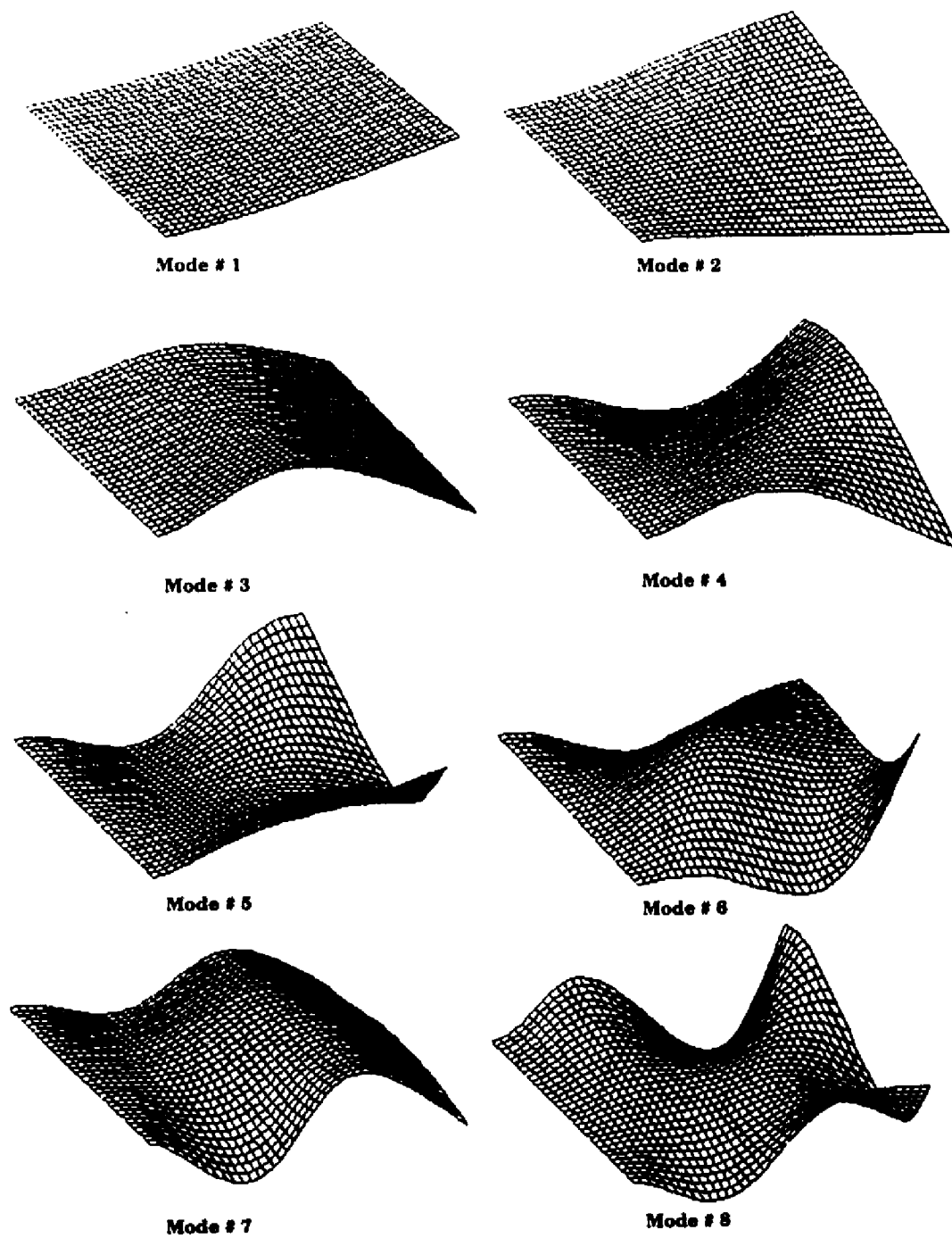Mode # 6

Mode # 7

Mode # 8
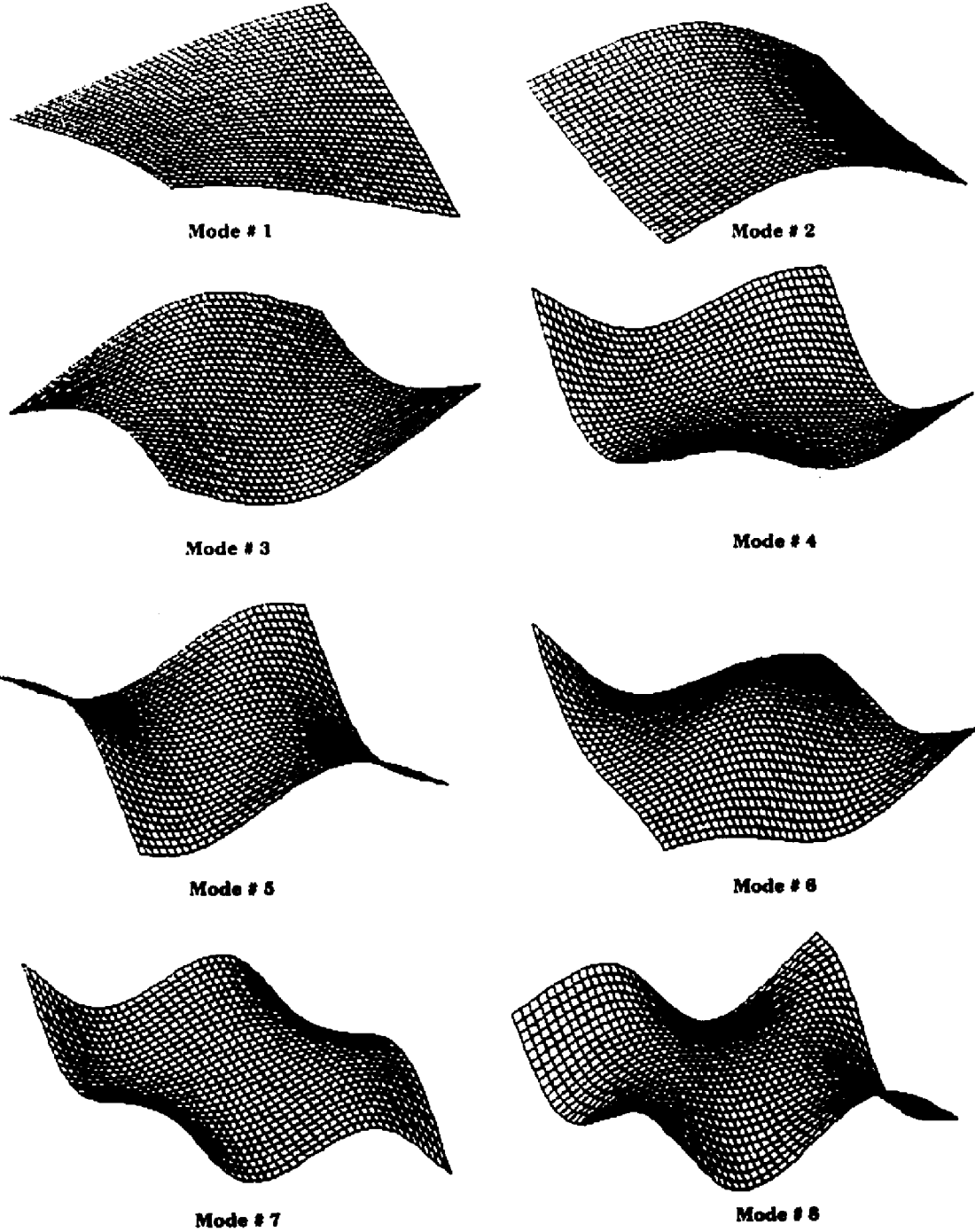
Fig. 74 Mode Shapes For Free-Free Unstiffened Composite Skew Plate

Case: 16

Plate: Crossply composite skew plate (20" x 16").
Stiffener: Single stiffener along 16" side symmetrically placed.
B.C.:   All sides free.
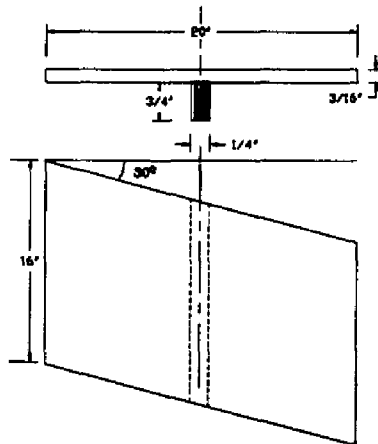
Fig. 75 Free-Free Single Stiffened Skew Plate

Table 24. Frequency in Cycles/sec (Hz.)

Mode No.	Type of Mode	Present (Hz.)	NASTRAN (Hz.)	Expt. (Hz.)
1	1st Twisting	34.72	38.78	30.00
2	1st Bending	70.22	64.36	68.00
3	2nd Twisting	83.64	79.45	78.00
4	Coupled	137.00	129.81	118.00
5	Coupled	171.82	150.62	142.00
6	2nd Bending	195.43	188.00	198.00
7	Coupled	232.05	199.12	202.00
8	Coupled	257.00	237.50	246.00
9	Coupled	278.41	259.62	271.00
10	Coupled	353.78	316.90	340.00

Mode # 1

Mode # 2

Mode # 3

Mode # 4

Mopde # 5

Mode # 6

Mode # 7

Mode # 8
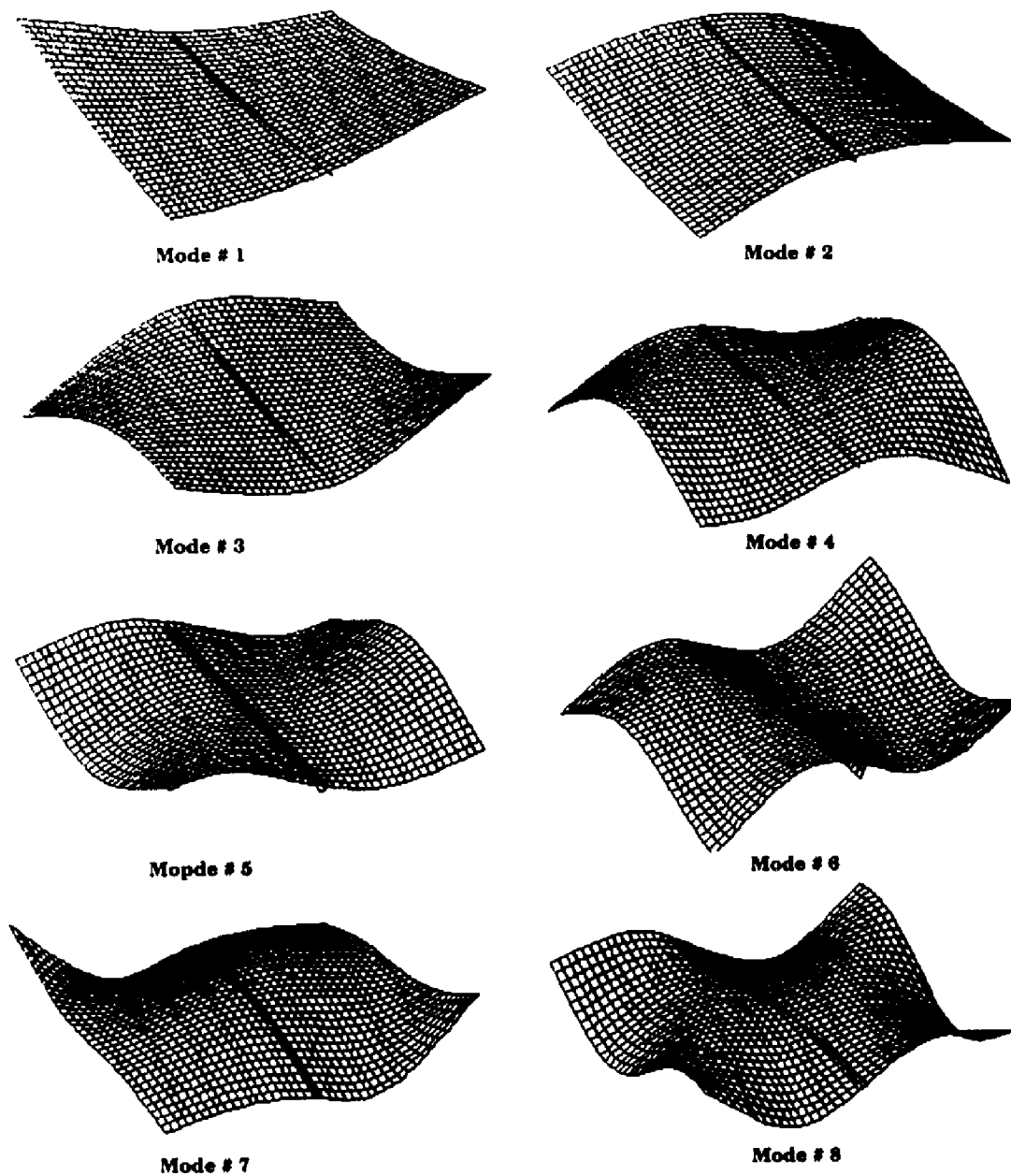
Fig. 76   Mode Shapes For Free-Free Single Stiffened Composite Skew Plate

A few points can be discussed regarding the result of these above cases. It can be seen that there is a good agreement between the results of the present theoretical model, experiment and NASTRAN. For the case of rectangular plates, the higher modes frequencies are greater for the finite element results than those of experimental ones by five percent approximately. This variance is due to the restricted flexure only at the nodes of the finite element and negligence of damping. The plate becomes stiffer and hence the frequencies are higher. For the cases of skew plate, even the first few modes also have a higher frequency value than those of experiment. As the plate becomes more and more skew, the obtuse angle of the plate element increases. So the isoparametric element becomes stiffer yielding a higher frequency.

Comparing the case 1 and case 2 for the clamped-clamped plate, it can be observed that by adding a stiffener to the plate, the first frequency has reduced from 80.43 to 76.01. That is because, by adding the stiffener parallel to the clamped edge, we only added some extra mass to the first bending mode and not any stiffness. Whereas by putting the same stiffener in a direction perpendicular to the clamped edge as shown in case 3, the first frequency has increased to 90.98. Here more than adding the stiffener mass, the stiffening effect of the stiffener is predominant for the first bending mode. As the plate becomes stiffer in this case, the frequency goes high. On contrast to the first mode, the second mode for this clamped plate behave in an opposite manner. This is the first twisting mode which decreases from 90.71 for case 1 to 86.34

for case 2 as the stiffening effect for the first twist is predominant. The same kind of variation can also be observed for the clamped-free (cantilever) plates in the case 5 through case 8. During the experiment, a few higher modes were missed because of the closer value of the adjacent mode and these are marked by (--) in the previous tables. The assignment of these conflicting modes are done based on the mode shape comparisons.

It can be stated here that, by adding an extra stiffener to the plate, along with the increased stiffness, the mass and hence the inertia force also increases. These two parameters have totally opposite effect on the natural frequency of the plate. Hence addition of a stiffener to plate decreases the value of bending frequency modes due to extra mass and increases the value of twisting frequency modes because of extra stiffness.

Another important factor can be marked about the higher modes. The 3rd bending mode for the clamped-clamped plate occurs as 8th mode for plate without any stiffener, and as 7th mode for plate with single stiffener. So the occurrence of these higher modes can be controlled by adding proper stiffening effect.

The cases 9 and 10 for rectangular plate and cases 15 and 16 for the skew plate are the study of free-free boundary conditions. In these cases, the first six mode obtained are the rigid body modes of translations and rotations. These modes had frequency values close to zero. In the case of experiment, a thin inelastic string was used to hang the plate in free-free condition and

hence the first six rigid body modes had values around 10 instead of close to zero. These values are discarded as of no use and only the flexural modes with their frequencies are listed in these cases.

In the case of NASTRAN, though the input was in the form of lamina properties and different layers, before any computation it converts these into a single layer plate element with isotropically defined properties. It also neglects the transverse shear. Because of this reason, there is a discrepancy in their results. For composite plates of the present nature (crossply orthotropic), the NASTRAN results can be accepted with minor error. But for anisotropic plates with different fiber orientation, these might lead to serious problems.

Out of personal curiosity, an aircraft all composite wing was modeled as a swept back cantilever stiffened plate and analyzed for its natural frequency and mode shape. The wing skin was composed of thirteen layers of crossply laminate supported on two sets of stiffeners. One set being parallel to the clamped boundary and has a constant depth. The other set along the length of the wing called as rib has a tapered cross section. The depth of this rib was varied from 0.75" at root to 0.65" at the tip. The wing modeled was having a symmetric aerofoil with four stiffeners and six ribs. The modal analysis for this structure was carried over using the super element solution of the NASTRAN. The first few natural frequencies with the corresponding mode shapes of this all composite aircraft wing are shown in the following page.
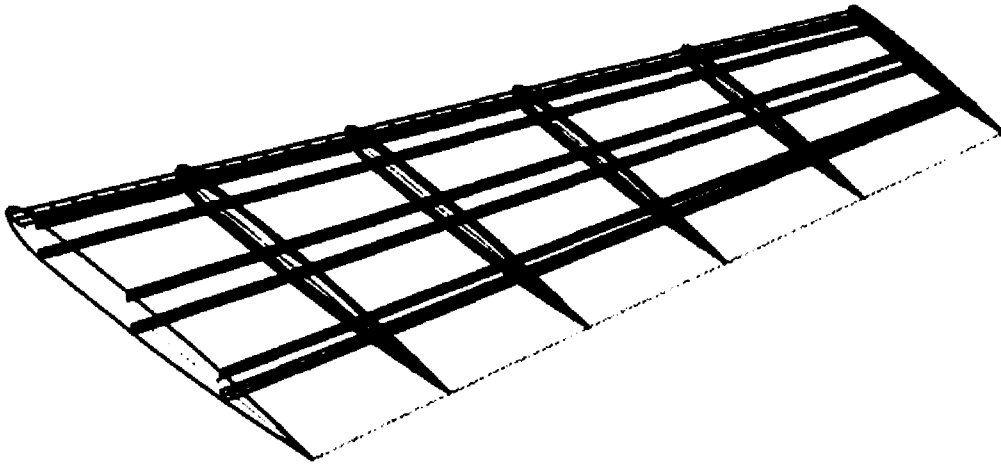
Fig. 77 Aircraft Wing Model Mesh, Ribs and Stiffeners.

Table 25.   Frequency in Cycles/sec (Hz.) for the Composite Aircraft Wing

Mode No.	Type of Mode	NASTRAN (Hz.)
1	1st Bending	74.09
2	2nd Bending	192.38
3	1st Twisting	227.05
4	Blow Mode	266.21
5	3rd Bending	317.28
6	Coupled	321.69
7	Coupled	395.48
8	Coupled	398.09
9	Coupled	461.19
10	Coupled	491.42
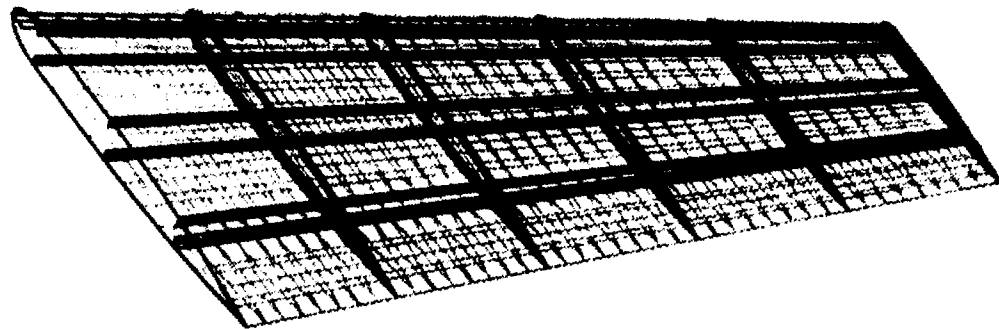
Fig. 78 Full Aircraft Wing Model Mesh

Mode # 1

Mode # 2

Mode # 3

Mode # 4

Mode # 5

Mode # 6

Mode # 7

Mode # 8
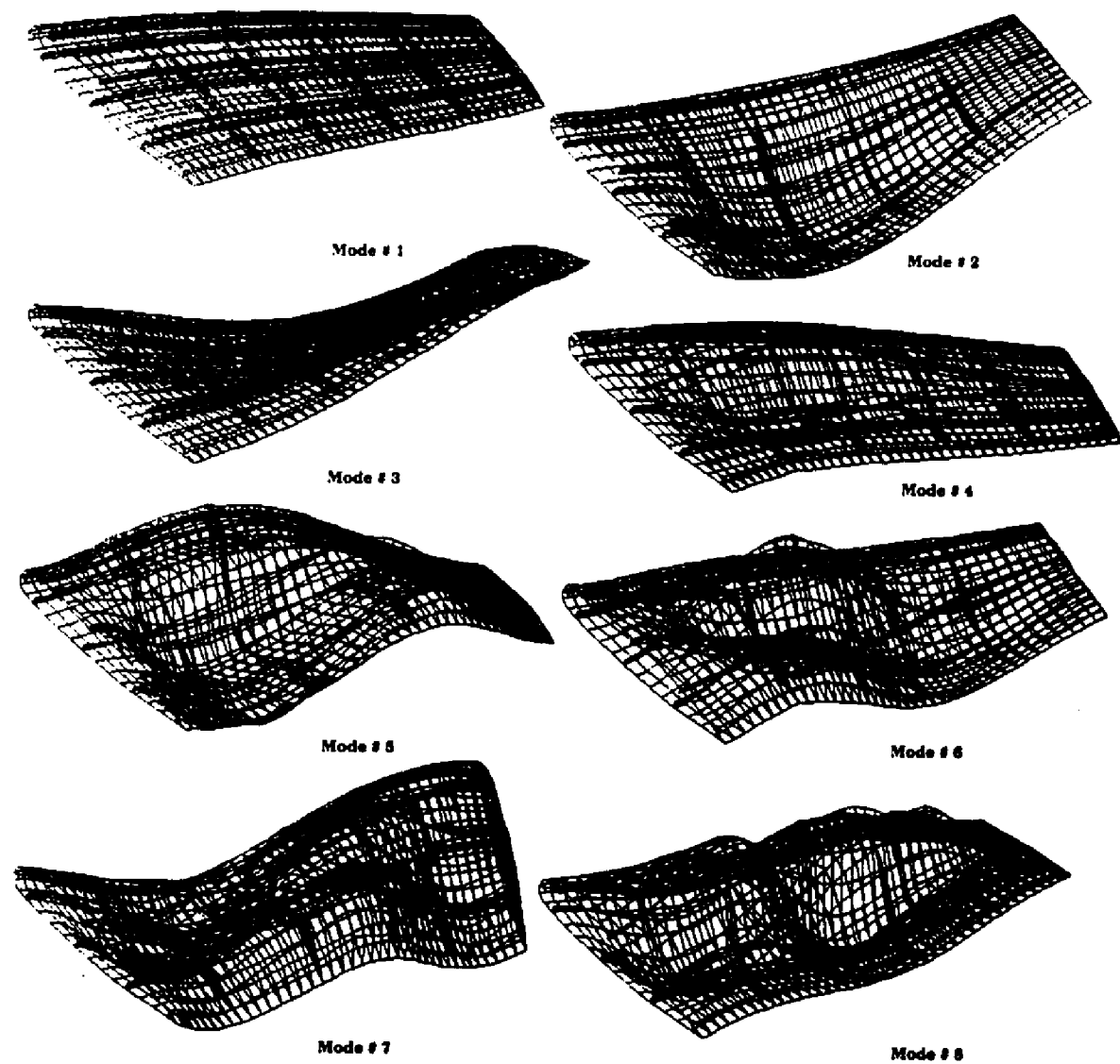
Fig. 79 Mode Shapes for Composite Aircraft Wing

CHAPTER 6. CONCLUSION AND FURTHER RECOMMENDATION

A finite element approach for the deflection analysis of laminated composite plates has been developed with stiffness matrix derivation based on the principle of minimum energy. Experiments were conducted for both unstiffened and stiffened plates of different materials (Aluminum 6061 T6 and Scotchply fiber glass composite) and the results are compared with the analytical ones. Based on these investigations, the following conclusions are drawn for the bending analysis only. The results of the dynamic part of this study is added towards end of this section.

Like other methods, the accuracy of the results obtained by using the finite element method to solve rhombic cantilever plate problems, also decreases with increase in the angle of sweep. It is concluded that the stresses at the rear triangle of the cantilever plate remains the same irrespective of the angle of sweep. There exists an optimized stiffener angle for minimum deflection of a plate of given skew angle, γ. This stiffener angle, θ, depends on the geometry (size) of the plate and stiffener. Hence for a plate of given boundary conditions, surface area, and skew angle, an optimum stiffener angle can be designed to reduce the maximum deflection and hence the stress. The number of elements used in the analysis gives results of adequate accuracy for skew angles up to 50°. Use of a better deflection polynomial expression that ensures continuity of both slopes and deflections over the complete plate would

perhaps, though not necessarily, lead to improved accuracy. Experimental results can also be improved by investigating a better way of producing the stiffeners for a given plate geometry. Such a method may include attaching stiffener sections instead of machining them.

Although only two types of boundary conditions have been analyzed, plates with any boundary condition and aspect ratio can also be analyzed by this finite element solution process. Further investigations can be carried out for designing the stiffest cross-section of stiffener to further reduce the deflection and stress values.

A second finite element approach for composite plates with low aspect to stiffener spacing ratio is formulated and validated well with the modal experimental results. The damping effect of these plates being very small, were neglected in this study. Several plates with different boundary conditions, plan form, and number of stiffeners were studied. It is concluded from this study that, by adding an extra stiffener to the plate, along with the increased stiffness, the mass and hence the inertia force also increases. These two parameters have totally opposite effect on the natural frequency of the plate. Hence addition of a stiffener to the plate decreases the value of the bending frequency modes due to an added extra mass and increases the value of twisting frequency modes because of the extra stiffness. Also the occurrence of the higher modes which is important in many structures, can be controlled by adding proper stiffening effect.

For further study, the following few things can be considered. The beam and plate finite element approach can be applied to analyze the bending of stiffened plates and the results can be compared with those from equivalent orthotropic Huber theory. The damping effect which is neglected in this work can be introduced in the finite element model and the results can be compared with the experimental damping effects. The isolators used in the experiment to obtain the perfect clamped support can be modeled in the finite element analysis with their damping property to have a better comparison of the results. A further study of finding the frequencies for the composite aircraft wing and validating with experiment may be proposed.

REFERENCES

1. Coull, A., "The Direct Stress Analysis of Swept Cantilever Plates of Low Aspect Ratio," *Aircraft Engineering*, pp. 182-190, 1965.

2. Mukhopadhyay, M., "A Galerkin Solution for Clamped Skew Plates in Bending," *The Aeronautical Journal of the Royal Aeronautical Society*, vol. 72, pp. 396-398, 1978.

3. Somashekar, B.R. and Prathap, G., "Stress Singularity in Swept Cantilever Plates," *Journal of Aeronautical Society of India*, vol. 35, No. 2, pp. 107-111, 1983.

4. Torres, J., Samartin, A., Arroyo, V. and Valle, J.D., "A C^1 Finite Element Family for Kirchhoff Plate Bending," *International Journal for Numerical Methods in Engineering*, vol. 23, pp. 2005-2029, 1986.

5. Dawe, D.J., "Parallelogramic Elements in the Solution of Rhombic Cantilever Plate Problems," *Journal of the Strain Analysis*, vol. 1, pp. 223-230, 1966.

6. Kan, Y.R. and Ito, Y.M., "On the Analysis of Unsymmetrical Cross-ply Rectangular Plates," *Journal of Applied Mechanics*, Transactions of the ASME, vol. 2, pp. 615-617, 1972.

7. Salerno, V.L. and Goldberg, M.A., "Effect of Shear Deformations on the Bending of Rectangular Plates," *Journal of Applied Mechanics*, pp. 54-58, 1960.

8. Rajaiah, K., "Flexure of Elastically Restrained Rhombic Plates," *Journal of Aeronautical Society of India*, vol. 35, No. 2, pp.119-124, 1983.

9. Huber, M.T., "Die Grundlagen Einer Rationellen Berechnung der Kreuzweise Bewehrten Eisenbeton Platten," Z. Osterreichischen Ing. Architekten, Ver. 66, pp. 557-560, 1914.

10. Pfluger, A., "Zum Beulproblem der Anisotropen Rechteckplatte, Ing. Arch. 16, pp. 111-120, 1947.

11. Hoppmann, W.H., "Bending of Orthogonally Stiffened Plates," *Journal of Applied Mechanics*, Trans. ASME, vol.77, pp. 267-271, 1955.

12. Hoppmann, W.H., Huffington, N.J. Jr. and Magness, L.S., "A Study of Orthogonally Stiffened Plates," *Journal of Applied Mechanics*, pp. 343-350, 1956.

13. Huffington, N.J. and Blackberg, V., "Theoretical Determination of Rigidity Properties of Orthogonally Stiffened Plates," *Journal of Applied Mechanics*, pp. 15-20, 1956.

14. Schade, H.A., "The orthogonally stiffened plate under uniform lateral load," Trans. ASME, vol. 62, pp. A-143-146, 1940.

15. Smith, C.B., Heebink, T.B. and Norris, C.B., "The Effective Stiffness of a Stiffener Attached to a Flat Plywood Plate," Forest Products Laboratory, Report No.-1557, 1946.

16. Karamanlidis, D. and Agrawal, V., "Analysis of Stiffened Shear-Flexible Orthotropic Panels," Univ. of Rhode Island, Dept. of Civil Engineering, 1988.

17. Davis, R.C., "Stress Analysis and Buckling of J-stiffened Graphite-Epoxy Panels," NASA Tech. Paper-1607, 1980.

18. Wegmuller, A.W., "Full Range Analysis of Eccentrically Stiffened Plates," ASCE, *Journal of the Structural Division*, pp. 143-159, January 1974.

19. Bushnell, D., "PANDA-Interactive Program for Minimum Weight Design of Stiffened Cylindrical Panels and Shells," *Computers and Structures*, vol. 16, No. 1-4, pp.167-185, 1983.

20. Bushnell, D., "PANDA2-Program for Minimum Weight Design of Stiffened, Composite, Locally Buckled Panels, *Computers & Structures*, vol. 25, No. 4, pp. 469-605, (1987).

21. Bushnell, D., "Theoretical Basis of the PANDA Computer Program for Preliminary Design of Stiffened Panels under Combined in plane Loads," *Computers and Structures*, vol. 27, No. 4, pp. 541-563, 1987.

22. Bushnell, D. and Bushnell, W., "Minimum Weight Design of a Stiffened Panel Via PANDA2 and Evaluation of the Optimized Panel Via STAGS," 33rd AIAA/ASME/AHS/ASC Structures, Structural Dynamics and Materials Conference, 1992.

23. Sheinman, I., "Nonlinear Equations of Laminated Panels with Laminated Stiffeners," *Composite Structures*, vol. 8, pp. 287-292, 1987.

24. Koko, T.S. and Olson, M.D., "Non-Linear Analysis of Stiffened Plates Using Super Elements," *International Journal for Numerical Methods in Engineering*, vol. 31, pp. 319-343, 1991.

25. Dawe, D.J., "A Finite Element Approach to Plate Vibration Problems," *Journal Mechanical Engineering Science*, vol. 7, No. 1, pp. 28-32, 1965.

26. Dawe, D.J., "Vibration of Rectangular Plates of Variable Thickness," *Journal Mechanical Engineering Science*, vol. 8, No. 1, pp.42-51, 1966.

27. Gorman, D.J. and Singal, R.K., "Analytical and Experimental Study of Vibrating Rectangular Plates on Rigid Point Supports," *AIAA Journal*, vol. 29, No. 5, pp. 838-844, 1991.

28. Singh, G., Rao, G.V., and Iyengar, N.G.R., "Large Amplitude Free Vibration of Simply Supported Anisotropic Cross-Ply Plates," *AIAA Journal*, vol. 29, No. 5, pp. 784-790, 1991.

29. Malhotra, S., Ganesan, N., and Veluswami, M.A., "Effect of Fiber Orientation and Boundary Conditions on the Vibration Behavior of Orthotropic Rhombic Plates," *Composites*, vol. 19, pp. 127-132, 1988.

30. Krishnan, A and Deshpande, J.V., "Vibration of Skew Laminates," *Journal of Sound and Vibration*, vol. 153, No. 2, 1992.

31. Krishnan, A and Deshpande, J.V., "A Study on Free Vibration of Trapezoidal Plates," *Journal of Sound and Vibration*, vol. 146, No. 3, pp. 507-515, 1991.

32. Bert, C.W. and Mayberry, B.L., "Free Vibrations of Unsymmetrically Laminated Anisotropic Plates with Clamped Edges," *Journal of Composite Materials*, vol. 3, pp. 282-289, 1969.

33. Dawe, D.J. and Roufaeil, O.L., "Rayleigh-Ritz Vibration Analysis of Mindlin Plates," *Journal of Sound and Vibration*, vol. 69, No. 3, pp. 345-359, 1980.

34. Rock, T.A. and Hinton, E., "A Finite Element Method for the Free Vibration of Plates Allowing for Transverse Shear Deformation, *Computers & Structures*, vol. 6, pp. 37-44, 1976.

35. Alam, N. and Asnani, N.T., "Vibration and Damping Analysis of Fiber Reinforced Composite Material Plates," *Journal of Composite Materials*, vol. 20, pp. 2-18, 1986.

36. Srinivas, S. and Rao, A.K., "Bending, Vibration and Buckling of Simply Supported Thick Orthotropic Rectangular Plates and Laminates," *International Journal of Solids and Structures*, vol. 6, pp. 1463-1481, 1970.

37. Chen, W.C. and Liu, W.H., "Deflections and Free Vibrations of Laminated Plates-Levy-Type Solutions," *International Journal of Mechanical Science*, vol. 32, No. 9, pp.779-793, 1990.

38. Kirk, C.L., "Natural Frequencies of Stiffened Rectangular Plates," *Journal of Sound and Vibration*, vol. 13, pp. 375-388, 1970.

39. Fahy, F.J. and Wee, R.B.S., "Some Experiments with Stiffened Plates Under Acoustic Excitation," *Journal of Sound and Vibration*, vol. 7, No. 3, pp. 431-436, 1968.

40. Aksu, G. and Ali, R., "Free Vibration Analysis of Stiffened Plates Using Finite Difference Method," *Journal of Sound and Vibration*, vol. 48, pp. 15-25, 1976.

41. Long, B.R., "A Stiffness-Type Analysis of the Vibration of a Class of Stiffened Plates," *Journal of Sound and Vibration*, vol. 16, pp. 323-335, 1971.

42. Bhandari, N.C., Juneja, B.L., and Pujara, K.K., "Free Vibration and Transient Forced Response of Integrally Stiffened Skew Plates on Irregularly Spaced Elastic Supports," *Journal of Sound and Vibration*, vol. 64, No. 4, pp. 475-496, 1979.

43. Lu, Y.P., Neilson, H.C., and Roscoe, A.J., "On the vibration Properties of Composite Materials and Structures," *Journal of Composite Materials*, vol. 27, No. 16, pp. 1598-1605, 1993.

44. Koko, T.S., "Super Finite Elements for Nonlinear Static and Dynamic Analysis of Stiffened Plate Structures," A Thesis for Ph. D. at The University of Columbia, 1990.

45. Ambur, D.R. and Reyfield, L.W., "Effect of Stiffness Characteristics on the Response of Composite Grid-Stiffened Structures," *Journal of Aircraft*, vol. 30, No. 4, pp. 541-546, 1993.

46. Liao, C. and Sun, Y.W., "Flutter Analysis of Stiffened Laminated Composite Plates and Shells in Supersonic Flow," *AIAA Journal*, vol. 31, No. 10, pp. 1897-1905, 1993.

47. Hachenberg, D. and Kossira, H., "Stringer Peeling Effects at Stiffened Composite Panels in the Postbuckling Range," *Journal of Aircraft*, vol. 30, No. 5, pp. 769-776, 1993.

48. Kassapoglou, C. and DiNicola, A.J., "Efficient Stress Solution at Skin Stiffener Interfaces of Composite Stiffened Panels," *AIAA Journal*, vol. 30, No. 7, pp. 1833-1839, 1992.

49. Mukherjee, A. and Mukhopadhyay, M., "Finite Element Free Vibration Analysis of Stiffened Plates," *Aeronautical Journal*, vol.90, pp. 267-273, 1986.

50. Mecitoglu, Z. and Dokmeci, M.C., "Free Vibration of a Thin, Stiffened Cylindrical Shallow Shell," *AIAA Journal*, vol. 30, pp. 848-850, 1992.

51. Mequita, L. and Kamat, M.P., "Simultaneous Design and Control of Stiffened Laminated Composite Structures," *Journal of Aerospace Engineering*, vol. 5, No. 1, pp. 111-117, 1992.

52. Liao, C.L. and Reddy, J.N., "Continuum-Based Stiffened Composite Shell Element for Geometrically Nonlinear Analysis," *AIAA Journal*, vol. 27, No. 1, pp. 95-101, 1989.

53. Vinson, J.R. and Sierakowski, R.L., *The Behavior Structures Composed of Composite Materials*, Kluwer Academic Publishers, pp. 35-57, 1987.

54. Lekhnitskii, S.G., *Anisotropic Plates*, (Translated from second edition by Tsai, S.W. and Cheron, T.), Gordon and Breach Science Publishers, 1968.

55. Timoshenko, S. and Woinowsky-Krieger, S., *Theory of Plates and Shells*, McGraw-Hill Book Company, 1959.

56. Ewing D.J. *Modal Testing: Theory and Practice*. Letchworth Research Study Press for Bruel & Kjaer, 1986.

57. Allemang R.J., Brown D.L. and Rost R.W. Course on Experimental Modal Analysis vol II, *Proceedings of the 15th International Seminar on Modal Analysis*. Measurement Techineques for Experimental Modal Analysis, 1960.

58. Randall R.B., Frequency Analysis. *Bruel & Kjaer: K.L. Larson & Son*, 1987.

59. Halvorsen W.G., Anatrol Corporation and Brown D.L., University of cincinnati. *Impulse Techniques for Structural Frequency Response*, 1977.

60. Ramsey K. A., Sound and Vibration 9 (11). *Effective measurements for structural Dynamics Testing*, part I, 1975.

61. Ramsey K. A., Sound and Vibration 10 (5). *Effective measurements for structural Dynamics Testing*, part II, 1976.

62. Leuridan J. Van Der Auweraer H and Mergay M, Course on Experimental Modal Analysis vol II, *Proceedings of the 15th International seminar on Modal Analysis*. Review of parameter estimation techniques, 1990.

63. Lembergts F, Course on Modal Analysis vol II, *Proceeoings of The 15th International Seminar on Modal Analysis*. Parameter Estimation in Modal Analysis, 1990.

VITA

Aruna Kumar Tripathy was born in Orissa, India on February 4, 1962. He finished his Bachelor of Science in Physics from Berhampur University, Orissa and then graduated from Institution of Engineers, Calcutta in Civil Engineering in the year 1986. He achieved his Master of Engineering in Aeronautical Engineering from Anna University, Madras. He then joined Indian Institute of Technology, Madras as a Research Scholar in the Department of Aerospace Engineering. Mr. Tripathy achieved his Doctor of Philosophy in Mechanical Engineering from the Louisiana State University in December 1995.

DOCTORAL EXAMINATION AND DISSERTATION REPORT

Candidate: Aruna Kumar Tripathy

Major Field: Mechanical Engineering

Title of Dissertation: Numerical and Experimental Analysis of Bending and
Vibration of Stiffened Laminated Composite Panels

Approved:

Su-Seng Pang
_____
Major Professor and Chairman

_____
Dean of the Graduate School

EXAMINING COMMITTEE:

_____

_____

_____

_____

_____

_____

_____

Date of Examination:

September 29, 1995